REVIEW

Gasotransmitter delivery for bone diseases and regeneration

Yaoyao Xu,[1] Yanyue Li,[1] Ang Gao,[1,*] Paul K. Chu,[2,*] and Huaiyu Wang[1,*]

*Correspondence: ang.gao1@siat.ac.cn (A. G.); paul.chu@cityu.edu.hk (P. C.); hy.wang1@siat.ac.cn (H. W.)

Received: April 28, 2023; Accepted: May 11, 2023; Published Online: June 2, 2023; https://doi.org/10.59717/j.xinn-life.2023.100015

GRAPHICAL ABSTRACT

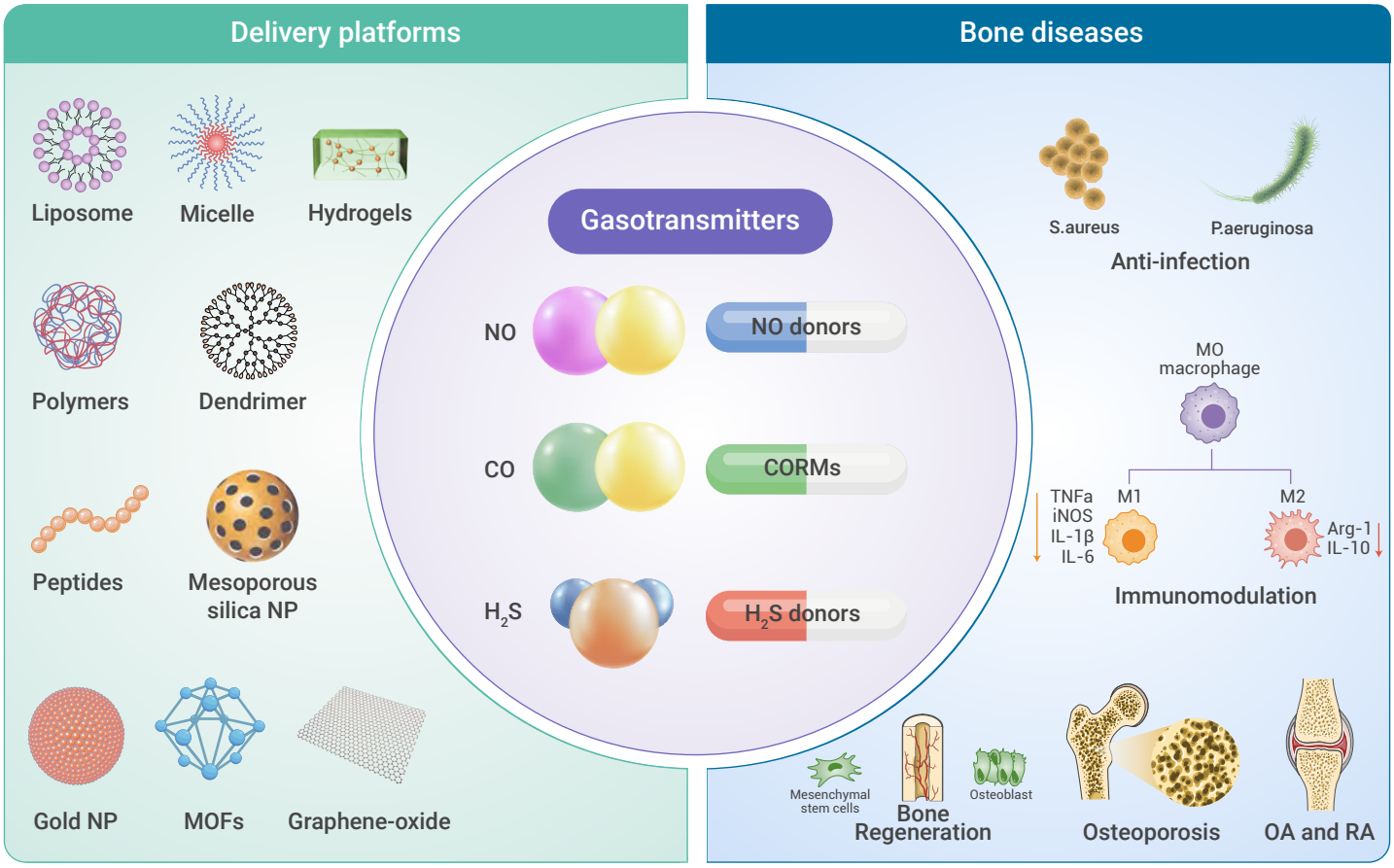

PUBLIC SUMMARY

- Endogenous gaseous signaling molecules (gasotransmitters) include nitric oxide, carbon monoxide, and hydrogen sulfide
- These gasotransmitters have gained significant interest due to their unique properties.
- Various donors and delivery platforms have been developed for controlled and targeted delivery of these gasotransmitters.
- Therapeutic application of these gasotransmitters in treating bone diseases are reviewed.

REVIEW

Gasotransmitter delivery for bone diseases and regeneration

Yaoyao Xu,[1] Yanyue Li,[1] Ang Gao,[1,*] Paul K. Chu,[2,*] and Huaiyu Wang[1,*]

[1]Center for Human Tissues and Organs Degeneration, Shenzhen Institute of Advanced Technology, Chinese Academy of Sciences, Shenzhen 518055, China

[2]Department of Physics, Department of Materials Science and Engineering, and Department of Biomedical Engineering, City University of Hong Kong, Hong Kong, China

*Correspondence: ang.gao1@siat.ac.cn (A. G.); paul.chu@cityu.edu.hk (P. C.); hy.wang1@siat.ac.cn (H. W.)

Received: April 28, 2023; Accepted: May 11, 2023; Published Online: June 2, 2023; https://doi.org/10.59717/j.xinn-life.2023.100015

Citation: Xu Y., Li Y., Gao A., et al., (2023). Gasotransmitter delivery for bone diseases and regeneration. The Innovation Life **1(1)**, 100015.

Endogenous gaseous signaling molecules, nitric oxide (NO), carbon monoxide (CO), and hydrogen sulfide (H_2S), collectively called gasotransmitters, regulate various physiological and pathophysiological processes. Thus, they offer significant advantages over traditional small-molecule drugs in treating bone diseases. However, their clinical use is limited by their gaseous nature, extensive reactivity, and short half-life. Also, these gasotransmitters behave as a double-edged sword, providing therapeutic effects at physiological concentrates while exhibiting acute toxicity at high concentrations. Therefore, controlled, sustained, and even targeted delivery of gasotransmitters is highly desirable. In this review, we emphasize recent significant advances in gasotransmitter delivery materials, including the gas-releasing molecules and their delivery platforms. We further focus on the therapeutic application of these gasotransmitters in treating bone diseases, including implant-associate infection, immunomodulation, bone regeneration, osteoporosis, and arthritis, aiming to provide references for the development of novel therapeutic strategies for bone diseases.

INTRODUCTION

Bone diseases encompass a wide range of skeletal-related disorders, including osteoporosis, osteoarthritis (OA), rheumatoid arthritis (RA), and bone defects associated with tumors or infections.[1] With the growing number of patients in an aging society, the medical and socioeconomic impacts of bone diseases will continue to rise. For instance, osteoporotic fractures can cause significant morbidity, leading to a loss of productivity and reduced quality of life for many individuals. The mortality rate in the first year following a hip fracture is 20–30%, and over half of those who experience a hip fracture are unable to return to their previous lifestyle.[2] As for bone defects, although bone tissue has an intrinsic capacity for repair, there are cases where bone healing is either impaired or insufficient, such as in diabetic or osteoporotic patients. Osteoarthritis is another age-related condition that will become more prevalent as the population ages.[3] Consequently, treating bone diseases poses significant challenges in clinical practice.

Limited effective treatments are available for some of the most common bone diseases such as OA and RA.[4,5] On the other hand, while current osteoporosis therapies using small-molecule drugs like bisphosphonates have proven successful in preventing osteoporotic fractures, concerns have been raised regarding their long-term safety, such as osteonecrosis of the jaw and a painful condition with exposed bone in the oral cavity.[2] The repair of bone defects usually utilizes various artificial implantable scaffolds, whereas the integration between the orthopedic implants and the native bone tissue is far from satisfying.[6] Therefore, there is an urgent need to develop new therapy strategy for safe and efficient clinical treatments of bone diseases.

Gas therapy, which involves the use of gasotransmitters to treat diseases, has gained significant interest as a promising therapeutic approach for bone diseases, due to its high therapeutic efficiency, low systemic side effects, and biosafety.[7] To date, three gasotransmitters have been identified: nitric oxide (NO), carbon monoxide (CO), and hydrogen sulfide (H_2S). These gasotransmitters have revolutionized conventional ideas of intercellular communication.[8] They play crucial roles in vasodilation, neurotransmission, and anti-inflammatory and antioxidative responses. The regulatory effects of gasotransmitters in various physiological functions open up the possibility to deliver them exogenously as therapeutic agents.[9] Therefore, these endogenous gas signaling molecules offer significant advantages over traditional small-molecule drugs for the treatment of bone diseases.[10]

The in vivo therapeutic application of these gasotransmitters through systemic administration is highly challenging due to their high diffusion rates, low solubility, and rapid systemic clearance.[11] Additionally, the therapeutic effects of these gases depend on factors such as concentration, diffusion velocity, location, and retention at the lesion site.[12] These gasotransmitters behave as a double-edged sword, exhibiting acute toxicity at high concentrations while providing therapeutic effects at physiological concentrations.[13–15] To improve the efficiency of gas therapy, it is crucial to utilize carriers to deliver the gases. Biocompatible materials that delivery gases in a sustained and controlled manner can be used as a single therapeutic method, or synergized with other strategies such as photothermal therapy.[16] To date, many kinds of materials are utilized to delivery gasotransmitters, mainly including various multifunctional polymer/organic/inorganic carriers with good biocompatibility, such as micelle, peptide amphiphiles, poly (lactic-co-glycolic acid) (PLGA), silica/mesoporous silica, metal-organic framework (MOF), Prussian blue (PB) nanoparticles, graphene, and upconversion nanoparticles (UCNP).

In this review, we firstly introduce the physiological roles and therapeutic mechanisms of NO, CO, and H_2S. Then the recent progress on the gas delivery materials, including gas-releasing donors, and delivery platforms is reviewed. Following is the discuss on the gas delivery materials for bone diseases, including the anti-infection application, immunomodulation, bone regeneration, osteoporosis, and arthritis, aiming to provide references for the development of novel therapeutic strategies for bone diseases.

PHYSIOLOGICAL MECHANISMS

NO

As first identified gasotransmitter, NO has been extensively studied and documented for its significant role in regulating various physiological processes in cardiovascular system, nervous system, and immune system. Endogenous NO is produced enzymatically from L-Arginine by three isoforms of nitric oxide synthase (NOS): endothelial NOS (eNOS), neuronal NOS (nNOS), and inducible NOS (iNOS).[17] NO can also be generated non-enzymatically through reduction of nitrite and decomposition of S-nitrosothiols.[18] The eNOS and nNOS act as constitutively expressed protein mainly in vascular endothelial cells and neurons, respectively.[19] Unlike eNOS and nNOS, which are tightly regulated and dependent on calcium fluxes entry into the cells, the iNOS is less susceptible to feedback inhibition by NO.[20] It predominates in immune cells to produce large amounts of NO that aids in the host defense mechanisms in response to extracellular stimuli, such as pro-inflammatory cytokines (IL-1, TNF-α) and bacterial lipopolysaccharide (LPS) endotoxin.[17]

NO is an excellent messenger molecule due to its highly reactive and diffusible properties. This short-lived signaling molecule operates across a wide physiological concentration ranging from subnanomolar levels (associated with cell survival signaling) to micromolar levels (linked to cytotoxic effects and apoptotic signaling) in different tissues.[21] The regulation role of NO is concentration-dependent. At low concentrations, NO produced by endothelial cells and neurons plays a vital role in regulating processes such as vasodilation, angiogenesis, and neurotransmission.[22] The primary function of NO is identified as endothelial-derived relaxation factor (EDRF), which plays a critical role in maintaining proper vascular tone and preventing leukocytes and platelets from adhering to the vascular wall. In addition, NO has been proven to enhance endothelization and promote angiogenesis, which is the indispensable process for the regeneration of damaged tissues.[23] In its classical physiological pathway, NO reacts to the heme group of the soluble guanylate cyclase (sGC), resulting in generation of cyclic guanosine monophosphate (cGMP) and following activation of protein kinase G (PKG).

NO also reacts with thiol group of a cysteine residues to form S-nitrosothiols (RSNOs). This reaction called S-nitrosylation has been shown to modify the activity of proteins involved in cellular regulatory mechanisms. Conversely, this radical gas produced at higher concentrations from macrophages and neutrophils react with oxygen or superoxide spontaneously, producing reactive nitrogen and oxygen intermediates. These resultant reactive nitrogen oxide species (RNOS) cause oxidative and nitrosative damage to pathogens by modifying DNA, inhibiting enzyme function, and inducing lipid peroxidation, contributing to the antimicrobial action of NO.[13] On the other hand, excessive NO also exerts pro-inflammatory effects by activating nuclear factor kappa B (NF-κB) and promoting oxidative stress.

CO

The colorless, odorless, and tasteless gas CO has long been regarded as a "silent killer" duo to its higher binding affinity (approximately 230-fold) for hemoglobin (Hb) than that of oxygen. It competitively displaces oxygen to form carboxyhemoglobin (COHb), thus reducing the oxygen-carrying capacity of the blood, leading to tissue hypoxia and eventually death.[24] Nowadays CO has been demonstrated to participate in multifaceted regulation of biological activities and has important cytoprotective and homeostatic properties.[25] The endogenous production of CO is mediated by the activity of heme oxygenases (HO), including both inducible (HO-1) and constitutive (HO-2 and HO-3) enzymes, which catalyze the degradation of heme, yielding biliverdin, Fe^{2+} and biological CO. As an inert gaseous molecule, CO is chemically much more stable under physiological conditions than other signaling molecules, (eg. NO and H_2S), and it also is freely diffusible and traverses all membranes. The typical biological reactivity of CO is exemplified by its interaction with transition metals, which are present in structural and functional proteins.[26] For example, the binding of CO to heme alters the conformation and thus the activity of various heme-containing proteins, such as sGC, heme-containing potassium channels, cytochrome c oxidase, nicotinamide adenine dinucleotide phosphate (NADPH) oxidase, and NOS.[27] These interactions endow the CO many potential pathophysiological effects, including modulation of vasomotor tone, anti-inflammation, redox control and cell apoptosis/proliferation.[28] CO shares similar vasoactive actions with NO involving the stimulation of the sGC–cGMP pathway.[29] It also serves as a significant regulator of intracellular ROS production through interaction with NADPH oxidase and cytochrome c oxidase, which is linked with redox homeostasis.[30] The anti-inflammatory effects of CO stem from its direct interaction with proteins participating in mitogen-activated protein kinases (MAPKs) signal transduction.[31] The pro-apoptosis and pro-proliferation effects of CO mainly dependent on its concentrations, which show different metabolic effects on mitochondria, the energy powerhouse of cells. The inhibition of the respiratory chain in bacteria and production of adenosine triphosphate (ATP) contributes the antimicrobial activity of CO.[32]

H_2S

H_2S, a colorless gas with a smell of rotten eggs, was considered as a highly toxic gas molecule. Now it has been identified as the third endogenous gasotransmitter following the NO and CO, playing an important role in many physiological processes.[33] H_2S is a lipophilic compound that easily permeates cell membranes without using specific transporters. The physiological effects of H_2S are closely correlated with its concentrations. At physiological concentration, H_2S exhibits cytoprotective effects that could protect cells and tissues from harmful oxidative injures, while prolonged and high-dose exposure disrupts normal biological processes, leading to cell dysfunction and apoptosis.[34] Dissolved gaseous H_2S is in a dynamic equilibrium under physiological conditions (pH = 7.4, 37 °C), with hydrosulfide anions (HS^-) constituting about 80% of the speciation, neutral H_2S about 20%, and dianionic S^{2-} less than 1%. These sulfur compounds are named as reactive sulfur species (RSS) that arguably contribute to most of the documented biological effects of H_2S.[35] Generally, the term "H_2S" refers to the equilibrium mixture of these total RSS. The protonation states of H_2S and HS^- confer water-solubility and lipophilicity, respectively. HS^- exhibits high nucleophilicity and can interact with various electrophilic targets within cells, including reactive sulfur, oxygen, and nitrogen species. These protonation states possess distinct metal-ligation and redox properties. The biological sulfur redox landscape is intricate, spanning from -2 in H_2S to +6 in SO_4^{2-}, indicating that H_2S/HS^- can be readily oxidized to other biologically significant sulfur species including persulfide and polysulfide.[35]

Endogenous H_2S can be generated through enzymatic and nonenzymatic pathways. In the enzymatic routine, the production of H_2S is directly catalyzed by cystathionineγ-lyase (CSE) and cystathionine-β-synthase (CBS), or indirectly by desulfhydration catalyzed by 3-mercaptopryruvate sulfurtransferase (3-MST) with the help of cysteine aminotransferase (CAT). CBS is mainly expressed in the liver and the central nervous system, while CSE is found primarily in the cardiovascular system. Both of them are distributed in the cytosol, and 3-MST is located predominantly in the mitochondria. The sulfur atom integrated into H_2S originates from the sulfhydryl group of either homocysteine or L-cysteine. Both CSE and CBS are pyridoxal 5'-phosphate-dependent enzymes that directly catalyze the conversion of L-cysteine into H_2S. CBS also catalyzes the condensation of homocysteine and L-serine to form L-cystathionine with the release of water. In the presence of L-cysteine, CBS performs the same β-replacement reaction but releases H_2S instead of water. In addition, CSE catalyzes the breakdown of cystathionine to L-cysteine, which supplies more H_2S sources.[15] In mitochondria, CAT utilizes L-cysteine and α-ketoglutarate to generate 3-mercaptopyruvate, which in turn is catalyzed to pyruvate and H_2S by 3-MST. In addition, the 3-MST pathway also accounts for H_2S formed from D-Cysteine, which is first converted to 3-mercaptopyruvate by D-amino acid oxidase.[35] The nonenzymatic pathway only accounts for a small portion of H_2S production. It involves the reduction of elemental sulfur to H_2S using reducing equivalents obtained from the oxidation of glucose. Not only glucose, other electron carriers such as NADH and NADPH may also help sulfur reduction.[36] Moreover, another non-enzymatic H_2S production in vivo has also been reported through a reaction specific for the cysteine serving as substrate and coordinated catalysis by pyridoxal(phosphate), and iron under physiological conditions.[37]

Endogenous H_2S serves as a versatile physiological mediator, exhibiting a wide range of properties, including anti-inflammatory, neuromodulating, cardioprotective, antioxidant defense, vasodilatory, pro-angiogenic, and cytoprotective effects. H_2S is known to exert its biological effects through three primary routes: interactions with metal centers in protein, scavenging reactive oxygen species (ROS)/reactive nitrogen species (RNS), and S-persulfidation.[38] Direct actions of H_2S on metal centers and the oxidized thiol products constitutes the chemical mechanisms of the physiological effects of H_2S.[39] In addition, H_2S is considered an endogenous reducing agent produced in response to oxidative stress. Evidence has shown that H_2S is a highly reactive molecule that readily reacts with ROS and RNS. Moreover, S-persulfidation of proteins is widely accepted as the key process through which H_2S operates in a signaling capacity. S-persulfidation is the process in which a thiol (R–SH) is converted into a perthiol (R–SSH). This post-translational modification process alters the structure and functionality of target proteins. Numerous proteins have been identified to be the targets of H_2S for S-sulfhydration modification, and these proteins mediates the biological effects of H_2S in regulating cell behaviors.[40]

MATERIALS FOR GAS DELIVERY

The simplest way to administer therapeutic gases is through inhalation, which has been widely used in clinical practice. However, the effectiveness of these gases greatly depends on their concentration at the target site.[41] Due to their low solubility in blood and short half-lives, the therapeutic potential of these gases through inhalation is limited. One solution is the use of chemical donors which act as gas releasing molecules.[42] Systemic administration of these donors are prone to nonspecific distribution, and small molecule donors also suffer from the burst release, rapid clearance, and even acute toxicity . In order to realize the accurate gas release and efficient gas delivery for the clinical translation of gas therapy, these gas releasing molecules have been encapsulated into a range of multifunctional nanocarriers (e.g. polymers, peptides, proteins, micelles, liposomes, mesoporous silica, organosilica, and inorganic multifunctional nanoparticles), which act as

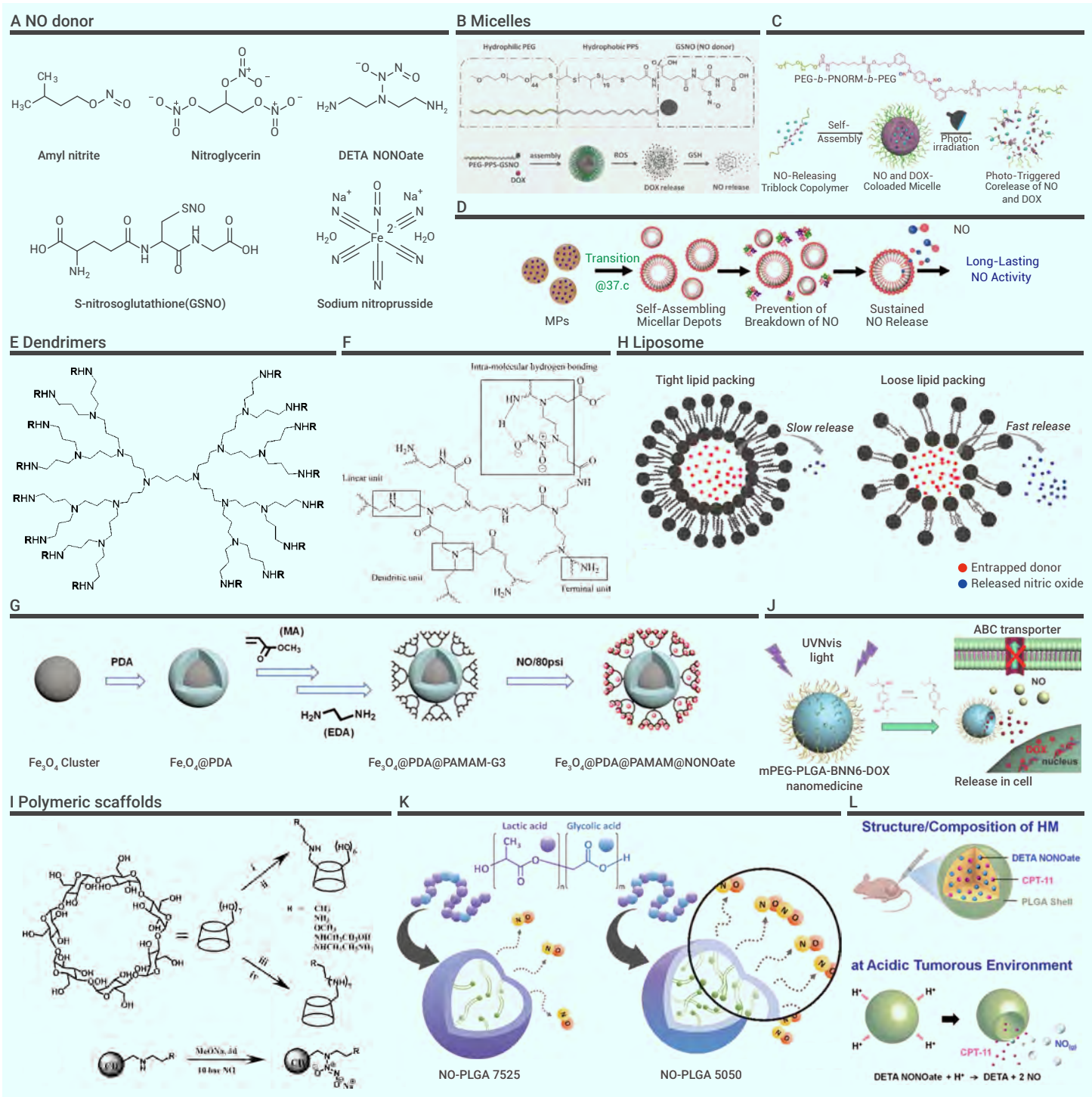

Figure 1. NO donors and organic delivery platforms (A) Chemical structures of commonly used NO donors. (B) Structure of copolymer, which self-assemble into micelles. Reprinted with permission from Wu et al.[59] Copyright 2020 Elsevier. (C) Structure of amphiphilic triblock copolymer. Reprinted with permission from Ding et al.[60] Copyright 2020 The Royal Society of Chemistry. (D) The functional mechanisms of the microparticles. Reprinted with permission from Wu et al.[61] Copyright 2018 Wiley-VCH. (E) Structure of 3 polypropylenimine dendrimer. Reprinted with permission from Stasko et al.[66] Copyright 2006 American Chemical Society. (F) Structure of N-Diazeniumdiolate NO donor-modified h-PAMAM. Reprinted with permission from Yang et al.[67] Copyright 2017 American Chemical Society. (G) Synthetic route of Fe_3O_4@PDA@PAMAM@NONOate. Reprinted with permission from Yu et al.[68] Copyright 2018 Wiley-VCH. (H) Schematic illustration for the liposome structure encapsulating NO donors. Reprinted with permission from Suchyta et al.[64] Copyright 2017 American Chemical Society. (I) Preparation protocols of secondary amine-modified CDs. Reprinted with permission from Jin et al.[75] Copyright 2018 American Chemical Society. (J) Schematic illustration of mPEG-PLGA-BNN6-DOX nanoparticles release NO and DOX inside cells. Reprinted with permission from Fan et al.[81] Copyright 2016 American Chemical Society. (K) Schematic illustration of the structure and anti-inflammatory effects of NO-releasing PLGA nanoparticle. Reprinted with permission from Oh et al.[77] Copyright 2020 American Chemical Society. (L) Schematic structure of the NO-releasing PLGA particles. Reprinted with permission from Chung et al.[80] Copyright 2015 Wiley-VCH.

physical barriers to extend the half-lives of gases, and to realize targeted and controlled delivery of gases for various biomedical applications.[43,44] This section will firstly introduce the recent advances in design of gas-releasing molecules and then summarize the materials and coatings for therapeutic gas delivery.

NO donors and NO delivery platforms

NO donors. Various NO donors have been designed to deliver exogenous NO into biological entities, including organic nitrates ($RONO_2$), nitrites (RONO), N-diazeniumdiolate (NONOate), S-nitrosothiol (RSNO), and metal–NO complexes (Figure 1A).[45]

Organic nitrates and nitrites, such as nitroglycerin, isosorbide mononitrate, and amyl nitrite, are the oldest category of NO donors and have been widely used as vasodilators for the treatment of angina pectoris. Among these, nitroglycerin is the most commonly used organic nitrate for clinically treating hypertension and angina pain.[46] Nitroglycerin releases one mole equivalent of NO upon bioactivation by mitochondrial aldehyde dehydrogenase (mtALDH).

NONOate is one of the most investigated NO donors synthesized by reactions between primary or secondary amines with NO under high pressure. It spontaneously generates two mole equivalents of NO per mole of donor via hydrolysis at physiological pH. The release of NO can also be triggered by different stimuli, including thermal, photochemical, or enzymatic reactions. Although NONOates donors face the drawbacks of burst NO release with short NO release duration, their ease of modification and relatively high thermal stability make them a promising candidate for the development of NO-releasing biomaterials.[47]

S-nitrosothiol (referred to as RSNOs), consisting of molecular bonding between thiol and nitric oxide, is another category of prominent and diverse NO donors.[48] Being different from NONOate, RNOS is endogenously exist in both tissue and blood, include S-nitrosoglutathione (GSNO), Snitrosocysteine (CysNO), S-nitrosoalbumin (AlbSNO), and S-nitrosohemoglobin (HbSNO). It can also be synthesized chemically by reacting thiols with nitrous acid. The release of NO from RSNOs can be induced by multiple pathways, including (1) Cu^{2+} mediated catalytic decomposition, (2) redox reaction with ascorbate, (3) light or thermal-triggered homolytic cleavage of S—NO bond, and (4) enzyme-mediated release.[49,50] GSNO and S-nitroso-N-acetylpenicillamine (SNAP) are two widely used RSNOs that have been intensively studied in biomedical applications. GSNO are found endogenously in mammalian systems and have intrinsically low toxicity, making them attractive NO donors for therapeutic applications. The SNAP is one of the most stable nonpeptide S-NOs reported. It releases NO slowly under physiologically relevant conditions and has already been shown to be a very promising candidate for fabricating long-term NO releasing polymeric materials.

Metal nitrosyl complexes are a class of NO donors that consists of nitric oxide bonded to a transition metal.[51] Sodium nitroprusside (SNP, $Na_2[Fe(CN)_5NO]$) has long been clinically used as a powerful vasodilator to alleviate hypertension. Other examples include Roussin's black salt (RBS, $[Fe_4S_3(NO)_7]^-$) and Roussin's red salt (RRS, $[Fe_2S_2(NO)_4]^{2-}$), which are synthetic iron–nitrosyl complexes mimicking the complexes found in nature, such as those in enzymes and metalloproteins.[52] Owing to the light responsive NO releasing properties, metal nitrosyl have drawn significant attention for spatially and temporally controlled NO delivery systems.[53–55]

NO delivery platforms. The direct application of these NO donors in clinical settings faces the limitations of rapid clearance, degradation, and non-targeted delivery. Therefore, they have been further physically encapsulated in or chemically conjugated onto a variety of biomaterial vectors to develop NO delivery systems, including organic (e.g. micelles, liposomes, dendrimers, polymeric nanoparticles, hydrogels and scaffolds) and inorganic (e.g. silica particles, metallic nanoparticles, zeolite and metal organic frameworks (MOFs)) biomaterial vectors. These NO-delivery platforms allows for a large control over the kinetics of NO release.[56]

Polymeric micelles are self-assembled nano-structures formed by amphiphilic block copolymers with a hydrophobic inner core stabilized by a hydrophilic outer shell. The hydrophobic NO donors can be conjugated with the hydrophilic hyaluronic acid to form a amphiphilic polymer, which could be self-assembled into micelles.[57] The hydrophobic microenvironment within the micellar core also protect the NONOates from proton-catalyzed NO liberation, facilitating delayed NO liberation over 3 weeks under physiological conditions without the initial burst release.[58] The NO donor GSNO has been conjugated to lipophilic end of the amphiphilic copolymer. The GSNO functionalized nanoparticles show high NO loading capacity, good stability and sustained NO release with specific GSH activated NO-releasing kinetics (Figure 1B).[59] The light-responsive NO donor can also be integrated into the middle block of an amphiphilic triblock copolymer, which self-assembles into micellar nanoparticles in aqueous solution without premature NO leakage. The obtained micelles thus release NO selectively under visible light irradiation both in vitro and in vivo (Figure 1C).[60] Besides, the micelles depots of NO can also be generated in situ after phase transition of surfactant molecules capric acid (CA), which instantly cover the NO bubbles generated from NONOate donor and protect NO against attack from hemoglobin (Hb). The entrapped NO passively diffuse through the micellar depots over time, performing a long-lasting therapeutic function (Figure 1D).[61]

Liposomes are spherical vesicles consisting an aqueous core surrounded by synthetic or natural phospholipid bilayers, with an overall structure mimicking the natural cell membranes.[62] They can either accumulate the hydrophobic donors inside the bilayer interface or encapsulating the hydrophilic donors in the hydrophilic core. Their main function also is to ensure a slow NO donor decomposition and consequently a prolonged NO release.[63] In addition, the compactness of the lipid chains upon liposome formation can also be tuned to regulate the water permeability of the lipid bilayer and further the NO-release kinetics of the loaded NO donors (Figure 1H).[64]

Dendrimers are globular macromolecules with a central core surrounded by a hyperbranched mantle and a highly branched corona with reactive surface groups.[65] They can be synthesized via a divergent (dendrimers are synthesized outward from a central core) method or the convergent (dendrimers are synthesized inward from the surface group toward the core) approach. Their accessible functional groups at the periphery allow a multiple functionalization of the structure, and they are an attractive tool for NO delivery owing to their high NO payload by functionalizing NO-releasing motifs on their hyperbranched side chains (Figure 1E).[66] For instance, hyperbranched polyamidoamines can be functionalized with NONOate donors achieving a wide range of NO storage capacities (~ 1-2.50 μmol/mg) and NO-release kinetics ($t_{1/2}$ ~ 30-80 min) (Figure 1F).[67] When the dendritic polyamidoamine is grafted on the surface of a nanoparticle core coated with polydopamine (PDA), which is an effective photoconversion agent, controllable NO release property under intermittent 808 nm laser irradiation can be obtained (Figure 1G).[68]

A wide range of natural and synthetic polymers also have been utilized for NO delivery applications. NO-releasing agents are either covalently linked with polymeric chains or physically encapsulated into polymers. Natural polymers, such as chitosan, dextran, hyaluronic acid, gelatin, and alginate are attractive as NO donor scaffolds due to their biodegradability, biocompatibility, and ease of gelation.[69–73] Cyclodextrins (CDs) with a hydrophobic central cavity and hydrophilic exterior have also been developed as tunable NO-releasing agents.[74–76] Jin et al. reported the synthesis of NONOate functionalized β-CD derivatives as NO-releasing biopolymers with variable NO payloads and highly tunable NO-release kinetics (Figure 1I).[75] Several biodegradable synthetic polymers have also been reported for the encapsulation of NO-releasing small molecules. Poly (lactic-co-glycolic acid) (PLGA) is a Food and Drug Administration (FDA) approved drug carrier owing to its excellent biocompatibility. NO-releasing PLGA nanoparticles can be prepared as a core-shell structure, consisting of hydrophilic NO donors in an aqueous core and a hydrophobic PLGA shell (Figure 1K and L).[77–80] When load the light-responsive NO donor, N,N '-di-sec-Butyl-N,N '-dinitroso-1,4-phenylenediamine (BNN6) into the PLGA nanoparticles, the resultant nanoformula exhibits stimuli-responsive decomposition of BNN6 for NO gas release upon ultraviolet-visible irradiation (Figure 1J).[81]

Silica nanoparticles and mesoporous silica nanoparticles (MSNs) have been widely used for storage and controlled release of NO due to their straightforward synthesis that enables tunable porous structures and tailorable surface functionalities. Various NO donors has been encapsulated into the mesoporous silica nanoparticles for controlled or responsive release of NO (Figure 2A and B).[82–87] Besides, the nitrosation of thiol containing silica nanoparticles synthesized by classical Stöber method facilitates the NO release durations exceed 48 h.[88] In addition, after the branched polyethylene imine (BPEI) polymer, which is rich in amine group, is self-assembled onto silica nanoparticles using electrostatic interactions, NONOate donors can be generated on the surface of silica nanoparticles via a high-pressure reaction with NO (Figure 2C).[89]

Recently, zeolites and metal-organic frameworks (MOFs) have garnered attention for their potential in NO storage and release applications.[90,91] Owing to their intriguing porous architecture, these materials possess high loading

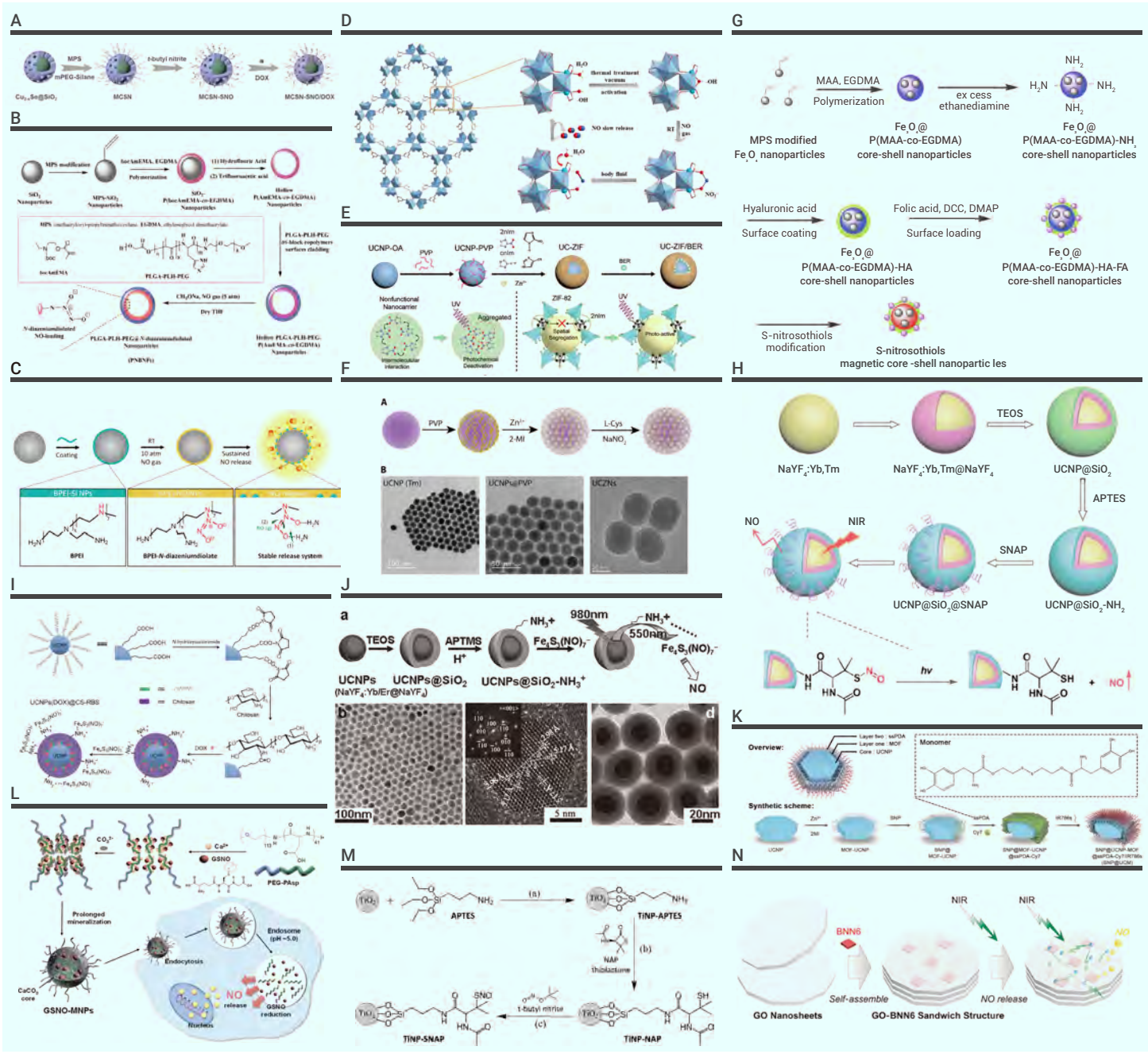

Figure 2. Inorganic vectors for NO delivery platforms (A) Schematic illustration of the synthetic procedure of MCSN-SNO/DOX. Reprinted with permission from Huang et al.[84] Copyright 2021 Elsevier. (B) Schematic diagrams of the synthetic route of the PNBNPs. Reprinted with permission from Liu et al.[87] Copyright 2021 The Royal Society of Chemistry. (C) Schematic illustration of the preparation of BPEI-functionalized NO NPs and mechanism of sustained NO release from NPs. Reprinted with permission from Jeong et al.[89] Copyright 2018 American Chemical Society. (D) MIP-177 microporosity and binding/release mechanism: viewed along the c-axis (left), adsorption and controlled release cycle of NO under the tested conditions (right) is shown. Reprinted with permission from Pinto et al.[94] Copyright 2020 Wiley-VCH. (E) Schematic illustration of the synthetic procedure of UC-ZIF/BER NPs. Reprinted with permission from Chu et al.[95] Copyright 2021 Wiley-VCH GmbH. (F) Synthesis and characterization of UCZN. Reprinted with permission from Jiang et al.[97] Copyright 2020 American Association for the Advancement of Science. (G) The synthetic route of the magnetic S-nitrosothiols core-shell nanoparticles. Reprinted with permission from Liu et al.[100] Copyright 2019 Elsevier. (H) The synthetic route of multilayered UCNP@SiO_2@SNAP nanoparticles and the chemistry of NIR-triggered release of NO by 980 nm laser. Reprinted with permission from Li et al.[103] Copyright 2017 Wiley-VCH. (I) Schematic synthesis procedure of UCNPs(DOX)@CS-RBS. Reprinted with permission from Tan et al.[104] Copyright 2017 Elsevier. (J) Scheme for the synthesis of the UPNCs@SiO_2 nanostructures and for NIR light triggered photochemical NO release. Reprinted with permission from Garcia et al.[107] Copyright 2012 Wiley-VCH. (K) Synthesis and characterization of SNP@UCM nanogenerators. Reprinted with permission from Yang et al.[108] Copyright 2021 Wiley-VCH. (L) Schematic illustration for block copolymer-templated fabrication of GSNO-loaded $CaCO_3$-mineralized nanoparticles and intracellular NO release. Reprinted with permission from Lee et al.[110] Copyright 2016 Elsevier. (M) Synthesis route of TiNP–APTES, TiNP–NAP, and TiNP–SNAP. Reprinted with permission from Massoumi et al.[111] Copyright 2022 American Chemical Society. (N) Self-assembly and NIR-responsive mechanism of the GOBNN6 sandwich structure, which was assembled by GO nanosheets and BNN6 molecules through π–π stacking. Reprinted with permission from Fan et al.[112] Copyright 2015 The Royal Society of Chemistry.

capacity to either NO gas molecules or NO donors, exhibiting remarkable stability for NO storage and controlled release (Figure 2D and E).[92–96] As an important subclass of MOF, zeolitic imidazolate framework 8 (ZIF-8), which is self-assembled from Zn^{2+} ion and 2-methylimidazolate, have attracted much attention for NO delivery duo to its simple and convenient synthesis protocol (Figure 2F).[97,98]

Metal nanoparticles, such as gold nanoparticles and iron oxide nanoparticles, and upconversion nanoparticles, serve as a versatile platform for gas delivery due to their unique physical, magnetic, optical, and electronic properties. Superparamagnetic iron oxide nanoparticles with NO release capability have been developed (Figure 2G).[99–101] Upconversion nanoparticles (UCNPs) efficiently harvest incident near-infrared (NIR) photons and upconvert them

into higher energy UV–vis photons, which sensitize NO precursors for NO release (Figure 2H-J).[102–107] NIR-light-driven NO release nanoplatform have been fabricated through coating an upconversion nanoparticle with a MOF layer loaded with SNP (Figure 2K).[108,109] Other inorganic nanoparticles, such as calcium carbonate ($CaCO_3$) (Figure 2L),[110] titanium dioxide (TiO_2) nanoparticles (Figure 2M),[111] graphene oxide (GO) nanosheets (Figure 2N),[112] and Prussian blue (m-PB) nanoparticles [113] have also been utilized as donors delivery platforms for NO delivery.

Although donors have been loaded to various platforms for NO delivery, there still exists a change for sustained NO release due to the finite donor payload. Therefore, alternative approaches have been proposed to catalyze endogenous NO prodrugs, such as GSNO, CysNO, and AlbSNO, for in situ and prolonged NO generation.[50] One of the well-known catalytic approaches is that Cu^{2+} effectively catalyze RSNOs to continuously generate nitric oxide (NO). Then it is loaded into various scaffolds through coordination effect,[114–116] directly doped into ZIF-8 nanoparticles [117] or SiO_2 nanoparticels.[118] In addition, ceria nanoparticles,[119] zinc oxide nanoparticles [120] and Se-contained enzyme mimics [121] have also been developed to initiate the release of NO from endogenous NO donors especially GSNO.

CO releasing molecules and CO delivery platforms

Carbon Monoxide Releasing Molecules (CORM). Controlled delivery of CO using CORMs as pharmaceutical agents represents an attractive and promising alternative to the administration of gaseous CO as an inhaled gas. Motterlini et al. pioneered the development of CORMs with identification of transition-metal carbonyl complexes ($Fe(CO)_5$, $Mn_2(CO)_{10}$ (CORM-1), and $[RuCl_2(CO)_3]_2$ (CORM-2)).[122] The limitation of CORM-2 with the poor solubility in water and short CO releasing half-life promotes the emergence of water-soluble CORMs, such as [Ru(Cl) $(CO)_3$(glycinate)] (CORM-3). These transition metal complexes are susceptible to ligand exchange in biological environments, resulting in CO leakage and the formation of protein adducts.[123] The commercially available CORM-2 and CORM-3 are the most frequently utilized CORMs to examine physiological functions of CO both in vitro and in vivo (Figure 3A).[124] Besides solvent-induced CORMs, photoCORMs which are stable in dark in aqueous solution while release CO at an appropriate wavelength upon photoactivation are also developed taking advantage of the inherent photolytic feature of CORMs.[125] PhotoCORMs allow for a spatial and temporal control in the CO delivery.[14,126] However, the release of CO from these photoresponsive metal carbonyls typically requires the irradiation of light in near-UV regions, which is not suitable for biomedical applications due to the poor tissue and inherent phototoxicity. Therefore, several metal-free photoCORMs have been developed, including 3-hydroxyflavone (3-HF) derivatives, xanthene-9-carboxylic acid, BODIPY derivatives, and unsaturated diketone derivatives, among others.[127] Notably, some of these photoCORMs can be selectively activated to release CO under visible and even NIR light, offering significant benefits for biomedical applications.[128] In recent decades, the development of CORMs has progressed considerably, resulting in an extensive library of compounds that can be categorized based on the mode of CO release activation. These categories include enzyme-triggered CORMs (ET-CORMs), thermal-triggered CORMs, oxidation-triggered CORMs, pH-triggered CORMs, etc.[14] This diverse range of activation methods has expanded the potential applications of CORMs in various biomedical contexts.

CO delivery platforms. CORMs have been chemically conjugated or physically encapsulated into various carriers to improve the delivery efficiency of CO.[129] Advantages of this strategy include 1) stabilization of the CORMs after CO release; 2) modulation of CO-releasing profiles; 3) improvement in solubility and stability of CORMs; 4) higher CO payloads; 5) targeted delivery to specific sites. The carriers can be categorized into organic macromolecules (e.g. peptides, proteins, polymers, and micelles) and inorganic nanoparticles (e.g. silica nanoparticles, Prussian blue nanoparticles, graphene-oxide nanoparticles, upconversion nanoparticles, and MOFs). Another potential remedy for CO delivery is based on endogenous substance or metabolic pathway, fully independent of delivery of CORMs. For example, photocatalytic nanomaterial can be delivered to act as a catalyst to convert endogenous substance into CO under the precise control of body penetrable 630 nm light.[130]

Similar with the carrier for NO delivery, polymeric micelles are a very promising carrier due to their high drug-loading capacity, easy formulation, and low toxicity. CO-releasing micelles have been prepared from triblock copolymers composed of a hydrophilic poly(ethylene glycol) block, a poly($Ru(CO)_3Cl$(ornithinate acrylamide) block capable of releasing CO, and a hydrophobic poly(n-butylacrylamide) block (Figure 3B).[131] In addition, copolymers consisting of hydrophilic endothelial cells-adhesive peptides covalently linked with hydrophobic polyhedral oligomeric silsesquioxane self-assemble into micelles allowing the high payload of CORM and controlled release of CO.[132] Moreover, a copolymer consisting a NO-releasing N-nitrosamine moiety and the CO-releasing 3-hydroxyflavone (3-HF) antenna self-assemble into spherical micelles that releases NO and CO simultaneously under visible light irradiation (Figure 3C).[133]

Peptide amphiphiles (PAs) have been extensively studied over the past three decades for biomedical application. They can self-assemble into various well-ordered nanostructures such as micelles, vesicles, and nanofibers.[134] It consists of a hydrophilic peptide sequence covalently bound to a hydrophobic alkyl tail, which provides driving force for self-assembly. After covalently attached with water-soluble CORM-3, the PA self-assembles to be nanofiber hydrogel that release CO with the half-life more than eight-fold longer than that of bare CORM-3. This can be ascribed to the slow water–gas ligand exchange of CORM-3 located onto the entangled nanofibril.[135] In addition, the self-assembly of the CORM-attached peptides with a gel-forming diphenylalanine-derivative gives rise to a syringe-injectable hydrogel exhibiting prolonged CO-releasing properties (Figure 3D).[136] The PA can also self-assemble into stable nanoparticles in aqueous solutions when using fluorinated amphiphilic dendritic peptide. The nanoparticles provide ample hydrophobic cores for the simultaneous physical encapsulation of photosensitizer Ce6 and H_2O_2-sensitive CORM, thus developing a photodynamic therapy (PDT)-driven CO-controlled delivery system. When irradiated with NIR light, CORM is oxidized by H_2O_2 generated during the PDT process to release CO (Figure 3E and F).[137,138]

Protein assemblies are a class of highly organized biomolecules that hold promise for development of a new gas delivery platform. One of the general methods involves encapsulation of CORMs within the protein scaffold. Protein crystals represent precise protein assemblies in the solid state with inner pores that suitable for use as nanovessels to immobilize CORMs.[139] Protein cages composed of multimeric protein assemblies have been used for development of biomaterials. Protein ferritin has been engineered to encapsulate CORM, providing a release rate that is 18-fold slower and uptake ratio that is 4-fold greater than those of CORM-3 (Figure 3G).[140]

The water insoluble and photoactive CROM-1 has also been non-covalently embedded into nanoporous poly(L-lactide-co-D/L-lactide) fibers via electrospinning to enable bioavailability and water accessibility of CORM-1.[141] CORM and glucose oxidase (GOx) are encapsulated in the biodegradable polymer PLGA, which is further covered with the red blood cell (RBC) membrane to obtain RBC membrane-biomimetic gas nanofactory.[142] In the presence of O_2, the GOx in the nanofactory effectively catalyze the conversion of endogenous glucose to H_2O_2, which further trigger CO release from CORM. In another study, photoCORM has also been embedded in polycaprolactone together with a triplet photosensitizer to fabricate nonwoven polymer fabrics using electrospinning. Under near-UV irradiation, energy transfer occurs from triplet excited-state photosensitizer to photoCORM and thus trigger the release of CO.[143]

A new strategy to prepare CO-releasing polymeric nanoparticles has been reported through phenylboronic acid-catechol complexation. The phenylboronic acid form cyclic boronate esters with compounds having cis diol groups and have especially high affinity toward catechol-containing compounds. So a catechol-bearing analogue of CORM-3 is synthesized and loaded to the nanoparticles by simply mixing them together at physiological pH. The resultant nanoparticles are stable in fetal bovine serum while release CO in the presence of cysteine (Figure 3H).[144] In addition, coordination assembled strategy has been proposed to fabricate Cu(II)-flavone coordination polymer (NCu-FleCP) CO nanoprodrug, which is stable in normal physiological conditions, and yet readily reduces to small size prodrug complex and releases CO on demand under glutathione (GSH) and NIR light (Figure 3I).[145]

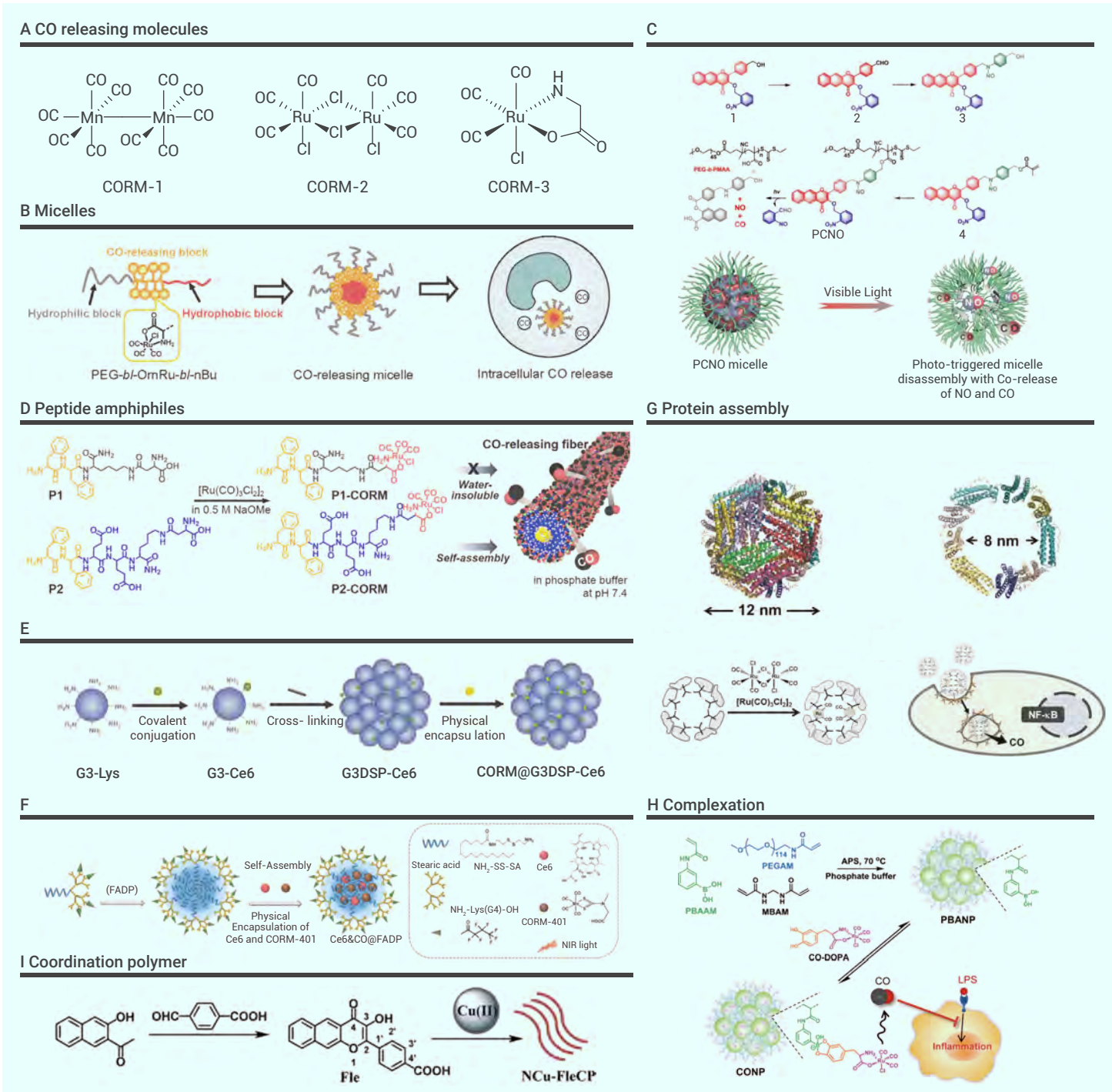

Figure 3. CO releasing molecules and their organic vectors (A) Chemical structures of CORMs. (B) Schematic illustration of micelle formation of PEG-b-OrnRu-b-nBu triblock copolymer and CO release after cellular uptake. Reprinted with permission from Hasegawa et al.[131] Copyright 2010 American Chemical Society. (C) Synthetic routes showing the covalent grafting of NO-releasing N-nitrosamine residue onto the CO-releasing extended 3-hydroxyflavone (3-HF) moiety and corresponding PCNO diblock copolymers. Reprinted with permission from Gao et al.[133] Copyright 2021 Wiley-VCH. (D) Molecular structures and synthesis of P1-CORM and P2-CORM from P1 and P2, respectively. Only P2-CORM self-assembles into a fibrillar structure that releases CO in phosphate buffer at pH 7.4. Reprinted with permission from Kim et al.[136] Copyright 2018 Wiley-VCH. (E) Schematic illustration for the design and application of CORM@G3DSP-Ce6 for controlled release of CO. Reprinted with permission from Wu et al.[137] Copyright 2018 Wiley-VCH. (F) Schematic illustration for the preparation of Ce6&CO@FADP. Reprinted with permission from Ma et al.[138] Copyright 2020 American Chemical Society. (G) CO releasing protein cage for induction of intracellular signaling. Reprinted with permission from Fujita et al.[140] Copyright 2014 American Chemical Society. (H) Synthesis of CO-releasing nanoparticles (CONPs) and their anti-inflammatory activity. Reprinted with permission from Van der Vlies et al.[144] Copyright 2016 American Chemical Society. (I) The preparation of NCu-FleCP. Reprinted with permission from Sun et al.[145] Copyright 2020 Wiley-VCH.

Inorganic nanomaterials have been proven an attractive platform for CO delivery, owing to their physiological stability and unique optical, electronic, and magnetic field response properties, which enable them to response to special stimuli to achieve CO release in an on-demand manner.

Solid SiO_2 nanoparticles and MSN have been wildly used as carriers for CORMs to fabricate CO-releasing materials (Figure 4A and B).[146–151] Photo-CORM is conjugated to the surface of the SiO_2 nanoparticles via the click reaction (Figure 4C).[152] Through a coordination linkage reaction between mercapto propyltriphenylphosphonium (TPP-SH) and CORM, a mitochondria-targeted and intramitochondrial microenvironment-responsive prodrug can be synthesized. This positively charged prodrug can be effectively loaded into the negatively charged MSNs through electrostatic assembly. The developed nanoparticles release the FeCO-TPP prodrug through acid-responsive disassembly, and further release of CO is triggered by the intracellular ROS

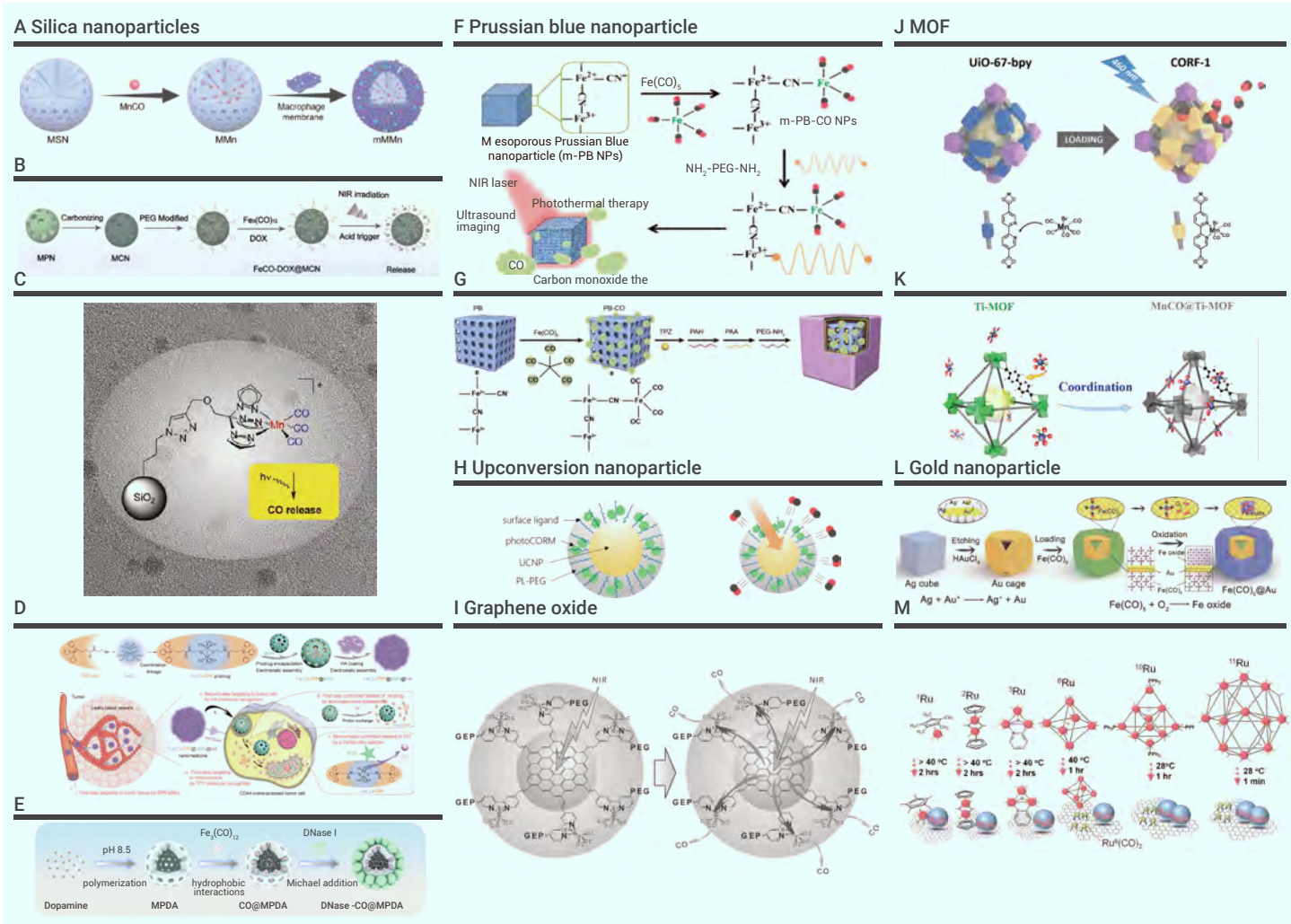

Figure 4. Inorganic vectors of CORMs (A) Schematic illustration of mMMn preparation. Reprinted with permission from Zhang et al.[150] Copyright 2020 Elsevier. (B) Preparation process of FeCO-DOX@MCN nanoparticles. Reprinted with permission from Yao et al.[151] Copyright 2019 Elsevier. (C) Covalent attachment of the $[Mn(CO)_3(tpm\text{-}L1)]^+$ complex to the surface of the (3-Azidoproply)-functionalized SiO_2 nanoparticles. Reprinted with permission from Dördelmann et al.[152] Copyright 2011 American Chemical Society. (D) Schematic illustration of multistage assembly method for construction of the FeCO-TPP@MSN@HA nanomedicine. Reprinted with permission from Meng et al.[153] Copyright 2020 American Association for the Advancement of Science. (E) Schematic illustration for the preparation of DNase–CO@MPDA NPs. Reprinted with permission from Yuan et al.[154] Copyright 2021 Wiley-VCH. (F) The composition of the nanoparticles and their CO release triggered by NIR irradiation. Reprinted with permission from Li et al.[157] Copyright 2016 American Chemical Society. (G) Schematic illustration of PPPPB-CO-TPZ NPs with enhanced bioreductive chemotherapy and CO-mediated pro-apoptotic gas therapy. Reprinted with permission from Li et al.[159] Copyright 2019 Elsevier. (H) Schematic illustration of a water-soluble nanocarrier used for CO uncaging. Upon 980 nm irradiation light (red arrow), the up-converted visible range emission from the UCNP gets re-absorbed by the photoCORM, leading to CO release. Reprinted with permission from Pierri et al.[161] Copyright 2015 The Royal Society of Chemistry. (I) Preparation of $Fe(CO)_5$@Au. Under aerobic conditions, the excess $Fe(CO)_5$ in solution is oxidized on the surface of the Au nanocage to form an iron oxide shell. Reprinted with permission from Wang et al.[163] Copyright 2020 American Chemical Society. (J) Schematic showing the loading of $MnBr(bpy)(CO)_3$ on UiO-67bpy to synthesize CORF-1, and the subsequent CO release upon light irradiation. Reprinted with permission from Diring et al.[165] Copyright 2017 The Royal Society of Chemistry. (K) Schematic representation of the coordination strategy for the construction of the MnCO@Ti-MOF. Reprinted with permission from Jin et al.[168] Copyright 2018 Wiley-VCH. (L) Molecular structure and NIR-responsive CO release mechanism of CORM loaded graphene oxide. Reprinted with permission from He et al.[169] Copyright 2015 Wiley-VCH. (M) Structures and reactivity of the various nuclearities of Ru–CO clusters on GO. Green stick represents carbon monoxide. Reprinted with permission from Tan et al.[170] Copyright 2018 Wiley-VCH.

(Figure 4D).[153]

Mesoporous polydopamine (MPDA) nanoparticles have also been utilized to delivery CORM because of their intrinsic biocompatibility, strong NIR photothermal conversion efficiency, and facile surface functionalization. Thermosensitive CORM is encapsulated into MPDA nanoparticles through hydrophobic interactions. Therefore, CO release can be triggered by the NIR irradiation (Figure 4E).[154,155]

Prussian blue (PB) nanoparticle is a novel and potential drug delivery system due to their favorable biocompatibility, porous and surface-modifiable features, as well as various unique properties, such as adsorbability, photoacoustic and magnetic resonance imaging ability, photothermal effects, and nanoenzyme activities.[156] PB has the structural composition composed of an Fe^{3+}–N≡C–Fe^{2+} unit that has endowed PB as an ideal candidate to process derivatization with iron carbonyl. The exposure of the cyano group $-CN^-$ acts as the active sites for the coordination of iron carbonyl. Taking advantage of the photothermal effects of PB, the photon-to-heat conversion upon exposure of NIR light is anticipated to cleave the Fe-CO coordinating bond, releasing CO from the PB nanoparticles (Figure 4F and G).[157–159]

Another mesoporous nanoplatform is constructed with hollow CuS nanoparticles carrying CORM. This CO delivery nanoplatform reveals superior properties in colloidal stability, photothermal conversion, H_2O_2/NIR-stimulated CO release and tumoral accumulation.[160]

Lanthanide ion doped upconversion NPs (UCNPs) have a specific optical characteristic that makes them absorb light in the NIR range and enables different ranges of UV-vis-NIR light emissions. A water-soluble NIR inducible CO delivery system is prepared by encapsulating the UCNPs with amphiphilic polymer, which incorporates a hydrophobic interior containing the photoCORM. Irradiation of this system with NIR light could induce the UCNPs core to emit visible range photons, which are then absorbed by the loaded photoCORM and ultimately results in photochemical uncaging of CO (Figure 4H).[161]

Gold nanoparticles exploit their unique chemical and physical properties for transporting and unloading the pharmaceuticals.[162] Au nanocage is utilized to

encapsulate the iron pentacarbonyl ($Fe(CO)_5$) under an oxygen-free atmosphere. $Fe(CO)_5$ in solution is oxidized to iron oxide on the surface of the Au nanocage under aerobic conditions, obtaining the nanoplatform with a core-shell structure. The formation of an iron oxide shell efficiently prevents the leakage and oxidation of caged $Fe(CO)_5$ and increases the stability and biocompatibility of $Fe(CO)_5$@Au. Under NIR irradiation, the photothermal effect of Au nanocages causes the decomposition of caged $Fe(CO)_5$, releasing CO gas and iron ions (Figure 4I).[163]

MOFs are receiving considerable attention for CO delivery due to their high payloads and simple synthesis protocol. The one-pot synthesis-encapsulation strategy has been proposed using hierarchical metal organic framework as a host of the photoCORM (Figure 4J).[164–166] Aluminum-based MOFs prepared by means of the coordination modulation method are synthesized to adsorb the photoCORM. The hybrid system retains the photoactive properties of the pristine CORM in both phosphate saline solution and solid state.[167] Besides, Ti-based MOF has also been utilized to realize an H_2O_2-triggered CO release and real-time CO release monitoring by fluorescence imaging (Figure 4K).[168]

GO has been noted for its favorable properties of high NIR photothermal conversion efficiency. A NIR-responsive nanomedicine for controlled CO release has been constructed through binding CORMs into GO nanosheets. The nanomedicine could collect and convert NIR light energy to break the bonds of CORM resulting in CO release (Figure 4L).[169] The NIR-responsive CO-release platform can also be developed by utilizing the size-dependent adsorption properties of CORM onto GO (Figure 4M).[170]

H_2S donors and H_2S delivery platforms

H_2S donors. Sodium hydrosulfide (NaHS) and sodium sulfide (Na_2S) are the most prevalent H_2S donors utilized in earlier biological research for elucidating endogenous roles and therapeutic prospects of H_2S. However, upon dissolution in water, they undergo immediate hydrolysis and spontaneously release H_2S, initially reaching supraphysiological levels before gradually declining due to H_2S gas volatilization. This makes it challenging to delivery H_2S that matches the slower, continuous, enzymatic production characteristic of endogenous H_2S synthesis. Plenty studies have reported even opposite biological effects of H_2S when utilizing sulfide salts and slow-releasing donors.[35] Unlike NaHS and Na_2S, other insoluble sulfide salts, such as ZnS,[171] FeS,[172,173] MnS,[174] and MoS_2,[175] generate H_2S under the attack of H^+ in acidic conditions (Figure 5A). For biomedical applications, these sulfide salts have been synthesized as nanoparticles for durable and targeted delivery of H_2S.

Hydrolysis-activated H_2S donors can spontaneously release H_2S in aqueous solutions (Figure 5B). Lawesson's reagent and its derivatives are phosphorodithioate-containing H_2S donors that exhibit slow-release properties.[176] Various Lawesson's reagents are commercially available, making them popular choices for studying H_2S physiology. Among these, GYY4137 is the most well-known and has been widely used in studies investigating the physiological effects of H_2S.[177] Another type of phosphorodithioate-containing H_2S donor is the JK donor, which possesses a unique acidic pH-accelerated H_2S releasing behavior.[178] Additionally, 1,2-dithiole-3-thiones (DTTs) are another class of compounds commonly considered to be in the family of hydrolysis-triggered H_2S donors.

Natural occurring polysulfides, such as diallyl disulfide (DADS) and diallyl trisulfide (DATS) isolated from garlic and other alliums, provide a source of sulfane sulfur that can be converted into H_2S upon reduction. Nucleophilic attack by GSH or other thiols on the polysulfides gives rise to release of H_2S.[179] Inspired by disulfide exchange chemistry, chemists have also developed various synthetic donors that are activated by nucleophilic attack by endogenous thiols, including N-(benzoylthio)benzamides, S-aroylthiooximes (SATOs), arylthioamides (ArC(S)–NH_2), and acyl perthiols. These donors are particularly suitable for controlled delivery of H_2S to the pathologically redox microenvironments (Figure 5C).[180]

As enzymes often exhibit substrate specificity and tissue localization, utilizing enzymes as triggers for H_2S release enables specific targeting to a tissue of interest (Figure 5D). For example, enzyme-activated H_2S donors hold great promise for targeted H_2S delivery to enzyme-overexpressed microenvironments of lesions. Design of enzyme-activated donors involve the incorporate an enzymatically cleaved trigger on a sulfide donor, which remains stable until the activating group is cleaved or modified by the target enzyme, subsequently releasing H_2S. A typical example is the H_2S donor containing a trimethyl lock group exhibit esterase-activated characteristics. In this system, esterase-mediated cleavage of an acyl-protecting group on the donor motif generates an unstable phenolic intermediate, which then undergoes intramolecular lactonization with a pendant thioacid to release H_2S.[181] Another example combines the concepts of enzyme-specific cleavable functionalities with the protected geminal dithiol as an H_2S releasing moiety.[182]

Light-triggered H_2S donors enable spatiotemporal control over H_2S release, allowing for noninvasive activation of H_2S release on skin or at shallow subcutaneous levels (Figure 5E). These donors typically contain photocaged species that, when exposed to the appropriate wavelength of light, cleave the protecting group and reveal the H_2S-releasing moiety. Examples include o-nitrobenzyl caged geminal dithiols and ketoprofenate caged H_2S donors, which release H_2S under ultraviolet (UV) light.[183,184] α-Thioetherketones are UV light-activated prodrugs of thioaldehydes, which subsequently release H_2S in the presence of amines.[185] Furthermore, p-hydroxyphenacyl photocaged H_2S donors respond to visible light to release H_2S.[186] Most current H_2S donors are activated by UV or visible light with limited tissue penetration depth. Developing NIR light-triggered donors, which can penetrate tissues more deeply, remains an area for further exploration.

Carbonyl sulfide (COS) can be rapidly hydrolyzed to H_2S by the ubiquitous enzyme carbonic anhydrase (CA). Therefore, a recent innovation in H_2S donor design is the synthesis of compounds that release COS (Figure 5F). The ring-opening polymerization of N-thiocarboxyanhydrides (NTA) by biological nucleophiles such as glycine is utilized to generate COS with peptides as byproducts.[187] Another class of COS-releasing prodrugs relies on a self-immolative reaction mechanism, in which COS release results from the decomposition of a thiocarbamate-containing compound in the presence of a specific trigger.[188] As a result, COS-based H_2S donors triggered by various stimuli, such as biothiols, enzymes, light, and reactive oxygen species (ROS), have emerged as versatile releasing templates.[34]

H_2S delivery platforms. Though lots of H_2S donors have been developed, they are usually unable to meet the requirements of in vivo applications, such as the poor stability, low solubility, short release duration, lack of target specificity, and the potential cytotoxicity. Therefore, various H_2S delivery platforms have been developed. Similar to NO and CO, H_2S donors can also be encapsulated or conjugated into various macromolecules, such as polymer conjugates, micelles, hydrogels and nanofibers, for controlled, targeted, and/or responsive delivery of H_2S.

Acid-sensitive H_2S donors, such as dithiocarbamate (DTC) and JK-1, have been encapsulated into the self-assembled micelle (Figure 5G),[189] sodium alginate (SA) dressing (Figure 5H),[190] collagen hydrogel,[191] hyaluronic acid (HA) hydrogel,[192] and electrospinning PCL fiber.[193] Additionally, thiol-initiated polysulfide-based donors are also loaded into PLGA microparticles (Figure 5I),[194] protein nanoemulsion formed by bovine serum albumin (BSA) (Figure 5J),[195,196] and nanoparticles formed by amphiphilic block polymers.[197,198] The release of H_2S is triggered by the intracellular GSH. The hydrophobic H_2S donor anethole dithiolethione (ADT) can also be doped in the phospholipid shell of liposomes. The release of ADT gives rise to large numbers of microsized H_2S bubbles via an enzymatic trigger.[199,200]

The polycaprolactone (PCL) electrospun scaffold is engineered to include azide functional groups with different densities through modular mixing of small amounts of a functional, low-molecular-weight azide-terminated PCL with a high-molecular-weight PCL. Then the surface of scaffold is modified using a straightforward click reaction with an alkynefunctionalized NTA (alkynyl-NTA), after which PCL scaffolds with controllable density of surface-bound, H_2S releasing NTAs are fabricated. These scaffolds showed dose-dependent release of H_2S based on the amount of NTA functionality attached to the surface.[201] In another study, H_2S donor 2-aminopyridine-5-thiocarboxamide is grafted to the partially oxidized alginate, which forming hydrogel through the Schiff base reaction with gelatin.[202]

Besides physical encapsulation, covalently binding of H_2S donor to the polymer scaffold ensures well-defined chemical structure and avoids uncontrolled leakage. A block copolymer consisting of a hydrophilic poly (N-acryloy morpholine) segment and a hydrophobic dithiolethione-bearing segment (PAM-PADT) has been synthesized using reversible addition–fragmentation

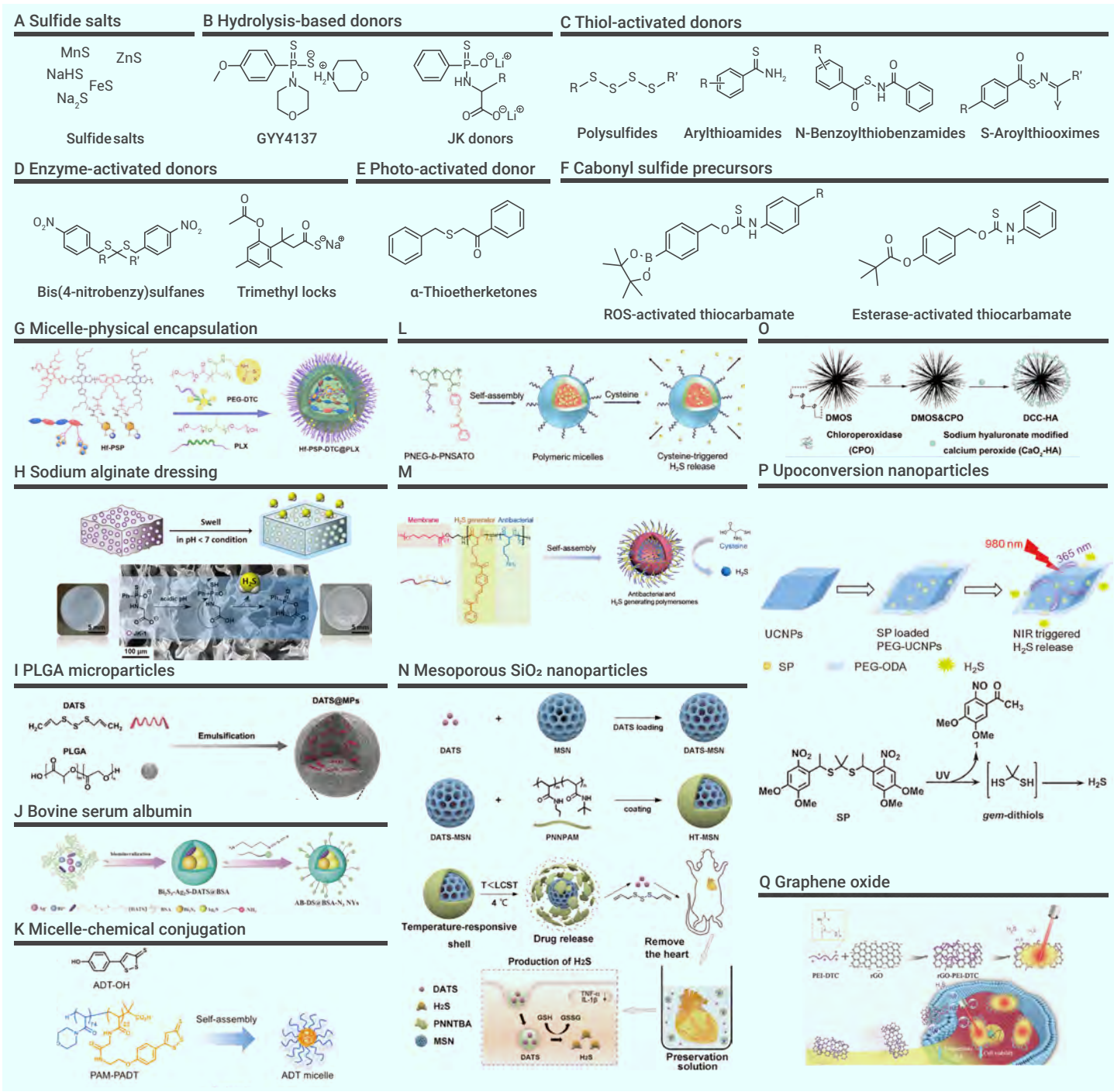

Figure 5. Some H_2S donors and H_2S delivery platforms (A) Chemical structures of sulfides salts. (B) Chemical structures of hydrolysis-based donors. (C) Chemical structures of thiol-activated donors. (D) Chemical structures of enzyme-activated donors. (E) Chemical structure of photo-activated donor. (F) Chemical structures of cabonyl sulfide precursors. (G) Schematic diagram of Hf-PSP-DTC@PLX nanosensitizer preparation. Reprinted with permission from Li et al.[189] Copyright 2022 Wiley-VCH. (H) Diagram illustrating the pH-dependent H_2S releasing SA sponge dressing. Reprinted with permission from Zhao et al.[190] Copyright 2019 Elsevier. (I) Composition/structure of DATS@MPs, which act as an in situ slow-releasing H_2S donor depot. Reprinted with permission from Hsieh et al.[194] Copyright 2019 Elsevier. (J) Schematic illustration of AB-DS@BSA-N_3NYs. Reprinted with permission from Zheng et al.[196] Copyright 2020 The Royal Society of Chemistry. (K) A block copolymer having ADT-groups (PAM-PADT) forms ADT micelles by self-assembly. Reprinted with permission from Takatani-Nakase et al.[203] Copyright 2017 The Royal Society of Chemistry. (L) Self-assemble and cysteine-triggered H_2S release of the PNEG-b-PNSATO polymeric micelles. Reprinted with permission from Le et al.[204] Copyright 2022 Elsevier. (M) PCL_{24}-b-P(Lys_{23}-stat-$SATO_{15}$) copolymer was self-assembled into polymersomes. Reprinted with permission from Liu et al.[205] Copyright 2021 American Chemical Society. (N) Schematic representation of hypothermia triggered H_2S releasing MSN coating and drug release. Reprinted with permission from Xia et al.[208] Copyright 2022 American Chemical Society. (O) Schematic illustration of the synthesis of the DCC-HA NCs. Reprinted with permission from Liu et al.[209] Copyright 2021 Wiley-VCH. (P) Construction of SP-loaded PEG-UCNPs platform for NIRtriggered H_2S release. Reprinted with permission from Chen et al.[212] Copyright 2015 The Royal Society of Chemistry. (Q) Illustration of the synthesis of a rGO–PEI-DTC nanocomposite and its H_2S photothermal release for suppression of cell viability. Reprinted with permission from Li et al.[213] Copyright 2019 The Royal Society of Chemistry.

chain-transfer polymerization. The PAM-PADT polymers self-assembled in water to form spherical micelles with an average hydrodynamic diameter of 34 nm (Figure 5K).[203] Through ring-opening metathesis polymerization, amphiphilic block copolymer consisting of norbornene-mPEG (Nor-mPEG) as a hydrophilic part and norbornene-conjugated SATO moiety (Nor-SATO) as a hydrophobic part is constructed. The block copolymer self-assembles into micelles with a range of sizes from 41 to 57 nm and release H_2S with the peak time of 60–70 min (Figure 5L).[204] In addition, polymersome is fabricated through self-assembly of poly(ε-caprolactone)$_{24}$-block-poly[lysine$_{23}$-stat-(SATO)$_{15}$]. The gradual generation of H_2S is realized by the multilayered poly-

mersome structure. Cysteine first reacts with the outer polymersome surface to produce H_2S, followed by a reaction with the lumen-facing inner surface after penetrating through the polymersome membrane (Figure 5M).[205] The SATO group is also attached to a short peptide. Upon dissolution in aqueous buffer, the peptide self-assembles into nanofibers and forms hydrogel in the presence of calcium. This gel delivered H_2S over the course of several hours in the presence of cysteine.[206]

MSNs are widely used drug delivery platform due to their biocompatibility and mesoporous architecture. Natural occurring H_2S donor DATS can be loaded into MSN (DATS-MSN) to construct an H_2S sustained-release system activated by endogenous GSH.[207] Further coating the DATS-MSN with temperature-sensitive polymer poly(N-n-propylacrylamide-co-Ntert-butyl acrylamide) (PNNTBA) gives rise to hypothermia-triggered hydrogen sulfide (H_2S) releasing particles (Figure 5N).[208]

Dendritic mesoporous silicon nanoparticles (DMSNs), which have larger pore sizes than traditional silicon nanoparticles, have been successfully applied as efficient nanocarriers. To enhance their biodegradability, the physiologically inert -Si-O-Si- frameworks in DMSNs are partially replaced with tetra-sulfide bonds. These tetra-sulfide bonds are sensitive to GSH, triggering the decomposition of the bonds and releasing H_2S. As a result, tetrasulfide bond-incorporating dendritic mesoporous organosilica can be used as a novel H_2S delivery platform (Figure 5O).[209] In addition, MOF is another promising platform for H_2S delivery under physiologically relevant conditions.[210,211]

Most H_2S donors are inherently responsive to UV–vis light and therefore have limited therapeutic utility. UCNPs can absorb long wavelength NIR light and emit narrow and sharp emissions ranging from UV to visible. A NIR light induced H_2S release platform based on UCNPs has been constructed. Under NIR light excitation, UCNPs can emit UV light which triggers H_2S release in a spatial and temporal pattern (Figure 5P).[212]

Reduced graphene oxide (rGO) has an excellent photothermal conversion rate for NIR and is a good carrier for photothermal therapy. H_2S donor DTC can be pyrolyzed to H_2S at high temperature. Therefore, a NIR-photoresponsive H_2S gas generation nanoplatform is developed through the electrostatic adsorption of positively charged DTC and negatively charged rGO. Under irradiation with NIR light, light energy is converted into thermal energy based on the photothermal effect of rGO, and a large amount of H_2S is released due to the thermal degradation of DTC (Figure 5Q).[213]

The ionization of insoluble sulfide salts provides an alternative strategy for sustainable H_2S release. For example, ZnS nanoparticles[171], metastable γ-phase manganese sulfide (MnS) nanoparticles,[174] and two-dimensional layered molybdenum disulfide (MoS_2) nanosheets have been synthesized. The as-prepared nanoparticles can be degraded in response to the mildly acidic tumor microenvironment, releasing H_2S for gas therapy. Furthermore, the ferrous sulfide has also been utilized for pH responsive release of H_2S. It can be embedded into BSA to form amorphous nanoclusters via a self-assembly approach,[172] or synthesized via a one-pot hydrothermal method to form crystalline nanoparticles.[173] Both of them release H_2S in acid conditions under physiological pH = 6.5 and pH = 5.5.

APPLICATION IN TREATING BONE DISEASES

Anti-infection

Infections related to orthopedic implants are a common and serious issue after orthopedic surgery, involving components such as prosthetic joints, fixation systems, artificial ligaments, and bone cements.[214] Typically caused by Staphylococcus aureus and other pathogens, orthopedic implant infections often stem from biofilms, where bacterial clusters tightly bind to the material surface and become encased in an abundant extracellular polymeric substance matrix.[215] To prevent infection, it is essential to avoid bacterial adhesion and biofilm formation by endowing orthopedic implants with the antibacterial ability. Antibacterial gas therapy has attracted much attention not only because they are endogenous signaling molecules, but also due to their critical roles in many pathological processes. These gases have also been utilized as potent bactericidal agents to kill bacteria, disperse biofilms, and prevent implant-associate infection while avoiding resistance.[216]

NO. NO demonstrates potent antibacterial activity against a wide range of bacteria, including both Gram-positive and Gram-negative species, as well as methicillin-resistant Staphylococcus aureus (MRSA). At low concentrations, NO can inhibit biofilm formation or break down existing biofilms, while at higher concentrations, it exhibits bactericidal properties. When NO is present at high concentrations (typically in the mM range), it reacts with the superoxide free radical (O^{2-}) to generate reactive species such as nitrogen dioxide (NO_2), dinitrogen trioxide (N_2O_3), and peroxynitrite ($ONOO^-$). These reactive species induce significant nitrosative and oxidative stress on bacteria, resulting in the disruption of bacterial membranes and impairment of cell function.

Although NO is clearly identified as a potent antimicrobial, its clinical utility is challenging as NO is a highly reactive gas with a short half-life. Therefore, NO releasing coatings have been fabricated on orthopedic implants to endow the implant with antibacterial ability. Joshua. et al. synthesized aminosilane-based xerogel films capable of storing large payloads of NO. NO releasing xerogel coatings can reduce bacterial colonization of external fixation pins up to 48 days post-implantation, despite the fact that the xerogel coatings have released the majority of their NO during the initial five days.[217]

Wang et al. proposed a magneto-based synergetic therapy to destruct biofilm on the orthopedic implants. Firstly, the fabricated magnetic nanoparticles generate sufficient thermal effect to cause dense biofilm dispersal under an alternating magnetic field. Loosened biofilms allow the penetration of magnetic nanoparticles, which are also coated with thermosensitive RSNO. The RSNO further release NO inside the biofilm, thus efficiently killing sessile bacteria under the magnetothermal effect of nanoparticles. As a result, the synthesized nanoparticles are able to disrupt the dense 3D biofilm structure, presenting the promising potential for the effective and durable control and elimination of implant-associated infections (Figure 6A).[218]

Yuan et al. reported a NIR light responsive hydrogel coating with NO plus superoxide ($\bullet O_2^-$) release ability. The Ti substrate is firstly coated with red phosphorus (RP) nanofilm, which produce $\bullet O_2^-$ under the irradiation of NIR. Then the substrate is modified with a hydrophilic and adhering hydrogel coating consisting of chitosan (CS), polydopamine (PDA) and NO release donor RSNO. Under the irradiation of NIR, peroxynitrite ($\bullet ONOO^-$) can be formed by the reaction between the released NO and $\bullet O_2^-$ produced by the RP nanofilm. The generated $\bullet ONOO^-$ is proven to effectively eradicate biofilm formed by methicillin-resistant Staphylococcus aureus (MRSA). Additionally, osteogenic differentiation is promoted and inflammatory polarization is regulated by the released NO without NIR irradiation through upregulating the expression of OPN and OCN genes and TNF-α. The in vivo results also confirms excellent osteogenesis and biofilm eradication by released NO under NIR irradiation (Figure 6B).[219]

Li et al. developed an efficient NO-releasing coating via functionalization of Ti with aminosilanes and the subsequent tethering of NONOates onto the silanes. They utilized the osseointegrative promoting silane containing a secondary amine (6-aminohexyl-3-aminopropyltrimethoxysilane (AHAP3)). The silane modified Ti substrates are then exposed to high pressures of NO (5 bar) over 72 h to allow formation of NONOate. At pH 4, AHAP3 modified surfaces released NO at a maximum instantaneous NO release concentration of 1.8 μM/s with 1005.4 μM NO being released in a burst during the first hour. The modified surface demonstrates a reduction in S. aureus and P. aeruginosa adhered to the surface. Of particular interest is that the modified surface is capable of prevention of biofilm formation while not displaying cytotoxicity toward human primary osteoblast cells (Figure 6C).[220]

A multifunctional coating which can be triggered by near-infrared II (NIR-II) light to achieve bone tumor treatment, anti-biofilm formation, as well as osseointegration simultaneously is designed and fabricated on Ti implants. The ytterbium (Yb) and erbium (Er) doped TiO_2 nano-shovel arrays are formed on the Ti implants by hydrothermal treatment. Incorporation of Yb and Er enhances the upconversion capability, thereby facilitating generation of reactive oxygen species (ROS) during exposure to NIR-II light. Quercetin (Qr) is immobilized covalently on the surface of the TiO_2 nano-shovel with organosilane as the coupling reagent, while the positively charged L-arginine adsorb electrostatically onto the negatively charged Qr. L-arginine can be catalyzed by ROS to release NO. In vitro and in vivo experiments indicate that the combined actions of ROS, Qr, and NO eliminate Staphylococcus aureus biofilms on the Ti implants at a mild temperature of 45 °C upon illumination with a 1,060 nm laser. Moreover, this surface promotes angiogenesis and osteogenic differentiation, reduces inflammation, and accelerates formation of new bone tissues (Figure 6D).[221]

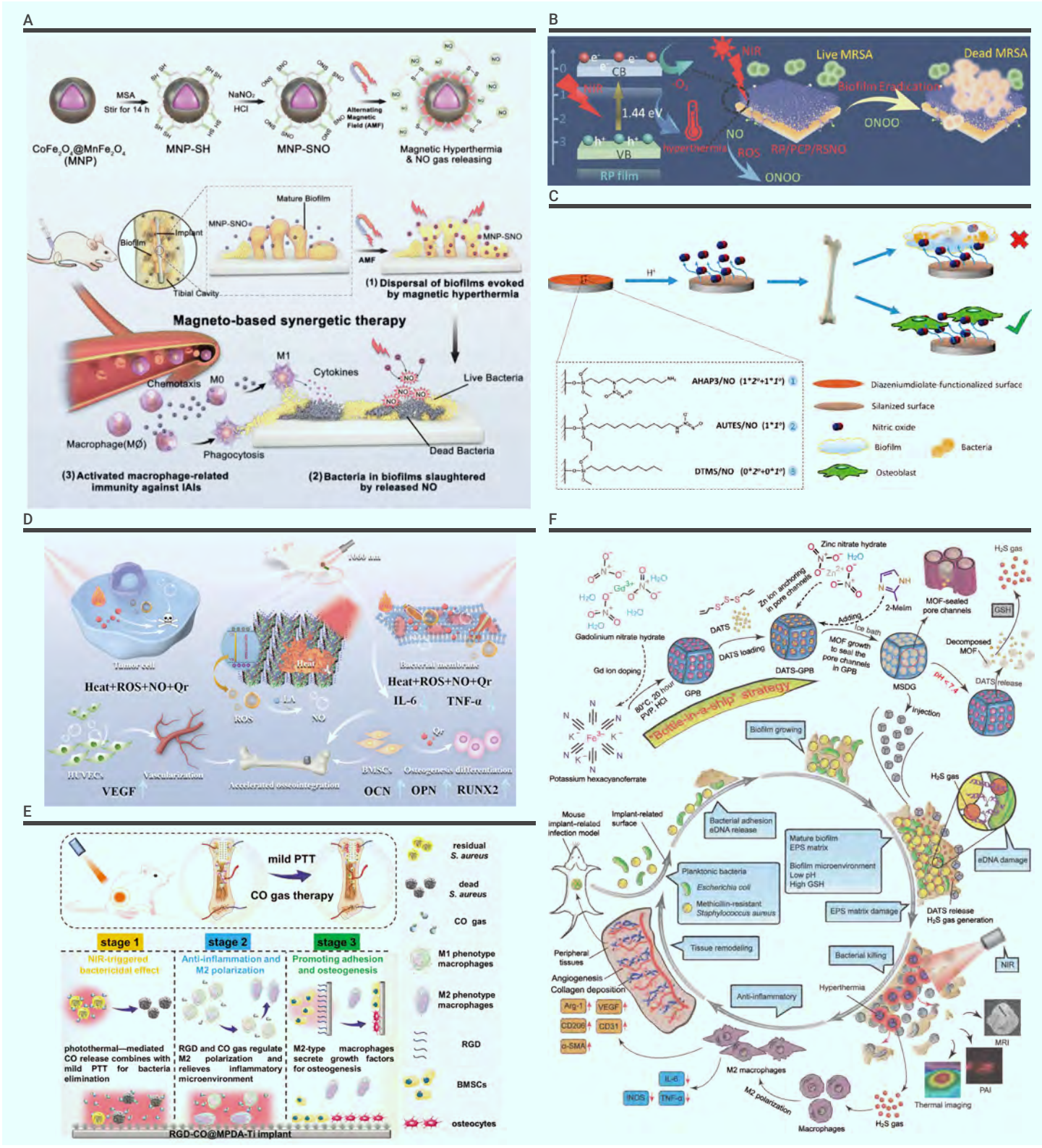

Figure 6. Gasotransmitter delivery for anti-infection application (A) Schematic illustration of the synthesis of MNP-SNOs and its in vivo magneto-based synergetic therapy. Reprinted with permission from Wang et al.[218] Copyright 2021 Wiley-VCH. (B) A schematic diagram of the mechanism of promoted bone formation through M1 polarization of macrophages and MRSA biofilm eradication through gene downregulation. Reprinted with permission from Li et al.[219] Copyright 2020 American Chemical Society. (C) Diazeniumdiolate functionalization of titanium surfaces for anti-infection application. Reprinted with permission from Li et al.[220] Copyright 2020 American Chemical Society. (D) Schematic illustration of TiO_2@UCN/Qr/LA nano-shovel on Ti implants for tumor ablation, biofilm elimination, vascularization and bone regeneration. Reprinted with permission from Zhang et al.[221] Copyright 2021 Elsevier. (E) Schematic illustration of RGD-CO@MPDA-Ti implant for accelerating infected bone repair through CO-potentiated antibiosis, CO-mediated anti-inflammation, and immunomodulation-osteogenic differentiation. Reprinted with permission from Yuan et al.[227] Copyright 2022 Wiley-VCH. (F) Schematic illustration of design, synthesis, and biomedical applications of MSDG. Reprinted with permission from Su et al.[229] Copyright 2022 American Association for the Advancement of Science.

CO. The bactericidal effect of CO arises from inhibiting the respiratory chain of bacteria and its action on adenosine triphosphate (ATP) production.[222–224] CO has also been shown to increase the concentration of ROS in the biofilms, resulting in bacterial membrane polarization and struc-

tural damage.[225] Besides, CO promotes phagocytosis of macrophage to uptake bacteria, such as Escherichia coli via p38-mediated surface expression of toll-like receptor 4 (TLR4) and to activate the host immune response.[226]

Zhang et al. proposed an interfacial functionalization strategy to modify the orthopedic Ti implants with a CO nanogenerator, followed by covalently grafting arginine-glycine-aspartic acid (RGD) polypeptide. Under NIR irradiation, the designed surface displays great light-activatable antibiosis through CO-potentiated mild photothermal therapy. More importantly, after bacteria elimination, on-demand CO delivery alleviated inflammatory response of infection microenvironment by inhibiting M1 macrophages to secrete pro-inflammatory cytokines. Light-activatable substrate further drive the polarization of M1 macrophages toward anti-inflammatory M2-phenotype, thereby remodeling the damaged microenvironment into a pro-regenerative microenvironment, which is beneficial for accelerated bone repair (Figure 6E).[227]

H_2S. The toxicity of H_2S to microorganisms is associated with the oxidative damage via inhibition of antioxidant proteins. In addition, it has also been reported to results from the DNA damage, lipid peroxidation, protein denaturation through disulfide disruption, and inactivation of redox centers in metalloenzymes due to its binding to the metals.[228] Zheng et al. proposed a "H_2S-sensitized hyperthermia" strategy to overcome drug resistance in bacterial biofilm infections. They fabricate a MOF–sealed Prussian blue–based nanocarrier (MSDG), which carries glutathione-responsive H_2S donor DATS. Upon reaching the biofilm, MOF is decomposed in response to the acidic biofilm microenvironment, allowing the release of DATS. The released DATS further reacts with the overexpressed glutathione within the biofilm to generate H_2S gas. Upon NIR irradiation, H_2S-sensitized hyperthermia arising from Prussian blue efficiently eliminate biofilms through H_2S-induced extracellular DNA damage and heat-induced bacterial death, thus realizing the renaissance of precision treatment of refractory implant related infections (Figure 6F).[229]

Immunomodulation

When an orthopedic implant is introduced into body, the immune system recognizes it as foreign and triggers an acute inflammatory response mediated by macrophages.[230] Although inflammation is essential for healing following an injury, its resolution is crucial for bone tissue repair, as excessive acute or chronic inflammation has been linked to impaired healing in both patients and animal models.[231,232] Macrophages, a type of immune cell, play a pivotal role in bone tissue repair and regeneration. In the early stages of bone repair, macrophages primarily differentiate into the M1 phenotype, which releases inflammatory factors such as TNF-α, IL-6, and IL-1β. These factors promote inflammation and help eliminate pathogenic microorganisms and aged or necrotic cells. Over time, macrophages polarize into the M2 phenotype, releasing anti-inflammatory factors like IL-4 and IL-10, which inhibit the inflammatory environment and promote bone regeneration.[233,234] Modulate the initial inflammatory phase and promoting its resolution create a favorable environment for bone regeneration. Biomaterial-assisted delivery of biomolecules with the ability of immunomodulation is an attractive strategy to these efforts.[235] Owing to the potent immunomodulatory ability of gaseous signaling molecules, delivery of NO, CO, and H_2S have natural advantages over other biomolecules to tailor a favorable immune environment for bone regeneration.

NO. NO has been shown to possess both pro- and anti-inflammatory properties. The balance between the two depends on the concentration and duration of released NO. Small amounts of NO, like those derived from eNOS, are thought to be beneficial, as they inhibit the adhesion and migration of inflammatory cells. In contrast, the relatively high amounts of NO, like those produced by iNOS upon stimulation by LPS or inflammatory cytokines (e.g. IL-1β and TNF-α), are thought to contribute to inflammatory response.[236] NO and its role in several models of inflammatory diseases, such as RA, have been well addressed.[237] NO produced by macrophages is responsible for tricarboxylic acid cycle alterations and citrate accumulation associated with polarization.[238] Therefore, special attention needs to be paid when using NO releasing materials for immunomodulatory purpose.

Won et al. developed a polymer capable of controlled NO release to promote the osteogenic capacity in artificial scaffolds. The synthesized NO-releasing compound modulates macrophage polarization toward a regenerative phenotype (from M1 to M2) under LPS stimulation. The compound also promotes ALP activity and mineralization in osteoblastic lineage. In bone defects, NO-releasing scaffolds enhanced angiogenesis and bone growth.[239]

Qi et al. reported a NIR light triggered nanoplatform with anti-inflammatory and antibacterial dual functions.[240] The nanoplatform consists of core-shell structure with photothermal agent gold nanorods as core and mesoporous silica as drug carrier shell. The mesoporous silica is loaded with indocyanine green (ICG) and the NO donor RSNO. Under the irradiation of NIR light, RSNO would be thermally activated to release NO, contributing to decrease of the inflammasome activation related components and inhibition of NF-κB pathway, thus consequently suppressing the inflammasome activation and improving local inflammatory status. Additionally, the nanoplatform also presents antibacterial abilities based on the photodynamic therapy (PDT), photothermal therapy (PTT), as well as NO gas therapy (Figure 7A).[240]

CO. The immunomodulatory role of CO is highlighted in innate immunity, especially in macrophages. In previous studies, both the in vivo and in vitro studies show that CO at low concentrations selectively inhibited the expression of LPS-induced pro-inflammatory cytokines TNF-α, IL-1β, and macrophage inflammatory protein-1β (MIP-1β) and increased the LPS-induced expression of the anti-inflammatory cytokine IL-10. In vivo experiments indicated that CORM-3 induced more M2 macrophages in periodontal tissues in mice with experimental periodontitis.[241]

Liu et al. presented a CO-releasing nano-platform for in vivo synergistic anti-inflammation, which could achieve targeted CORMs delivery and spatiotemporally controllable in situ CO release. The hollow mesoporous MnO_2 nanoparticles were chosen as the carriers and used for encapsulating Fla, a small molecule prodrug for CO release. Then the MnO_2 nanoparticles were further coated with neutrophil cell membrane to target the nanoparticles to the inflammatory sites. In an LPS-induced paw inflammation model, the subsequently administrated nanoparticles are primed by the chemoattractants and migrate to the inflammatory sites. Afterward, nanoparticles achieve in situ rapid photo-induced CO release in the presence of ample oxygen and the light and thus produce a significant synergistic anti-inflammatory effect (Figure 7B).[242]

In addition, the aforementioned CO nanogenerator possesses immunomodulatory effects to suppress M1 polarization while activating macrophages transformation toward the M2 phenotype. The underlying anti-inflammatory mechanisms have been speculated that CO gas participates in the activation of HO-1 antioxidant system and downregulation of pro-inflammatory signaling pathways such as p38 MAPK and NF-κB (p50/p65) simultaneously, resulting in inhibited oxidative stress and diminished secretion of pro-inflammatory cytokine. The positive induction of HO-1 upregulates the expression of typical polarization-related M2 markers such as CD206 and Arg-1 by activating JAK-STAT6 signaling pathways, thereby driving the phenotype shift of macrophages (Figure 7C).[227]

Zhang et al. fabricated a biomimetically hierarchical scaffold composed of deferoxamine@poly(ε-caprolactone) nanoparticles (DFO@PCL NPs), manganese carbonyl (MnCO) nanosheets, gelatin methacryloyl hydrogel, and a polylactide/hydroxyapatite (HA) matrix. This 3D printed stiff scaffold augment bone repair by facilitating the balance of the immune system and bone metabolism. A Fenton-like reaction between MnCO and endogenous H_2O_2 generated at the implant-tissue site triggers continuous release of CO and Mn^{2+}, thus significantly lessening inflammatory response by upregulating the M2 phenotype of macrophages, which also secretes vascular endothelial growth factor to induce vascular formation. The immunomodulatory, angiogenic, and osteogenic abilities of such an osteoimmunity-regulating scaffold present a profound effect on improving bone regeneration (Figure 7D).[243]

H_2S. H_2S is rapidly gaining ground as a physiological mediator of inflammation. The regulatory role for H_2S has been reported in both pro- and anti-inflammatory processes, highlighting that the varied effects of H_2S on the inflammatory process could be due to H_2S concentration and rate of its generation. For example, NaHS had a biphasic effect and at high concentrations (>200 μm) increases the synthesis of pro-inflammatory cytokines IL-1β, IL-6, TNF-α, and PGE-2. In contrast, GYY4137 significantly inhibits LPS-induced release of proinflammatory mediators but increases the synthesis of

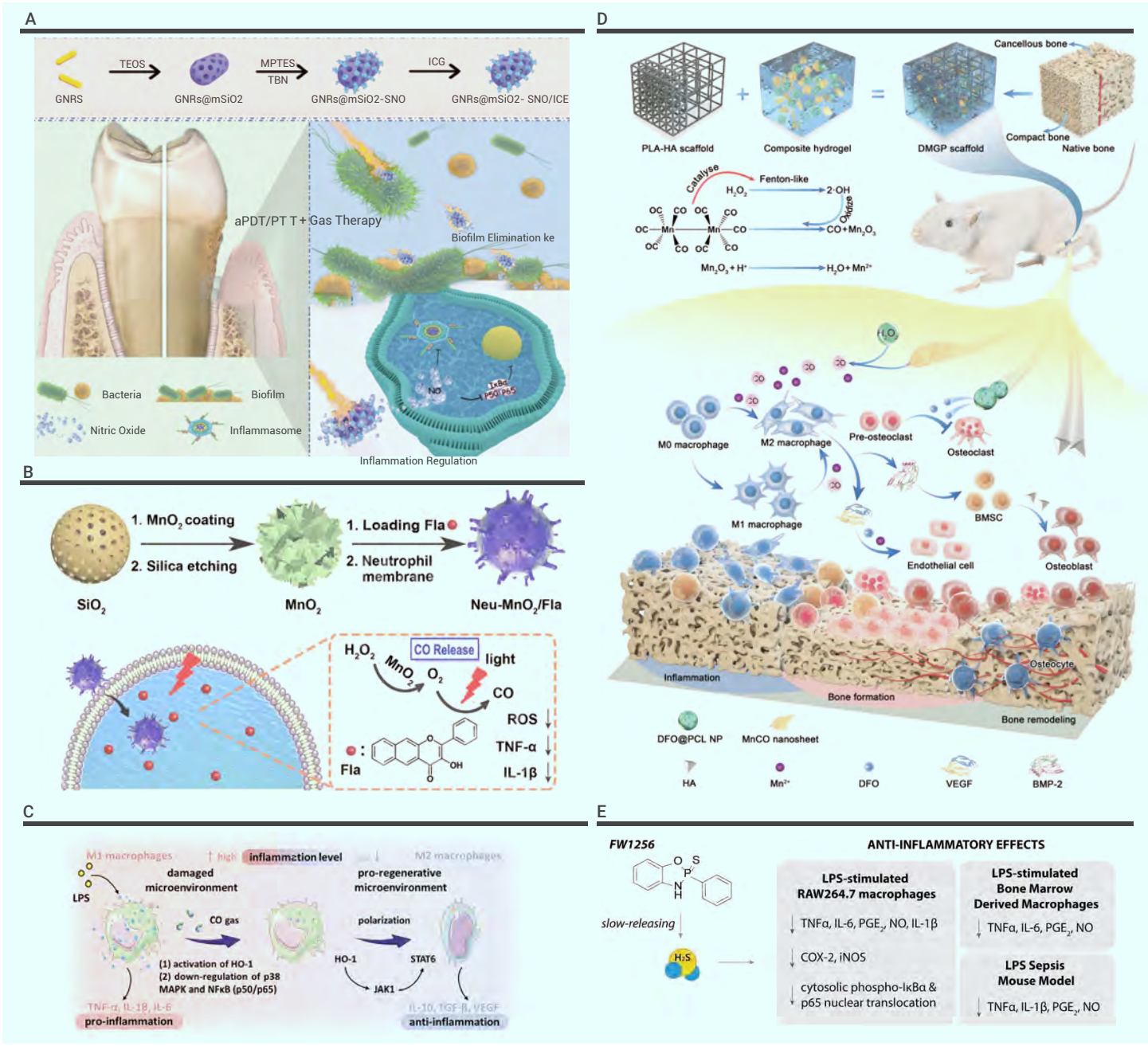

Figure 7. Gasotransmitter delivery for immunomodulation application (A) Schematic illustration of design of GNRs@mSiO$_2$-SNO/ICG NPs and their anti-biofilm and inflammatory regulation functions to target periodontal diseases. Reprinted with permission from Qi et al.[240] Copyright 2022 Elsevier. (B) Schematic representation of synergistic anti-inflammation. Reprinted with permission from Liu et al.[242] Copyright 2022 Elsevier. (C) Schematic illustration of potential mechanism of anti-inflammation and M2-type macrophage polarization by NIR-triggered CO release. Reprinted with permission from Yuan et al.[227] Copyright 2022 Wiley-VCH. (D) Schematic illustration of osteoimmunity-regulating biomimetically hierarchical scaffold for augmented bone regeneration. Reprinted with permission from Zhang et al.[243] Copyright 2022 Wiley-VCH. (E) Structure and immunomodulation performance of H_2S delivery platform. Reprinted with permission from Huang et al.[245] Copyright 2019 Elsevier

the antiinflammatory chemokine IL-10 through NF-κB/ATF-2/HSP-27–dependent pathways.[244] Similarly, Huang et al. recently reported that 3-dihydro2-phenyl-2-sulfanylenebenzo[d] [1,3,2]oxazaphosphole (FW1256) releases H_2S in vitro over a period of several hours. FW1256 decreases TNF-α, IL-6, PGE_2 and NO generation in LPS-stimulated RAW264.7 macrophages in concentration-dependent manner via inhibition of the NF-κB system (Figure 7E).[245] Zheng et al. encapsulated a pH-responsive H_2S donor JK1 into collagen hydrogel (Col-JK1). This hydrogel could control the release of H_2S by responding to the condition that mimic the intervertebral disc degeneration environment (acidic pH and overexpression of matrix metalloproteinases). In vitro studies indicate that Col-JK1 could inhibit apoptosis of nucleus pulposus cells (the major cells in discs), which eventually contributes to the recovery of disc degeneration by restoring the stability of disc ECM through up-regulation of the expression of anabolic proteins (for example, collagen II, aggrecan and sox-9), and down-regulation of the expression of catabolic proteins (for example, MMP13 and ADAMST5).[191] H_2S also can promote the polarization of macrophages toward M2 phenotype for ameliorating the immune microenvironment through activation of adenosine monophosphate-activated protein kinase (AMPK) (Figure 6F).[229] Recent studies utilizing the inflammatory regulation effect of H_2S are mainly focus on the wound healing, and there is a limited number of studies to treat bone diseases.[192,193,202]

Bone regeneration

Bone defects caused by trauma, tumor and inflammation diseases seriously reduce the quality of life of patients. The limited intrinsic regenerative ability of the bone following destruction remains a notable medical problem, and thus it is important to develop methods of stimulating bone

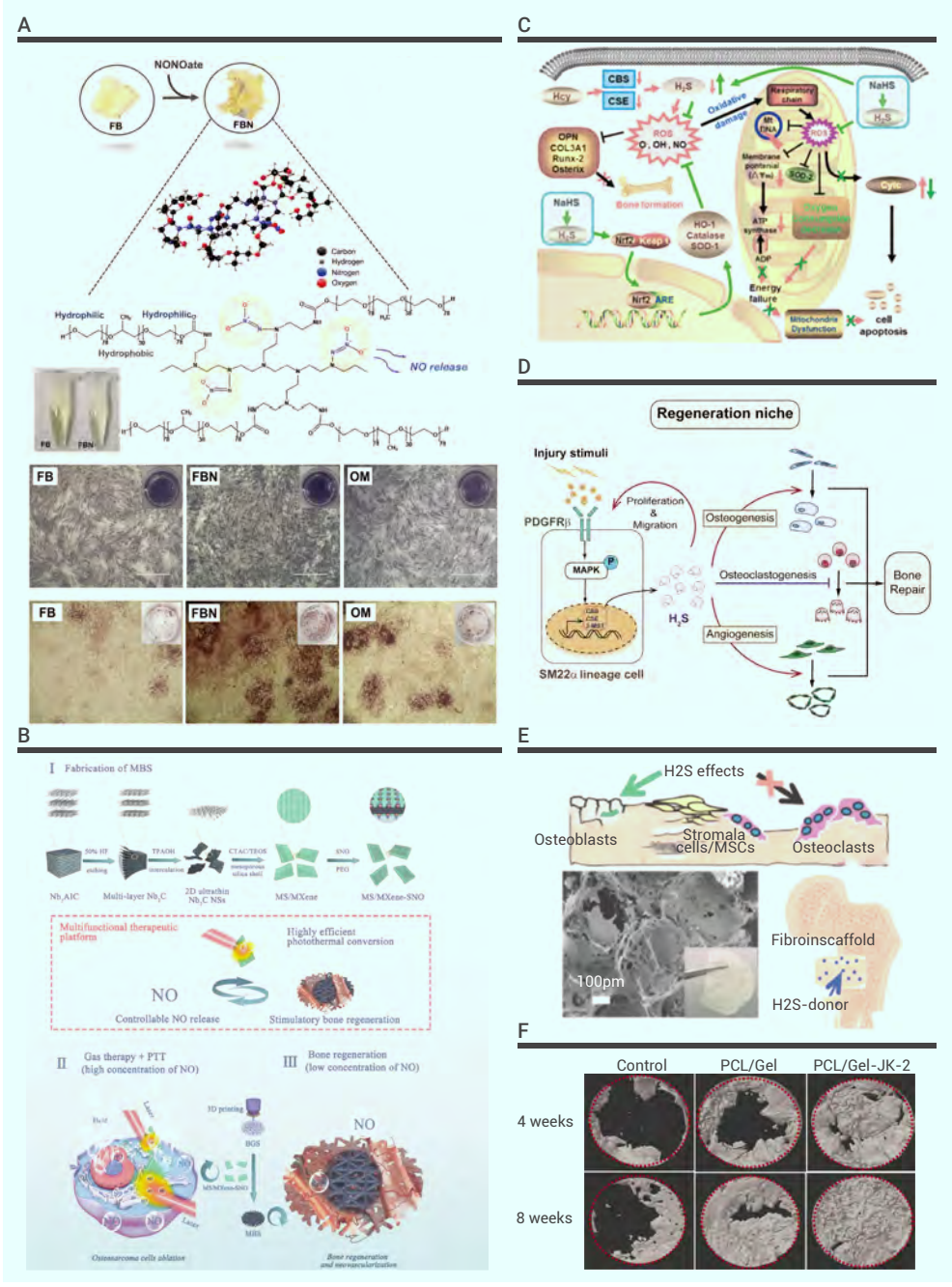

Figure 8. Gasotransmitter delivery for bone regeneration application (A) Schematic illustration and characterization of the FB and FBN, and their promotion effects on osteogenic differentiation of MG63 cells. Reprinted with permission from Won et al.[239] Copyright 2022 Wiley-VCH. (B) Schematic illustration of the multifunctional therapeutic platform. Reprinted with permission from Yang et al.[253] Copyright 2020 Wiley-VCH. (C) Schematic of proposed hypothetical mechanism of NaHS mediated recovery of osteoblast function via mitochondrial biogenesis in Hcy - treated condition. Reprinted with permission from Zhai et al.[260] Copyright 2019 Wiley-Periodicals. (D) SM22α-lineage stromal cells regulate diverse processes of intramembranous bone regeneration through PDGFRb/H_2S-dependent regulatory mechanism. Reprinted with permission from Zhou et al.[264] Copyright 2022 Elsevier. (E) Embedding an H_2S-releasing donor in silk fibroin scaffold is a suitable strategy to achieve a long-lasting release of H_2S that preserves cell viability and allows local delivery at sites of tissue injury. Reprinted with permission from Raggio et al.[266] Copyright 2018 American Chemical Society. (F) 3D reconstructed images of rabbits head implantation model after 4 and 8 weeks. Reprinted with permission from Al-Bishari et al.[267] Copyright 2021 Elsevier.

regeneration.[246] Bone marrow mesenchymal stem cells (MSCs) have the capacity to differentiate into multiple cell lineages and are a major source of osteoblast precursors. Scaffolding biomaterials loaded with the osteogenic signals hold the potential to promote bone regeneration.

NO. NO plays a crucial role in physiology and pathology related to osteogenesis and bone regeneration. It exhibits a biphasic, dose-dependent effects on the activity of osteoblasts. A rapid release and high concentrations of NO lead to osteoblast apoptosis, while a slow and moderate release of NO encourages osteoblast differentiation, proliferation, and survival.[247] The specific concentration of NO in a localized area depends on the release kinetics of NO from the donor species. Of note is the timing and dosage of localized NO delivery.[248] NO donors with slow NO releasing property enhance bone regeneration by stimulating expression of osteoblastic genes, e.g. ALP, osteocalcin, and collagen-I, and increasing bone matrix synthesis and mineralization.[249] Via activation of sGC and cGMP-dependent protein kinases (PKGs), NO promotes the osteogenic differentiation of osteoblasts by increasing the expression and activity of the osteoblast master transcription factor Runx2.[250]

Angiogenesis is a key component of bone repair. New blood vessels bring oxygen and nutrients to the highly metabolically active regenerating callus and serve as a route for inflammatory cells and cartilage and bone precursor cells to reach the injury site.[251] NO is well recognized as a mediator of angiogenesis.[252] Therefore, the NO-releasing orthopedic implants hold the potential to enhance the bone regeneration through promote the angiogenesis. Won et al. utilized the positive charge branching in branched polyethylenimine (BPEI) as carrier of NO donor NONOate. The obtained macromolecule stably carries NONOate and releases NO more slowly for a longer time with less cytotoxicity. In vitro studies indicate that the NO releasing macromolecule induces enhanced ALP activity and ECM mineralization of MG63 and MC3T3-E1 cells of osteoblastic lineage cells. In vivo results shows that collagen scaffold loading the NO releasing macromolecule promote osteogenesis and angiogenesis simultaneously, which is valuable for bone regeneration in critical-sized defects (Figure 8A).[239]

Yang et al. construct a 3D-printing scaffold by integration of 2D Nb_2C MXene wrapped with S-nitrosothiol with bioactive glass. The NIR-triggered photonic hyperthermia of MXene precisely control release of NO, which plays a crucial role in sequential adjuvant tumor ablation, combinatory promotion of coupled vascularization, and bone regeneration (Figure 8B).[253]

CO. In previous study, CORM-3 has been shown to promote the osteogenic differentiation of rat bone marrow mesenchymal stem cells (BMSCs) in vitro. Levels of Runx2, osteocalcin (OCN) and osteopontin (OPN) mRNA and protein in the CORM-3-osteogenic group are significantly increased compared with the osteogenic group.[254] The association of CO with bone homeostasis and orthopedic diseases need to be further investigated.

H_2S. In recent years, H_2S is emerging as a critical gasotransmitter in bone homeostasis.[255] It regulates multiple signaling pathways in mammalian cells, and abnormal H_2S metabolism has been linked to defects in bone homeostasis. It has become recognized to impact various aspects during bone regeneration such as calcium uptake regulation, oxidative stress reduction, and angiogenesis promotion. H_2S has been found to play an important role in supporting the osteogenic differentiation of bone marrow mesenchymal stem

cells (BMSCs). BMSCs are the original source of osteoblasts for bone formation. BMSCs produce H_2S to regulate their self-renewal and osteogenic differentiation. H_2S deficiency results in decreased intracellular Ca^{2+} influx and then downregulates PKC/ERK-mediated Wnt/β-catenin signaling which controls osteogenic differentiation of BM-MSCs.[256] CSE majorly contributed to endogenous H_2S production in the primary osteoblast. Overexpressed CSE increases osteoblast differentiation and maturation with higher BMP-2 and OPN expression, ALP activity, and calcium nodule formation via RUNX2 pathway; in contrast, knockdown of CSE has opposite effects. Implantation of a gelatin sponge containing the CSE adenovirus in a rat bone fracture resultes in repair of the fracture lesion after 2 weeks.[257,258] Exogenous H_2S prevents high glucose-induced damage to osteoblasts through regulation of K_{ATP} channels.[259] H_2S also mediates recovery of osteoblast dysfunction by maintaining mitochondrial biogenesis in homocysteine - treated [260] and dexamethasone-treated [261] osteoblast cultures in vitro (Figure 8C). H_2S protects MC3T3-E1 osteoblastic cells against oxidative stress caused by H_2O_2 via an MAPK-dependent mechanism.[262]

H_2S has been reported to enhance the proliferation and migration of endothelial cells and activate vascular endothelial growth factor (VEGF) receptors and K_{ATP} channels, contributing to angiogenesis, which is crucial for tissue regeneration.[263] Angiogenesis and vascularization is a primary driving force for both intramembranous and endochondral ossification, and the close relationship between new vasculature formation and osteogenesis is of paramount importance. Zhou et al. found that platelet-derived growth factor receptor β (PDGFRβ)-triggered H_2S generation in SM22α-lineage niche cells facilitates osteogenesis and angiogenesis while suppressing overactive osteoclastogenesis (Figure 8D).[264]

Administration of H_2S both holds good therapeutic potential for bone regeneration. To control the delivery of potential therapeutic agents in bone, researchers have developed various scaffolds that can be embedded into the defect site. For example, the common H_2S donor GYY4137 has been embedded in a silk fibroin scaffold for bone regeneration while promoting neovascularization. H_2S-releasing silk fibroin scaffold is shown to support adhesion, proliferation and viability of BMSCs. Moreover, H_2S activates genes and proteins involved in ossification, osteoblast differentiation, bone mineral metabolism and angiogenesis allowing a high and early mineralization (Figure 8E).[265,266]

Al-Bishari fabricated an electrospun membrane loaded with H_2S donor JK-2 for promoting bone regeneration. After 4 and 7 d of culture, the ALP activity and expression of osteogenic genes of MC3T3-E1 cells cultured on this scaffold is significantly higher than that in the control group. After 2 months implantation of scaffolds in the rabbit skull, this scaffold is nearly covered with new bone whereas the control group shows a significantly lesser amount of new bone formation, indicating JK-2 donor loaded nanofiber membrane could be a promising candidate for bone tissue regeneration (Figure 8F).[267]

Osteoporosis

Osteoporosis is an emerging medical and socioeconomic threat with an ageing population. It is characterized by a systemic impairment of bone mass, strength, and microarchitecture, which increases the propensity of fragility fractures.[3] Under normal physiological conditions, the metabolism of bone is a dynamic balance between bone formation and bone resorption. Osteoblasts mediated bone formation and osteoclasts mediated resorption are key processes that are necessary for the constant remodeling of bone tissue to keep it healthy. Osteoporosis results from an imbalance of bone resorption and bone formation that causes bone fragility and increases the risk of fracture. Postmenopausal osteoporosis is the most common type of osteoporosis.[268] Due to the lack of estrogen, the bone resorption process is primarily increased by osteoclast maturation.[269]

NO. Estrogen exerts its positive effects on bone partly through the NO/cGMP pathway.[250,270] Hence NO donor therapy serves as an alternative to estrogen, estrogen agonists-antagonists, and androgen receptor modulator therapy for preventing and treating osteoporosis.[248] Nitrates, which generate NO, improved bone mineral density in estrogen-deficient rats and improve bone formation markers and bone mineral density in postmenopausal women in clinical trials.[271] However, clinical benefits of organic nitrates are limited by development of tolerance and induction of oxidative stress. Kalyanaraman et al. developed a NO-releasing donor nitrosyl-cobinamide (NO-Cbi) for treating osteoporosis. In murine primary osteoblasts, NO-Cbi increases intracellular cGMP, Wnt/β-catenin signaling, proliferation, and osteoblastic gene expression, and protectes cells from apoptosis. NO-Cbi reduces osteoclasts in intact mice and preventes the known increase in osteoclasts in ovariectomized (OVX) mice.[272] Lin et al. delivered NO donor by encapsulation into an injectable microparticle system, which consists of phase-change materials capric acid (CA) and octadecane. Upon subcutaneous administration, the MPs undergo a phase transition, leaching out the NO donor and generating NO bubbles that are instantly covered by a micellar depots, thus effectively reversing OVX-induced osteoporosis (Figure 9A).[61] Ye et al. developed a NO delivery nanoplatform with bone targeting property based on the UCNPs that can convert NIR light into UV/blue light, and further stimulate the release of NO. Both in vitro and in vivo experiments demonstrate the bone targeting ability of the nanoparticles and a favorable curative effect of reversing osteoporosis (Figure 9B).[273] Lee et al. fabricated a NO-releasing bioinspired scaffold with bioactive agents for the exquisite regeneration of osteoporotic bone. Nanoparticles containing bioactive agents of zinc oxide (ZO), alendronate, and BMP2 are incorporated to the biomimetic scaffold. The scaffold imparts multifunctionality such as anti-inflammation, angiogenesis, anti-osteoclastogenesis, and bone regeneration. These synergistic effects contribute to enhanced new bone formation even in the osteoporotic rat model (Figure 9C).[274]

CO. CO has been demonstrated to provide remarkable therapeutic benefits at low doses by suppressing inflammatory reaction of macrophages, which are also precursors for osteoclasts. Intraperitoneal injection of CORM-2 into mice with reduced bone mass due to ovariectomy results in a significant increase in bone mass. Treatment with CORM-2 also reduces the serum levels of collagen-type I fragments, tartrate-resistant acid phosphatase 5b, and ROS, all of which are increased due to ovariectomy. In vitro study indicate that CORM-2 hinders receptor activator of nuclear factor-κB ligand (RANKL)-induced osteoclast formation without affecting bone resorption. CORM-2 lowers long-lasting ROS levels and NF-κB activation in response to RANKL. Collectively, the inhibitory effect of CO on osteoclastogenesis is a result of impaired RANKL signaling due to defective NF-κB activation and decreased levels of long-lasting ROS (Figure 9D).[275–277]

H_2S. Decrease in serum H_2S levels and the bone marrow levels of two key H_2S-generating enzymes, CBS and CSE, has been observed in ovariectomy mice, a model of postmenopausal bone loss (Figure 9E).[278] Pharmacological administration of H_2S has achieved encouraging results in preclinical studies in the treatment of osteoporosis. Treatment with the H_2S donor GYY4137 normalizes serum H_2S in OVX mice, increases bone formation, and completely prevents the loss of trabecular bone induced by OVX. Mechanistic studies revealed that GYY4137 increases osteoblastogenesis by activating Wnt signaling (Figure 9F).[278] In another study, NaHS dose-dependently decreases human osteoclast differentiation at concentrations which did not induce toxicity. The inhibition of human osteoclast differentiation is associated with a down-regulation in RANKL-dependent intracellular ROS levels in human pre-osteoclasts cells.[279] Moreover, oxidative damage is an important contributor to the pathological development of osteoporosis. H_2S has been reported to protect MC3T3-E1 osteoblastic cells against H_2O_2 induced oxidative injury. H_2S not only increases cell viability and reduces cell apoptosis caused by H_2O_2, but also stimulates osteoblast proliferation by enhancing both transcription and activity of ALP in MC3T3-E1 osteoblastic cells. Moreover, treatment with NaHS stimulated the transcriptional level of OCN, the main bone matrix protein, and the protein expression of collagen, a major constituent of bone tissue. The above effects are mediated by the antioxidant effect of H_2S.[262]

RA and OA

RA and OA are the most prevalent forms of arthritis. RA is an autoimmune disease characterized by joint swelling, tenderness, and eventual destruction of synovial joints.[280] OA is characterized by subchondral bone remodeling, synovial inflammation and the progressive degeneration of articular

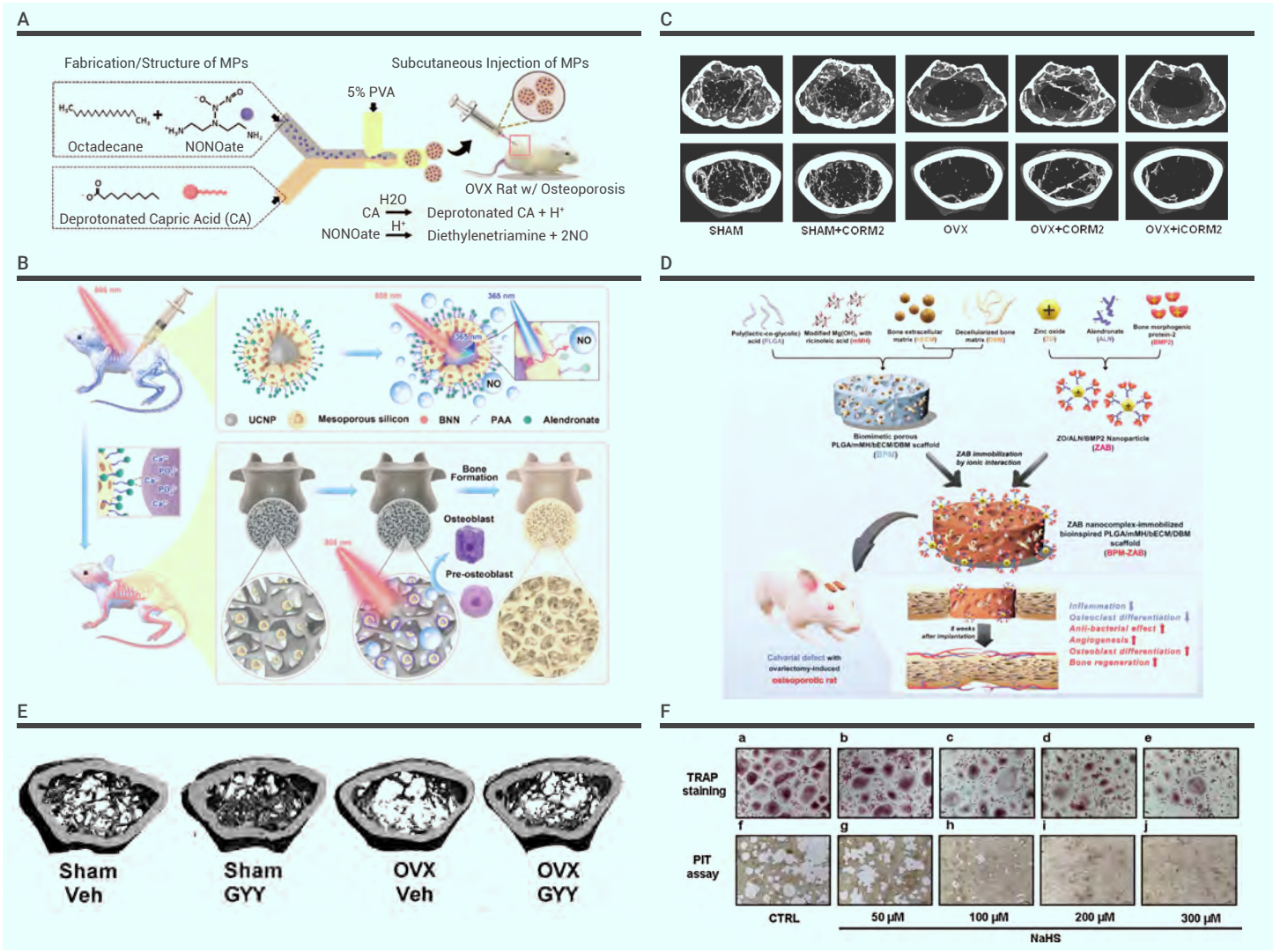

Figure 9. Gasotransmitter delivery for treating osteoporosis (A) Fabrication/structure of test MPs and the functional mechanisms. Reprinted with permission from Lin et al.[61] Copyright 2018 Wiley-VCH. (B) The UCPA-BNN can specifically chelate calcium ion in bone tissue. Reprinted with permission from Ye et al.[273] Copyright 2021 American Chemical Society. (C) Schematic illustration of the ZAB-immobilized bioinspired polymeric scaffold. Reprinted with permission from Lee et al.[274] Copyright 2022 Wiley-VCH. (D) CO protects against bone loss induced by OVX in mice. Reprinted with permission from Van Phan et al.[275] Copyright 2013 Elsevier. (E) 3D image reconstruction of one representative femur per group. Reprinted with permission from Grassi et al.[278] Copyright 2015 American Society for Bone and Mineral Research. (F) Representative pictures showing the effect of NaHS on osteoclasts differentiation and function. Reprinted with permission from Gambari et al.[279] Copyright 2014 Elsevier.

cartilage.[281] Monocytes/macrophages have been found to massively infiltrate synovial membranes, playing a central role in the pathophysiology of inflammation. Inflammatory cytokines are crucial factors in the onset of OA. In response to inflammatory stimuli including IL-1β, TNF-α, and NO, chondrocytes synthesize the MMPs involved in the degradation of the extracellular matrix (ECM) of the cartilage.[282]

NO. Although the exact mechanism of the initiation of RA disease is unclear, overproduction of NO is closely related to RA development.[283] NO contributes to the enhancement of the activation and production of MMPs, the inhibition of synthesis of anabolic molecules and the promotion of chondrocyte apoptosis. Therefore, the selective depletion of NO using NO-scavenging agents has shown promising potential for RA treatment. Yeo et al. developed a NO-scavenging nanosized hydrogel (NO-Scv) for treating RA. The NO-Scv gel is prepared by solution polymerization between acrylamide and a NO-cleavable cross-linker, which is readily cleaved by consuming the NO molecule. The NO-Scv gel reduces inflammation levels by scavenging NO in vitro and shows excellent biocompatibility. Furthermore, the NO-Scv gel suppresses the onset of RA in a mouse RA model when compared to the effects of commercial drug dexamethasone (Figure 10A).[284] In another studies, Kim et al. developed a polymeric aggregate-embodied hybrid NO scavenging and sequential drug-releasing "click" hydrogel (M-NO) for the combinatorial treatment of RA. The M-NO gel could also fulfill an on-demand drug-release depending on the severity of the diseases in response to NO concentration as a hallmark. Moreover, consecutive NO-scavenging action reduces pro-inflammatory cytokine levels in LPS-stimulated macrophage cell lines in vitro. Finally, the intraarticularly injected M-NO gel with anti-inflammatory dexamethasone significantly alleviates the symptoms of RA, with negligible toxicity, in animal models (Figure 10B).[285]

As for the treating of OA, an opposite strategy is proposed. More NO is delivery to the joint to facilitate decrease activity of the macrophage. Chen et al. constructed a novel photothermal-triggered NO generation platform for the precise therapy of OA by combining photothermal agents, NO and Notch1-siRNA into a single particle. NO nanogenerator exhibits precisely controlled NO production under the irradiation of a 650 nm laser in an aqueous solution and RAW 264.7 cells, effectively inhibit the activity of macrophages and the level of proinflammatory cytokines. In vivo experiments indicate that the nanoparticles can effectively accumulate in OA region, reduce the inflammatory response and efficiently prevent cartilage erosion, without causing toxic side effects in the major organs (Figure 10C).[286]

CO. CORM is an interesting strategy for the development of new treatments in articular conditions. Recently study reported CORMs are protective in OA. CORM-2 exhibits protecting effects on cartilage metabolism through the depression of catabolic activities and the stimulation of glycosaminoglycan synthesis.[287] CORM-2 also regulates the inflammatory process in

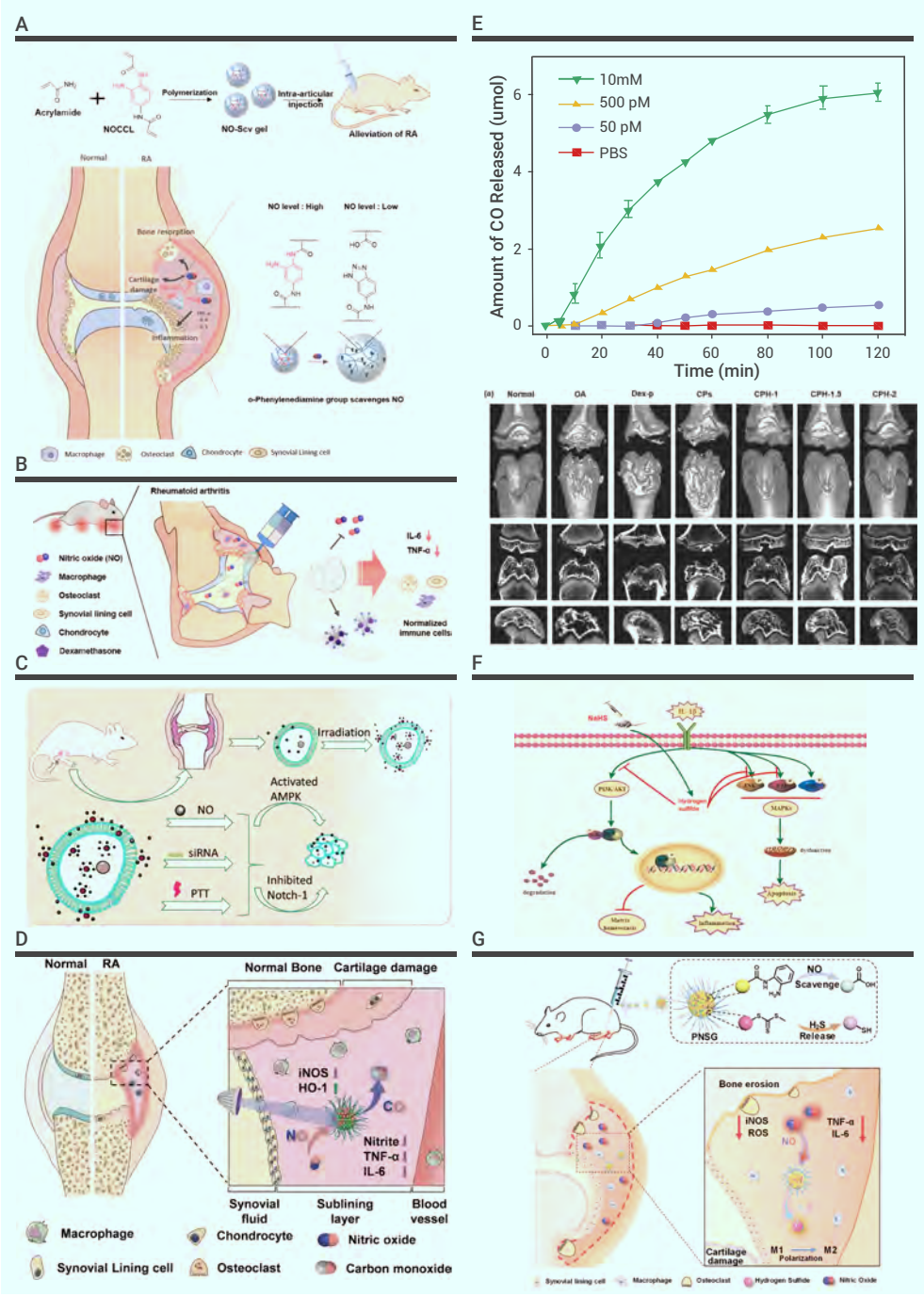

Figure 10. Gasotransmitter delivery for treating OA and RA (A) Mechanism of NO-induced inflammatory effect in RA and alleviation of RA by NO-Scv gel. Reprinted with permission from Yeo et al.[284] Copyright 2019 American Chemical Society. (B) Combinatorial treatment of RA with M-NO gel. Reprinted with permission from Kim et al.[285] Copyright 2021 Wiley-VCH. (C) The process of nanoparticles inhibiting the macrophage inflammatory response after being triggered by the photothermal effect. Reprinted with permission from Chen et al.[286] Copyright 2019 The Royal Society of Chemistry. (D) BM exerts a combinatorial anti-inflammatory effect for RA treatment. Reprinted with permission from Tao et al.[290] Copyright 2020 Wiley-VCH. (E) CO release profiles under different H_2O_2 concentrations, and the representative micro-CT 2D images of the rat knee joints following 23 days treatment. Reprinted with permission from Yang et al.[291] Copyright 2020 Elsevier. (F) Schematic of the potential protective effects of H_2S in osteoarthritis development. Reprinted with permission from Wang et al.[294] Copyright 2020 Wiley-Periodicals. (G) PNSG scavenges overproduced NO and releases therapeutic H_2S to attenuate inflammation for synergistic treatment of RA. Reprinted with permission from Geng et al.[299] Copyright 2022 Wiley-VCH.

osteoarthritic chondrocytes. Treatment of chondrocytes with CORM-2 strongly down-regulates NOS-2 and mPGES-1 protein expression, as well as the production of ROS, nitrite, PGE2, and IL-1β-induced TNF-α.[288] CORM-3 reduces the cellular infiltration into the joints and production of relevant inflammatory mediators such as cytokines and PGE2. CORM-3 inhibits IL-1β, TNF-α and IL-6 production, which may result in a decreased infiltration and activation of inflammatory cells in arthritic joints leading to an amelioration of the disease.[289]

Tao et al. developed a "breathing" micellar platform that can inhale NO and exhale CO. The micelle can simultaneously scavenge overproduced NO and release CO to attenuate proinflammatory cytokines in LPS-challenged macrophage cells. In vivo studies reveal that the micelle outperformed conventional nonsteroidal anti-inflammatory drugs such as dexamethasone in treatment of RA in adjuvant-induced arthritis (AIA) rats (Figure 10D).[290] Yang et al. fabricated a peptide dendrimer nanogel, which physically encapsulates CO donor CORM-401 and wraps its surface with folic acid (FA)-modified hyaluronic acid (HA). The naongel is capable of efficiently entering activated macrophages via FA- and HA-mediated specific targeting effects and then rapidly release large amounts of CO by massive consumption of H_2O_2. The anti-inflammatory effects results from the generated CO, together with the depletion of intracellular H_2O_2, contribute to the suppression of articular cartilage degradation (Figure 10E).[291]

H_2S. The effect of H_2S on joint inflammation has been investigated in the last few years due to its anti-inflammatory effect. H_2S shows a protective effect on cartilage damage in OA patients in different studies. The H_2S-release donor exerts anti-inflammatory effects of in multiple cell types relevant for the pathogenesis of arthritis. NaHS treatment of FLSs obtained from OA patients reduces both spontaneous and IL-1β-induced secretion of IL-6, IL-8, and various MMPs such as MMP-2 and MMP-14. H_2S partially antagonizes IL-1β stimulation via selective manipulation of the MAPK and the PI3K/Akt pathways.[292,293]

Pretreatment with the H_2S donor NaHS dramatically attenuates IL - 1β - induced overproduction of inflammatory cytokines (IL-8、IL-6、TNF-α) and improves the balance between anabolic and catabolic chondrocyte capacities via PI3K/AKT pathway - mediated inhibition of NF - κB. Moreover, mitochondrial dysfunction - related apoptosis is significantly reversed by NaHS in IL - 1β - stimulated chondrocytes though suppressing IL - 1β - induced phosphorylation of the MAPK cascades. Furthermore, in the destabilization of the medial meniscus mouse model, OA progression is ameliorated by NaHS administration. Surgery-induced activation of p-p38 and p-JNK MAPKs (including p-ERK1/2) are elevated, which are markedly reversed after NaHS treatment (but not p-ERK1/2) (Figure 10F).[294]

Another in vitro study reveals that GYY4137 exerts anti-inflammatory properties on LPS-treated normal human synoviocytes (HFLS) and articular chondrocytes (HAC). When cells are treated with GYY4137 previously (for 1 h prior to LPS addition) and subsequently (at 6 or 18 h after LPS addition), the levels of pro-inflammatory markers PGE_2, TNF-α, IL-6 and NO are reduced. Intracellular levels of COX-2 and iNOS and NF-κB activation in both cell types

are also reduced when GYY4137 is administered 1 h prior to LPS.[295] Both H_2S sources NaHS and GYY4137 show anti-inflammatory and anti-catabolic properties when added to IL-1β activated osteoarthritic human chondrocytes. Supplementation with exogenous H_2S sources can regulate the expression of relevant genes in OA pathogenesis and progression, counteracting IL-1β pro-inflammatory signals that lead to cartilage destruction in part by reducing NF-κB activation.[296] In addition, co-culture the OA cartilage disks with H_2S-forming reagents NaHS and GYY4137 for long-term up to 21 days effectively avoids GAGs destruction.[297]

Yu et al. prepared and constructed the dendritic mesoporous silica nanoparticles (DMSN) and a sustained H_2S delivery system consisted of SPRC and DMSN (SPRC@DMSN). The SPRC@DMSN could elevate the H_2S concentration for 3 days with single oral administration, while the SPRC lasted for only 6 h. The SPRC@DMSN suppresses the expression of LPS-induced pro-inflammatory cytokines (TNF-α, IL-1β and IL-6) release and increases the release of IL-10 detected in AIA rats. In SPRC@DMSN group, decrease level of paw volume and arthritis index could be observed. The SPRC@DMSN-treated rats have a marked reduction in cartilage degradation and bone erosion in comparison with the AIA group or SPRC-treated group.[298]

Geng et al. fabricated a block polymer composed of an NO-responsive monomer and a cysteine-triggered H_2S donor. The block polymer self-assembles to nanomicelles, which simultaneously scavenges NO and releases therapeutic H_2S for RA treatment. In vitro experiments demonstrate that the polymer exhibits a synergistic effect on suppressing ROS levels and pro-inflammatory cytokine production via NF-κB signaling pathway. In vivo studies with an RA rat model show that the system mitigates the synovial inflammation, osteoporosis, and clinical symptoms of RA rats (Figure 10G).[299]

CONCLUSION AND OUTLOOK

In summary, gas therapy, which utilizes endogenous gas signaling molecules to treat diseases, holds natural advantages over traditional therapy strategies in dealing with bone diseases. Various multifunctional gas delivery platforms have been developed, with the abilities not only to delivery gasotransmitters in a sustained and controlled manner, but also to realize responsive release to endogenous or exogenous stimuli, synergize with other therapy strategies such as photothermal treatment, and to target a desired site of release through systemic administration. Despite the encouraging results in treatment of bone diseases, several challenges remain in the field of gasotransmitter delivery for further development, and more effort is required to accelerate the clinical application of this novel therapy approach.

a Biocompatibility and biosafety of gas delivery platforms. Although the gas delivery platforms show low cytotoxicity and good biocompatibility at suitable concentration, the platforms still suffer from the long-term biosafety concern, including biodistribution, biodegradation, metabolism, and hemocompatibility. For example, photoresponsive gasotransmitter donors usually yield cytotoxic byproducts. Additionally, some gas delivery platforms are initially developed for cancer treatment, the long-term toxicity of these materials needs to be studied in depth when utilize them to treat bone diseases.

b The mechanism of gas therapy. Although gas therapy has been studied for many years, with its therapeutic potential evaluated in vitro and in animal models for various diseases, the underlying mechanisms remain incompletely understood. This is especially true for gas therapies assisted by gas-releasing materials. For example, the precise concentration threshold has yet to be determined. Clinical trials involving gas therapy are scarce, but highly desirable. Future research should focus on elucidating the specific action mechanisms of gas therapy, which will aid in the development of gas-releasing platforms with improved biocompatibility and controlled release behaviors for clinical applications. Moreover, advanced techniques need to be developed for accurately measuring the concentrations of these therapeutic gases when administered to the body.

c Controllable gas release and precise delivery of platforms. Delivering gases to specific targets and achieving controllable release through a feasible trigger are crucial for obtaining optimal therapeutic effects. Therefore, it is essential to develop more platforms with high sensitivity to exogenous and endogenous stimuli to enable efficient and controlled release of gaseous donors. It is important to note that if administered at inappropriate levels (either too high or too low), these gases may produce adverse effects.

d Orthopedic application. Gas-releasing molecules hold great potential for orthopedic applications. With the help of platforms, gaseous molecules can be delivered to specific bone sites through injection or implantation, ensuring in situ release of the corresponding gas under stimuli and enhancing therapeutic efficacy. More importantly, the dosage and release rate of gaseous molecules within the platforms need to be precisely tuned through molecular design and further regulated by internal or external stimuli specific for the microenvironment of bone tissues.

e Co-delivery of multiple gasotransmitters. An intriguing and currently underexplored area for future research is the development of delivery systems that co-activate multiple therapeutic gases simultaneously for potential combination therapy. There is evidence that crosstalk exists among these gases, with some displaying similar pharmacological profiles and even acting on the same targets. For instance, both H_2S and CO are widely known as potent anti-inflammatory agents that act on the Nrf2 pathway. Additionally, synergistic effects have been observed between some gasotransmitters. As such, it would be highly desirable to create drug delivery systems designed for the co-delivery of multiple gasotransmitters.

REFERENCES

1. Wei, H., Cui, J., Lin, K., et al. (2022). Recent advances in smart stimuli-responsive biomaterials for bone therapeutics and regeneration. Bone Res. ***10***, 17.
2. Kawai, M., Mödder, U. I., Khosla, S., et al. (2011). Emerging therapeutic opportunities for skeletal restoration. Nat. Rev. Drug Discov. ***10***, 141–156.
3. Rachner, T. D. and Khosla, P. S. (2011). Osteoporosis: now and the future. The Lancet ***377***, 1276–1287.
4. Rahimi, M., Charmi, G., Matyjaszewski, K., et al. (2021). Recent developments in natural and synthetic polymeric drug delivery systems used for the treatment of osteoarthritis. Acta Biomater. ***123***, 31–50.
5. Guo, Q., Wang, Y., Xu, D., et al. (2018). Rheumatoid arthritis: pathological mechanisms and modern pharmacologic therapies. Bone Res. ***6***, 15.
6. Jiang, P., Zhang, Y., Hu, R., et al. (2023). Advanced surface engineering of titanium materials for biomedical applications: From static modification to dynamic responsive regulation. Bioact. Mater. ***27***, 15–57.
7. Wang, Z., Rong, F., Li, Z., et al. (2023). Tailoring gas-releasing nanoplatforms for wound treatment: an emerging approach. Chem. Eng. J. ***452***, 139297.
8. Mustafa, A. K., Gadalla, M. M. and Snyder, S. H. (2009). Signaling by gasotransmitters. Sci. Signal. ***2***, 268re2.
9. Yu, L., Hu, P. and Chen, Y. (2018). Gas-generating nanoplatforms: material chemistry, multifunctionality, and gas therapy. Adv. Mater. ***30***, 1801964.
10. Szabo, C. (2016). Gasotransmitters in cancer: from pathophysiology to experimental therapy. Nat. Rev. Drug Discov. ***15***, 185–203.
11. Zhou, Y., Yang, T., Liang, K., et al. (2021). Metal-organic frameworks for therapeutic gas delivery. Adv. Drug Deliv. Rev. ***171***, 199–214.
12. Wallace, J. L., Ianaro, A., Flannigan, K. L., et al. (2015). Gaseous mediators in resolution of inflammation. Semin. Immunol. ***27***, 227–233.
13. Farah, C., Michel, L. Y. M. and Balligand, J.-L. (2018). Nitric oxide signalling in cardiovascular health and disease. Nat. Rev. Cardiol. ***15***, 292–316.
14. Ling, K., Men, F., Wang, W.-C., et al. (2018). Carbon monoxide and its controlled release: therapeutic application, detection, and development of carbon monoxide releasing molecules (CORMs): miniperspective. J. Med. Chem. ***61***, 2611–2635.
15. Ding, H., Chang, J., He, F., et al. (2022). Hydrogen sulfide: an emerging precision strategy for gas therapy. Adv. Healthc. Mater. ***11***, 2101984.
16. Qian, Y. and Matson, J. B. (2017). Gasotransmitter delivery via self-assembling peptides: treating diseases with natural signaling gases. Adv. Drug Deliv. Rev. ***110–111***, 137–156.
17. Forstermann, U. and Sessa, W. C. (2012). Nitric oxide synthases: regulation and function. Eur. Heart J. ***33***, 829–837.
18. Kapil, V., Khambata, R. S., Jones, D. A., et al. (2020). The noncanonical pathway for in vivo nitric oxide generation: the nitrate-nitrite-nitric oxide pathway. Pharmacol. Rev. ***72***, 692–766.
19. Bogdan, C. (2001). Nitric oxide and the immune response. Nat. Immunol. ***2***, 907–916.
20. MacMicking, J., Xie, Q. and Nathan, C. (1997). Nitric oxide and macrophage function. Annu. Rev. Immunol. ***15***, 323–350.
21. Jin, G., Gao, Z., Liu, Y., et al. (2021). Polymeric nitric oxide delivery nanoplatforms for treating cancer, cardiovascular diseases, and infection. Adv. Healthc. Mater. ***10***, 2001550.
22. Vidanapathirana, A. K., Psaltis, P. J., Bursill, C. A., et al. (2021). Cardiovascular bioimaging of nitric oxide: achievements, challenges, and the future. Med. Res. Rev. ***41***, 435–463.
23. Wo, Y., Brisbois, E. J., Bartlett, R. H., et al. (2016). Recent advances in thromboresistant and antimicrobial polymers for biomedical applications: just say yes to nitric oxide (NO). Biomater. Sci. ***4***, 1161–1183.
24. Romão, C. C., Blättler, W. A., Seixas, J. D., et al. (2012). Developing drug molecules for

therapy with carbon monoxide. Chem. Soc. Rev. ***41***, 3571.
25. Motterlini, R. and Otterbein, L. E. (2010). The therapeutic potential of carbon monoxide. Nat. Rev. Drug Discov. ***9***, 728–743.
26. Heinemann, S. H., Hoshi, T., Westerhausen, M., et al. (2014). Carbon monoxide – physiology, detection and controlled release. Chem Commun ***50***, 3644–3660.
27. Boczkowski, J., Poderoso, J. J. and Motterlini, R. (2006). CO—metal interaction: vital signaling from a lethal gas. Trends Biochem. Sci. ***31***, 614–621.
28. Zhou, Y., Yu, W., Cao, J., et al. (2020). Harnessing carbon monoxide-releasing platforms for cancer therapy. Biomaterials ***255***, 120193.
29. Durante, W., Johnson, F. K. and Johnson, R. A. (2006). Role of carbon monxide in cardiovascular function. J. Cell. Mol. Med. ***10***, 672–686.
30. Bedard, K. and Krause, K.-H. (2007). The NOX family of ROS-generating NADPH oxidases: physiology and pathophysiology. Physiol. Rev. ***87***, 245–313.
31. Ryter, S. W. and Choi, A. M. K. (2016). Targeting heme oxygenase-1 and carbon monoxide for therapeutic modulation of inflammation. Transl. Res. ***167***, 7–34.
32. Nguyen, D. and Boyer, C. (2015). Macromolecular and inorganic nanomaterials scaffolds for carbon monoxide delivery: recent developments and future trends. ACS Biomater. Sci. Eng. ***1***, 895–913.
33. Szabó, C. (2007). Hydrogen sulphide and its therapeutic potential. Nat. Rev. Drug Discov. ***6***, 917–935.
34. Rong, F., Wang, T., Zhou, Q., et al. (2023). Intelligent polymeric hydrogen sulfide delivery systems for therapeutic applications. Bioact. Mater. ***19***, 198–216.
35. Hartle, M. D. and Pluth, M. D. (2016). A practical guide to working with H_2S at the interface of chemistry and biology. Chem. Soc. Rev. ***45***, 6108–6117.
36. Wang, R. (2012). Physiological implications of hydrogen sulfide: a whiff exploration that blossomed. Physiol. Rev. ***92***, 791–896.
37. Yang, J., Minkler, P., Grove, D., et al. (2019). Non-enzymatic hydrogen sulfide production from cysteine in blood is catalyzed by iron and vitamin B6. Commun. Biol. ***2***, 194.
38. Wallace, J. L. and Wang, R. (2015). Hydrogen sulfide-based therapeutics: exploiting a unique but ubiquitous gasotransmitter. Nat. Rev. Drug Discov. ***14***, 329–345.
39. Cuevasanta, E., Möller, M. N. and Alvarez, B. (2017). Biological chemistry of hydrogen sulfide and persulfides. Arch. Biochem. Biophys. ***617***, 9–25.
40. Paul, B. D. and Snyder, S. H. (2012). H_2S signalling through protein sulfhydration and beyond. Nat. Rev. Mol. Cell Biol. ***13***, 499–507.
41. Yao, X., Yang, B., Xu, J., et al. (2022). Novel gas - based nanomedicines for cancer therapy. VIEW ***3***, 20200185.
42. Chen, L., Zhou, S.-F., Su, L., et al. (2019). Gas-mediated cancer bioimaging and therapy. ACS Nano ***13***, 10887–10917.
43. Manoharan, D., Li, W.-P. and Yeh, C.-S. (2019). Advances in controlled gas-releasing nanomaterials for therapeutic applications. Nanoscale Horiz. ***4***, 557–578.
44. Carné-Sánchez, A., Carmona, F. J., Kim, C., et al. (2020). Porous materials as carriers of gasotransmitters towards gas biology and therapeutic applications. Chem. Commun. ***56***, 9750–9766.
45. Yang, L., Feura, E. S., Ahonen, M. J. R., et al. (2018). Nitric oxide-releasing macromolecular scaffolds for antibacterial applications. Adv. Healthc. Mater. ***7***, 1800155.
46. Divakaran, S. and Loscalzo, J. (2017). The role of nitroglycerin and other nitrogen oxides in cardiovascular therapeutics. J. Am. Coll. Cardiol. ***70***, 2393–2410.
47. Midgley, A. C., Wei, Y., Li, Z., et al. (2020). Nitric - oxide - releasing biomaterial regulation of the stem cell microenvironment in regenerative medicine. Adv. Mater. ***32***, 1805818.
48. Park, D., Saravanakumar, G. and Kim, W. J. (Elsevier, 2019). Nitric oxide-releasing functional nanomaterials for anticancer therapy. 191–218. doi:10.1016/B978-0-12-816545-4.00010-4.
49. Wu, M., Lu, Z., Wu, K., et al. (2021). Recent advances in the development of nitric oxide-releasing biomaterials and their application potentials in chronic wound healing. J. Mater. Chem. B ***9***, 7063–7075.
50. Yang, T., Zelikin, A. N. and Chandrawati, R. (2020). Enzyme mimics for the catalytic generation of nitric oxide from endogenous prodrugs. Small ***16***, 1907635.
51. Xiang, H., Guo, M. and Liu, J. (2017). Transition - metal nitrosyls for photocontrolled nitric oxide delivery. Eur. J. Inorg. Chem. ***2017***, 1586–1595.
52. Li, L. and Li, L. (2016). Recent advances in multinuclear metal nitrosyl complexes. Coord. Chem. Rev. ***306***, 678–700.
53. Huang, P.-J., Garcia, J. V., Fenwick, A., et al. (2019). Nitric oxide uncaging from a hydrophobic chromium (III) photoNORM: visible and near-infrared photochemistry in biocompatible polymer disks. ACS Omega ***4***, 9181–9187.
54. Rose, M. J. and Mascharak, P. K. (2008). Photoactive ruthenium nitrosyls: effects of light and potential application as NO donors. Coord. Chem. Rev. ***252***, 2093–2114.
55. Eroy-Reveles, A. A., Leung, Y., Beavers, C. M., et al. (2008). Near-infrared light activated release of nitric oxide from designed photoactive manganese nitrosyls: strategy, design, and potential as NO donors. J. Am. Chem. Soc. ***130***, 4447–4458.
56. Paul, S., Pan, S., Mukherjee, A., et al. (2021). Nitric oxide releasing delivery platforms: design, detection, biomedical applications, and future possibilities. Mol. Pharm. ***18***, 3181–3205.
57. Hou, L., Zhang, Y., Yang, X., et al. (2019). Intracellular NO-generator based on enzyme trigger for localized tumor-cytoplasm rapid drug release and synergetic cancer therapy. ACS Appl. Mater. Interfaces ***11***, 255–268.
58. Jo, Y. S., van der Vlies, A. J., Gantz, J., et al. (2009). Micelles for delivery of nitric oxide. J. Am. Chem. Soc. ***131***, 14413–14418.
59. Wu, W., Chen, M., Luo, T., et al. (2020). ROS and GSH-responsive S-nitrosoglutathione functionalized polymeric nanoparticles to overcome multidrug resistance in cancer. Acta Biomater. ***103***, 259–271.
60. Ding, Z., He, K., Duan, Y., et al. (2020). Photo-degradable micelles for co-delivery of nitric oxide and doxorubicin. J. Mater. Chem. B ***8***, 7009–7017.
61. Lin, Y.-J., Chen, C.-C., Chi, N.-W., et al. (2018). In situ self-assembling micellar depots that can actively trap and passively release NO with long-lasting activity to reverse osteoporosis. Adv. Mater. ***30***, 1705605.
62. van der Meel, R., Fens, M. H. A. M., Vader, P., et al. (2014). Extracellular vesicles as drug delivery systems: lessons from the liposome field. J. Controlled Release ***195***, 72–85.
63. Elnaggar, M. A., Seo, S. H., Gobaa, S., et al. (2016). Nitric oxide releasing coronary stent: a new approach using layer-by-layer coating and liposomal encapsulation. Small ***12***, 6012–6023.
64. Suchyta, D. J. and Schoenfisch, M. H. (2017). Controlled release of nitric oxide from liposomes. ACS Biomater. Sci. Eng. ***3***, 2136–2143.
65. Svenson, S. (2015). The dendrimer paradox – high medical expectations but poor clinical translation. Chem. Soc. Rev. ***44***, 4131–4144.
66. Stasko, N. A. and Schoenfisch, M. H. (2006). Dendrimers as a scaffold for nitric oxide release. J. Am. Chem. Soc. ***128***, 8265–8271.
67. Yang, L., Wang, X., Suchyta, D. J., et al. (2018). Antibacterial activity of nitric oxide-releasing hyperbranched polyamidoamines. Bioconjug. Chem. ***29***, 35–43.
68. Yu, S., Li, G., Liu, R., et al. (2018). Dendritic Fe_3O_4@Poly(dopamine)@PAMAM nanocomposite as controllable NO-releasing material: a synergistic photothermal and NO antibacterial study. Adv. Funct. Mater. ***28***, 1707440.
69. Ahonen, M. J. R., Suchyta, D. J., Zhu, H., et al. (2018). Nitric oxide-releasing alginates. Biomacromolecules ***19***, 1189–1197.
70. Li, M., Aveyard, J., Doherty, K. G., et al. (2022). Antimicrobial nitric oxide-releasing electrospun dressings for wound healing applications. ACS Mater. Au ***2***, 190–203.
71. Hoang Thi, T. T., Lee, Y., Le Thi, P., et al. (2018). Nitric oxide-releasing injectable hydrogels with high antibacterial activity through in situ formation of peroxynitrite. Acta Biomater. ***67***, 66–78.
72. Huang, S., Liu, H., Liao, K., et al. (2020). Functionalized GO nanovehicles with nitric oxide release and photothermal activity-based hydrogels for bacteria-infected wound healing. ACS Appl. Mater. Interfaces ***12***, 28952–28964.
73. Yang, Y., Zhou, Y., Li, Y., et al. (2021). Injectable and self-healing hydrogel containing nitric oxide donor for enhanced antibacterial activity. React. Funct. Polym. ***166***, 105003.
74. Deng, Y., Jia, F., Chen, X., et al. (2020). ATP suppression by pH - activated mitochondria - targeted delivery of nitric oxide nanoplatform for drug resistance reversal and metastasis inhibition. Small ***16***, 2001747.
75. Jin, H., Yang, L., Ahonen, M. J. R., et al. (2018). Nitric oxide-releasing cyclodextrins. J. Am. Chem. Soc. ***140***, 14178–14184.
76. Deng, Y., Jia, F., Chen, S., et al. (2018). Nitric oxide as an all-rounder for enhanced photodynamic therapy: hypoxia relief, glutathione depletion and reactive nitrogen species generation. Biomaterials ***187***, 55–65.
77. Oh, Y., Jeong, H., Lim, S., et al. (2020). Controlled nitric oxide release using poly(lactic-co-glycolic acid) nanoparticles for anti-inflammatory effects. Biomacromolecules ***21***, 4972–4979.
78. Hasan, N., Cao, J., Lee, J., et al. (2019). PEI/NONOates-doped PLGA nanoparticles for eradicating methicillin-resistant Staphylococcus aureus biofilm in diabetic wounds via binding to the biofilm matrix. Mater. Sci. Eng. C ***103***, 109741.
79. Lautner, G., Meyerhoff, M. E. and Schwendeman, S. P. (2016). Biodegradable poly(lactic-co-glycolic acid) microspheres loaded with S-nitroso-N-acetyl-D-penicillamine for controlled nitric oxide delivery. J. Controlled Release ***225***, 133–139.
80. Chung, M., Liu, H., Lin, K., et al. (2015). A pH - responsive carrier system that generates NO bubbles to trigger drug release and reverse P - glycoprotein - mediated multidrug resistance. Angew. Chem. Int. Ed. ***54***, 9890–9893.
81. Fan, J., He, Q., Liu, Y., et al. (2016). Light-responsive biodegradable nanomedicine overcomes multidrug resistance via NO-enhanced chemosensitization. ACS Appl. Mater. Interfaces ***8***, 13804–13811.
82. Soto, R. J., Yang, L. and Schoenfisch, M. H. (2016). Functionalized mesoporous silica via an aminosilane surfactant ion exchange reaction: controlled scaffold design and nitric oxide release. ACS Appl. Mater. Interfaces ***8***, 2220–2231.
83. Choi, H. W., Kim, J., Kim, J., et al. (2016). Light-induced acid generation on a gatekeeper for smart nitric oxide delivery. ACS Nano ***10***, 4199–4208.
84. Huang, Y., Zhang, J., Zhang, Y., et al. (2021). P-glycoprotein suppression by photothermal-responsive nitric oxide releasing nanoplatform for triple-combination therapy of multidrug resistant cancer. Mater. Des. ***211***, 110160.
85. Fan, W., Lu, N., Huang, P., et al. (2017). Glucose - responsive sequential generation of hydrogen peroxide and nitric oxide for synergistic cancer starving - like/gas therapy. Angew. Chem. ***129***, 1249–1253.
86. Yin, H., Guan, X., Lin, H., et al. (2020). Nanomedicine - enabled photonic thermogaseous cancer therapy. Adv. Sci. ***7***, 1901954.
87. Liu, T., Wei, J., Fu, G., et al. (2021). Surface charge switchable nanoparticles capable of controlled nitric oxide release for the treatment of acidity-associated bacterial

infections. Polym. Chem. ***12***, 1023–1029.

88. Riccio, D. A., Nugent, J. L. and Schoenfisch, M. H. (2011). Stöber synthesis of nitric oxide-releasing *S* -nitrosothiol-modified silica particles. Chem. Mater. ***23***, 1727–1735.
89. Jeong, H., Park, J.-H., Shin, J. H., et al. (2018). Prolonged release period of nitric oxide gas for treatment of bacterial keratitis by amine-rich polymer decoration of nanoparticles. Chem. Mater. ***30***, 8528–8537.
90. Hinks, N. J., McKinlay, A. C., Xiao, B., et al. (2010). Metal organic frameworks as NO delivery materials for biological applications. Microporous Mesoporous Mater. ***129***, 330–334.
91. Gregg, S. T., Yuan, Q., Morris, R. E., et al. (2017). Functionalised solids delivering bioactive nitric oxide gas for therapeutic applications. Mater. Today Commun. ***12***, 95–105.
92. Wan, S.-S., Zeng, J.-Y., Cheng, H., et al. (2018). ROS-induced NO generation for gas therapy and sensitizing photodynamic therapy of tumor. Biomaterials ***185***, 51–62.
93. Ji, H. B., Kim, S.-N., Kim, C. R., et al. (2023). Metal-organic framework for biomimetic nitric oxide generation and anticancer drug delivery. Biomater. Adv. ***145***, 213268.
94. Pinto, R. V., Wang, S., Tavares, S. R., et al. (2020). Tuning cellular biological functions through the controlled release of NO from a porous Ti - MOF. Angew. Chem. Int. Ed. ***59***, 5135–5143.
95. Chu, X., Jiang, X., Liu, Y., et al. (2021). Nitric oxide modulating calcium store for Ca^{2+} - initiated cancer therapy. Adv. Funct. Mater. ***31***, 2008507.
96. Neidrauer, M., Ercan, U. K., Bhattacharyya, A., et al. (2014). Antimicrobial efficacy and wound-healing property of a topical ointment containing nitric-oxide-loaded zeolites. J. Med. Microbiol. ***63***, 203–209.
97. Jiang, Y., Fu, P., Liu, Y., et al. (2020). Near-infrared light-triggered NO release for spinal cord injury repair. Sci. Adv. ***6***, eabc3513.
98. An, J., Hu, Y.-G., Li, C., et al. (2020). A pH/ultrasound dual-response biomimetic nanoplatform for nitric oxide gas-sonodynamic combined therapy and repeated ultrasound for relieving hypoxia. Biomaterials ***230***, 119636.
99. Yu, Y.-T., Shi, S.-W., Wang, Y., et al. (2020). A ruthenium nitrosyl-functionalized magnetic nanoplatform with near-infrared light-controlled nitric oxide delivery and photothermal effect for enhanced antitumor and antibacterial therapy. ACS Appl. Mater. Interfaces ***12***, 312–321.
100. Liu, T., Zhang, P., Huang, X., et al. (2019). Magnetic core-shell S-nitrosothiols nanoparticles as tumor dual-targeting theranostic platform. Colloids Surf. B Biointerfaces ***181***, 400–407.
101. Yang, F., Li, M., Liu, Y., et al. (2016). Glucose and magnetic-responsive approach toward in situ nitric oxide bubbles controlled generation for hyperglycemia theranostics. J. Controlled Release ***228***, 87–95.
102. Zhang, X., Tian, G., Yin, W., et al. (2015). Controllable generation of nitric oxide by near-infrared-sensitized upconversion nanoparticles for tumor therapy. Adv. Funct. Mater. ***25***, 3049–3056.
103. Li, C., Shen, J., Yang, J., et al. (2018). NIR-triggered release of nitric oxide with upconversion nanoparticles inhibits platelet aggregation in blood samples. Part. Part. Syst. Charact. ***35***, 1700281.
104. Tan, L., Huang, R., Li, X., et al. (2017). Controllable release of nitric oxide and doxorubicin from engineered nanospheres for synergistic tumor therapy. Acta Biomater. ***57***, 498–510.
105. Zhang, X., Guo, Z., Liu, J., et al. (2017). Near infrared light triggered nitric oxide releasing platform based on upconversion nanoparticles for synergistic therapy of cancer stem-like cells. Sci. Bull. ***62***, 985–996.
106. Wang, H., Liu, Y., Wang, Z., et al. (2018). 808 nm-light-excited upconversion nanoprobe based on LRET for the ratiometric detection of nitric oxide in living cancer cells. Nanoscale ***10***, 10641–10649.
107. Garcia, J. V., Yang, J., Shen, D., et al. (2012). NIR-triggered release of caged nitric oxide using upconverting nanostructured materials. Small ***8***, 3800–3805.
108. Yang, Y., Huang, K., Wang, M., et al. (2021). Ubiquitination flow repressors: enhancing wound healing of infectious diabetic ulcers through stabilization of polyubiquitinated hypoxia - inducible factor - 1α by Theranostic nitric oxide nanogenerators. Adv. Mater. ***33***, 2103593.
109. Sun, J., Fan, Y., Ye, W., et al. (2021). Near-infrared light triggered photodynamic and nitric oxide synergistic antibacterial nanocomposite membrane. Chem. Eng. J. ***417***, 128049.
110. Lee, H. J., Kim, D. E., Park, D. J., et al. (2016). pH-responsive mineralized nanoparticles as stable nanocarriers for intracellular nitric oxide delivery. Colloids Surf. B Biointerfaces ***146***, 1–8.
111. Massoumi, H., Kumar, R., Chug, M. K., et al. (2022). Nitric oxide release and antibacterial efficacy analyses of *S* -nitroso- *N* -acetyl-penicillamine conjugated to titanium dioxide nanoparticles. ACS Appl. Bio Mater. ***5***, 2285–2295.
112. Fan, J., He, N., He, Q., et al. (2015). A novel self-assembled sandwich nanomedicine for NIR-responsive release of NO. Nanoscale ***7***, 20055–20062.
113. Feng, T., Wan, J., Li, P., et al. (2019). A novel NIR-controlled NO release of sodium nitroprusside-doped prussian blue nanoparticle for synergistic tumor treatment. Biomaterials ***214***, 119213.
114. Li, Z., Huang, X., Lin, L., et al. (2021). Polyphenol and Cu^{2+} surface-modified chitin sponge synergizes with antibacterial, antioxidant and pro-vascularization activities for effective scarless regeneration of burned skin. Chem. Eng. J. ***419***, 129488.
115. Zhang, F., Zhang, Q., Li, X., et al. (2019). Mussel-inspired dopamine-CuII coatings for sustained in situ generation of nitric oxide for prevention of stent thrombosis and restenosis. Biomaterials ***194***, 117–129.
116. Lyu, N., Du, Z., Qiu, H., et al. (2020). Mimicking the nitric oxide - releasing and glycocalyx functions of endothelium on vascular stent surfaces. Adv. Sci. ***7***, 2002330.
117. Zhou, Y., Yang, T., Namivandi-Zangeneh, R., et al. (2021). Copper-doped metal–organic frameworks for the controlled generation of nitric oxide from endogenous *S* -nitrosothiols. J. Mater. Chem. B ***9***, 1059–1068.
118. Kulyk, K., Azizova, L., Cunningham, J. M., et al. (2020). Nanosized copper(ii) oxide/silica for catalytic generation of nitric oxide from *S* -nitrosothiols. J. Mater. Chem. B ***8***, 4267–4277.
119. Luo, Z., Zhou, Y., Yang, T., et al. (2022). Ceria nanoparticles as an unexpected catalyst to generate nitric oxide from *S* - nitrosoglutathione. Small ***18***, 2105762.
120. Yang, T., Fruergaard, A. S., Winther, A. K., et al. (2020). Zinc oxide particles catalytically generate nitric oxide from endogenous and exogenous prodrugs. Small ***16***, 1906744.
121. Chen, Y., Gao, P., Huang, L., et al. (2021). A tough nitric oxide-eluting hydrogel coating suppresses neointimal hyperplasia on vascular stent. Nat. Commun. ***12***, 7079.
122. Motterlini, R., Clark, J. E., Foresti, R., et al. (2002). Carbon monoxide-releasing molecules: characterization of biochemical and vascular activities. Circ. Res. ***90***, 17–24.
123. Santos-Silva, T., Mukhopadhyay, A., Seixas, J. D., et al. (2011). CORM-3 reactivity toward proteins: the crystal structure of a Ru(II) dicarbonyl–lysozyme complex. J. Am. Chem. Soc. ***133***, 1192–1195.
124. García-Gallego, S. and Bernardes, G. J. L. (2014). Carbon-monoxide-releasing molecules for the delivery of therapeutic co in vivo. Angew. Chem. Int. Ed. ***53***, 9712–9721.
125. Schatzschneider, U. (2011). PhotoCORMs: light-triggered release of carbon monoxide from the coordination sphere of transition metal complexes for biological applications. Inorganica Chim. Acta ***374***, 19–23.
126. Gonzales, M. A. and Mascharak, P. K. (2014). Photoactive metal carbonyl complexes as potential agents for targeted CO delivery. J. Inorg. Biochem. ***133***, 127–135.
127. Hu, J., Fang, Y., Huang, X., et al. (2021). Engineering macromolecular nanocarriers for local delivery of gaseous signaling molecules. Adv. Drug Deliv. Rev. ***179***, 114005.
128. Cheng, J., Gan, G., Shen, Z., et al. (2021). Red light - triggered intracellular carbon monoxide release enables selective eradication of MRSA infection. Angew. Chem. ***133***, 13625–13632.
129. Inaba, H., Fujita, K. and Ueno, T. (2015). Design of biomaterials for intracellular delivery of carbon monoxide. Biomater. Sci. ***3***, 1423–1438.
130. Zheng, D.-W., Li, B., Li, C.-X., et al. (2017). Photocatalyzing CO_2 to CO for enhanced cancer therapy. Adv. Mater. ***29***, 1703822.
131. Hasegawa, U., van der Vlies, A. J., Simeoni, E., et al. (2010). Carbon monoxide-releasing micelles for immunotherapy. J. Am. Chem. Soc. ***132***, 18273–18280.
132. Wang, X., Gao, B., Sebit Ahmed Suleiman, G., et al. (2021). A "controlled CO release" and "pro-angiogenic gene" dually engineered stimulus-responsive nanoplatform for collaborative ischemia therapy. Chem. Eng. J. ***424***, 130430.
133. Gao, L., Cheng, J., Shen, Z., et al. (2022). Orchestrating nitric oxide and carbon monoxide signaling molecules for synergistic treatment of MRSA infections. Angew. Chem. Int. Ed. ***61***, 202112782.
134. Sun, W., Gregory, D. A. and Zhao, X. (2023). Designed peptide amphiphiles as scaffolds for tissue engineering. Adv. Colloid Interface Sci. ***314***, 102866.
135. Matson, J. B., Webber, M. J., Tamboli, V. K., et al. (2012). A peptide-based material for therapeutic carbon monoxide delivery. Soft Matter ***8***, 6689.
136. Kim, I., Han, E. H., Bang, W.-Y., et al. (2018). Supramolecular carbon monoxide-releasing peptide hydrogel patch. Adv. Funct. Mater. ***28***, 1803051.
137. Wu, L., Cai, X., Zhu, H., et al. (2018). PDT-driven highly efficient intracellular delivery and controlled release of CO in combination with sufficient singlet oxygen production for synergistic anticancer therapy. Adv. Funct. Mater. ***28***, 1804324.
138. Ma, W., Chen, X., Fu, L., et al. (2020). Ultra-efficient antibacterial system based on photodynamic therapy and CO gas therapy for synergistic antibacterial and ablation biofilms. ACS Appl. Mater. Interfaces ***12***, 22479–22491.
139. Tabe, H., Fujita, K., Abe, S., et al. (2015). Preparation of a cross-linked porous protein crystal containing ru carbonyl complexes as a CO-releasing extracellular scaffold. Inorg. Chem. ***54***, 215–220.
140. Fujita, K., Tanaka, Y., Sho, T., et al. (2014). Intracellular CO release from composite of ferritin and ruthenium carbonyl complexes. J. Am. Chem. Soc. ***136***, 16902–16908.
141. Bohlender, C., Gläser, S., Klein, M., et al. (2014). Light-triggered CO release from nanoporous non-wovens. J Mater Chem B ***2***, 1454–1463.
142. Wang, Y., Liu, Z., Wang, H., et al. (2019). Starvation-amplified CO generation for enhanced cancer therapy via an erythrocyte membrane-biomimetic gas nanofactory. Acta Biomater. ***92***, 241–253.
143. Askes, S. H. C., Reddy, G. U., Wyrwa, R., et al. (2017). Red light-triggered CO release from $Mn_2(CO)_{10}$ using triplet sensitization in polymer nonwoven fabrics. J. Am. Chem. Soc. ***139***, 15292–15295.
144. Van der Vlies, A. J., Inubushi, R., Uyama, H., et al. (2016). Polymeric framboidal nanoparticles loaded with a carbon monoxide donor via phenylboronic acid-catechol complexation. Bioconjug. Chem. ***27***, 1500–1508.

145. Sun, P., Jia, L., Hai, J., et al. (2021). Tumor microenvironment - "and" near - infrared light - activated coordination polymer nanoprodrug for on - demand CO - sensitized synergistic cancer therapy. Adv. Healthc. Mater. ***10***, 2001728.
146. Carmona, F. J., Jiménez-Amezcua, I., Rojas, S., et al. (2017). Aluminum doped MCM-41 nanoparticles as platforms for the dual encapsulation of a CO-releasing molecule and cisplatin. Inorg. Chem. ***56***, 10474–10480.
147. Chakraborty, I., Carrington, S. J., Hauser, J., et al. (2015). Rapid eradication of human breast cancer cells through trackable light-triggered CO delivery by mesoporous silica nanoparticles packed with a designed photoCORM. Chem. Mater. ***27***, 8387–8397.
148. Gonzales, M. A., Han, H., Moyes, A., et al. (2014). Light-triggered carbon monoxide delivery with Al-MCM-41-based nanoparticles bearing a designed manganese carbonyl complex. J. Mater. Chem. B ***2***, 2107.
149. Jin, Z., Wen, Y., Xiong, L., et al. (2017). Intratumoral H_2O_2 -triggered release of CO from a metal carbonyl-based nanomedicine for efficient CO therapy. Chem. Commun. ***53***, 5557–5560.
150. Zhang, C., Peng, S.-Y., Hong, S., et al. (2020). Biomimetic carbon monoxide nanogenerator ameliorates streptozotocin induced type 1 diabetes in mice. Biomaterials ***245***, 119986.
151. Yao, X., Yang, P., Jin, Z., et al. (2019). Multifunctional nanoplatform for photoacoustic imaging-guided combined therapy enhanced by CO induced ferroptosis. Biomaterials ***197***, 268–283.
152. Dördelmann, G., Pfeiffer, H., Birkner, A., et al. (2011). Silicium dioxide nanoparticles as carriers for photoactivatable CO-releasing molecules (PhotoCORMs). Inorg. Chem. ***50***, 4362–4367.
153. Meng, J., Jin, Z., Zhao, P., et al. (2020). A multistage assembly/disassembly strategy for tumor-targeted CO delivery. Sci. Adv. ***6***, eaba1362.
154. Yuan, Z., Lin, C., Dai, L., et al. (2021). Near - infrared light - activatable dual - action nanoparticle combats the established biofilms of methicillin - resistant staphylococcus aureus and its accompanying inflammation. Small ***17***, 2007522.
155. Wu, D., Duan, X., Guan, Q., et al. (2019). Mesoporous polydopamine carrying manganese carbonyl responds to tumor microenvironment for multimodal imaging - guided cancer therapy. Adv. Funct. Mater. ***29***, 1900095.
156. Qin, Z., Li, Y. and Gu, N. (2018). Progress in applications of prussian blue nanoparticles in biomedicine. Adv. Healthc. Mater. ***7***, 1800347.
157. Li, W.-P., Su, C.-H., Tsao, L.-C., et al. (2016). Controllable CO release following near-infrared light-induced cleavage of iron carbonyl derivatized prussian blue nanoparticles for CO-assisted synergistic treatment. ACS Nano ***10***, 11027–11036.
158. Li, Y., Dang, J., Liang, Q., et al. (2019). Thermal-responsive carbon monoxide (CO) delivery expedites metabolic exhaustion of cancer cells toward reversal of chemotherapy resistance. ACS Cent. Sci. ***5***, 1044–1058.
159. Li, Y., Dang, J., Liang, Q., et al. (2019). Carbon monoxide (CO)-strengthened cooperative bioreductive anti-tumor therapy via mitochondrial exhaustion and hypoxia induction. Biomaterials ***209***, 138–151.
160. Zheng, S., Dou, P., Jin, S., et al. (2021). Tumor microenvironment/NIR-responsive carbon monoxide delivery with hollow mesoporous CuS nanoparticles for MR imaging guided synergistic therapy. Mater. Des. ***205***, 109731.
161. Pierri, A. E., Huang, P.-J., Garcia, J. V., et al. (2015). A photoCORM nanocarrier for CO release using NIR light. Chem. Commun. ***51***, 2072–2075.
162. Ghosh, P., Han, G., De, M., et al. (2008). Gold nanoparticles in delivery applications. Adv. Drug Deliv. Rev. ***60***, 1307–1315.
163. Wang, X.-S., Zeng, J.-Y., Li, M.-J., et al. (2020). Highly stable iron carbonyl complex delivery nanosystem for improving cancer therapy. ACS Nano ***14***, 9848–9860.
164. Carmona, F. J., Rojas, S., Romão, C. C., et al. (2017). One-pot preparation of a novel CO-releasing material based on a CO-releasing molecule@metal–organic framework system. Chem. Commun. ***53***, 6581–6584.
165. Diring, S., Carné-Sánchez, A., Zhang, J., et al. (2017). Light responsive metal–organic frameworks as controllable CO-releasing cell culture substrates. Chem. Sci. ***8***, 2381–2386.
166. Carmona, F. J., Rojas, S., Sánchez, P., et al. (2016). Cation exchange strategy for the encapsulation of a photoactive CO-releasing organometallic molecule into anionic porous frameworks. Inorg. Chem. ***55***, 6525–6531.
167. Carmona, F. J., Maldonado, C. R., Ikemura, S., et al. (2018). Coordination modulation method to prepare new metal–organic framework-based CO-releasing materials. ACS Appl. Mater. Interfaces ***10***, 31158–31167.
168. Jin, Z., Zhao, P., Zhang, J., et al. (2018). Intelligent metal carbonyl metal–organic framework nanocomplex for fluorescent traceable H_2O_2 - triggered CO delivery. Chem. – Eur. J. ***24***, 11667–11674.
169. He, Q., Kiesewetter, D. O., Qu, Y., et al. (2015). NIR-responsive on-demand release of CO from metal carbonyl-caged graphene oxide nanomedicine. Adv. Mater. ***27***, 6741–6746.
170. Tan, M. J., Pan, H.-C., Tan, H. R., et al. (2018). Flexible modulation of CO-release using various nuclearity of metal carbonyl clusters on graphene oxide for stroke remediation. Adv. Healthc. Mater. ***7***, 1701113.
171. Fang, C., Cen, D., Wang, Y., et al. (2020). ZnS@ZIF-8 core-shell nanoparticles incorporated with ICG and TPZ to enable H_2S-amplified synergistic therapy. Theranostics ***10***, 7671–7682.
172. Xie, C., Cen, D., Ren, Z., et al. (2020). FeS@BSA nanoclusters to enable H_2S - amplified ROS - based therapy with MRI guidance. Adv. Sci. ***7***, 1903512.
173. Yang, Z., Luo, Y., Hu, Y., et al. (2021). Photothermo - promoted nanocatalysis combined with H_2S - mediated respiration inhibition for efficient cancer therapy. Adv. Funct. Mater. ***31***, 2007991.
174. He, T., Qin, X., Jiang, C., et al. (2020). Tumor pH-responsive metastable-phase manganese sulfide nanotheranostics for traceable hydrogen sulfide gas therapy primed chemodynamic therapy. Theranostics ***10***, 2453–2462.
175. Zheng, H., Ma, B., Shi, Y., et al. (2021). Tumor microenvironment-triggered MoS2@GA-Fe nanoreactor: a self-rolling enhanced chemodynamic therapy and hydrogen sulfide treatment for hepatocellular carcinoma. Chem. Eng. J. ***406***, 126888.
176. Ozturk, T., Ertas, E. and Mert, O. (2007). Use of lawesson's reagent in organic syntheses. Chem. Rev. ***107***, 5210–5278.
177. Li, L., Whiteman, M., Guan, Y. Y., et al. (2008). Characterization of a novel, water-soluble hydrogen sulfide–releasing molecule (GYY4137): new insights into the biology of hydrogen sulfide. Circulation ***117***, 2351–2360.
178. Kang, J., Li, Z., Organ, C. L., et al. (2016). pH-controlled hydrogen sulfide release for myocardial ischemia-reperfusion injury. J. Am. Chem. Soc. ***138***, 6336–6339.
179. Pluth, M., Bailey, T., Hammers, M., et al. (2015). Natural products containing hydrogen sulfide releasing moieties. Synlett ***26***, 2633–2643.
180. Powell, C. R., Dillon, K. M. and Matson, J. B. (2018). A review of hydrogen sulfide (H_2S) donors: chemistry and potential therapeutic applications. Biochem. Pharmacol. ***149***, 110–123.
181. Zheng, Y., Yu, B., Ji, K., et al. (2016). Esterase-sensitive prodrugs with tunable release rates and direct generation of hydrogen sulfide. Angew. Chem. Int. Ed. ***55***, 4514–4518.
182. Shukla, P., Khodade, V. S., SharathChandra, M., et al. (2017). "On demand" redox buffering by H_2S contributes to antibiotic resistance revealed by a bacteria-specific H_2S donor. Chem. Sci. ***8***, 4967–4972.
183. Devarie-Baez, N. O., Bagdon, P. E., Peng, B., et al. (2013). Light-induced hydrogen sulfide release from "caged" gem -dithiols. Org. Lett. ***15***, 2786–2789.
184. Fukushima, N., Ieda, N., Sasakura, K., et al. (2014). Synthesis of a photocontrollable hydrogen sulfide donor using ketoprofenate photocages. Chem Commun ***50***, 587–589.
185. Xiao, Z., Bonnard, T., Shakouri-Motlagh, A., et al. (2017). Triggered and tunable hydrogen sulfide release from photogenerated thiobenzaldehydes. Chem. - Eur. J. ***23***, 11294–11300.
186. Venkatesh, Y., Das, J., Chaudhuri, A., et al. (2018). Light triggered uncaging of hydrogen sulfide (H_2S) with real-time monitoring. Chem. Commun. ***54***, 3106–3109.
187. Powell, C. R., Foster, J. C., Okyere, B., et al. (2016). Therapeutic delivery of H_2S via COS: small molecule and polymeric donors with benign byproducts. J. Am. Chem. Soc. ***138***, 13477–13480.
188. Steiger, A. K., Pardue, S., Kevil, C. G., et al. (2016). Self-immolative thiocarbamates provide access to triggered H_2S donors and analyte replacement fluorescent probes. J. Am. Chem. Soc. ***138***, 7256–7259.
189. Li, J., Xie, L., Sang, W., et al. (2022). A metal - phenolic nanosensitizer performs hydrogen sulfide - reprogrammed oxygen metabolism for cancer radiotherapy intensification and immunogenicity. Angew. Chem. Int. Ed. ***61***, 202200830.
190. Zhao, X., Liu, L., An, T., et al. (2020). A hydrogen sulfide-releasing alginate dressing for effective wound healing. Acta Biomater. ***104***, 85–94.
191. Zheng, Z., Chen, A., He, H., et al. (2019). pH and enzyme dual-responsive release of hydrogen sulfide for disc degeneration therapy. J. Mater. Chem. B ***7***, 611–618.
192. Wu, J., Chen, A., Zhou, Y., et al. (2019). Novel H_2S-releasing hydrogel for wound repair via in situ polarization of M2 macrophages. Biomaterials ***222***, 119398.
193. Wu, J., Li, Y., He, C., et al. (2016). Novel H_2S releasing nanofibrous coating for in vivo dermal wound regeneration. ACS Appl. Mater. Interfaces ***8***, 27474–27481.
194. Hsieh, M.-H., Tsai, H.-W., Lin, K.-J., et al. (2019). An in situ slow-releasing H_2S donor depot with long-term therapeutic effects for treating ischemic diseases. Mater. Sci. Eng. C ***104***, 109954.
195. Ciocci, M., Iorio, E., Carotenuto, F., et al. (2016). H_2S-releasing nanoemulsions: a new formulation to inhibit tumor cells proliferation and improve tissue repair. Oncotarget ***7***, 84338–84358.
196. Zheng, Z., Chen, Q., Dai, R., et al. (2020). A continuous stimuli-responsive system for NIR-II fluorescence/photoacoustic imaging guided photothermal/gas synergistic therapy. Nanoscale ***12***, 11562–11572.
197. Li, J., Li, X., Yuan, Y., et al. (2020). Efficient polysulfide - based nanotheranostics for triple - negative breast cancer: ratiometric photoacoustics monitored tumor microenvironment - initiated H_2S therapy. Small ***16***, 2002939.
198. Li, J., Xie, L., Li, B., et al. (2021). Engineering a hydrogen - sulfide - based nanomodulator to normalize hyperactive photothermal immunogenicity for combination cancer therapy. Adv. Mater. ***33***, 2008481.
199. Liu, Y., Yang, F., Yuan, C., et al. (2017). Magnetic nanoliposomes as in situ microbubble bombers for multimodality image-guided cancer theranostics. ACS Nano ***11***, 1509–1519.
200. Liu, Y., Li, J., Chen, H., et al. (2019). Magnet-activatable nanoliposomes as intracellular bubble microreactors to enhance drug delivery efficacy and burst cancer cells. Nanoscale ***11***, 18854–18865.
201. Yao, T., van Nunen, T., Rivero, R., et al. (2022). Electrospun scaffolds functionalized with a hydrogen sulfide donor stimulate angiogenesis. ACS Appl. Mater. Interfaces

14, 28628–28638.
202. Liang, W., Chen, J., Li, L., et al. (2019). Conductive hydrogen sulfide-releasing hydrogel encapsulating ADSCs for myocardial infarction treatment. ACS Appl. Mater. Interfaces *11*, 14619–14629.
203. Takatani-Nakase, T., Katayama, M., Matsui, C., et al. (2017). Hydrogen sulfide donor micelles protect cardiomyocytes from ischemic cell death. Mol. Biosyst. *13*, 1705–1708.
204. Le, T.-N., Ru, H., Lee, C.-K., et al. (2022). Polynorbornene-derived block copolymer micelles via ring - opening metathesis polymerization with capacity of hydrogen sulfide generation. Eur. Polym. J. *173*, 111294.
205. Liu, D., Liao, Y., Cornel, E. J., et al. (2021). Polymersome wound dressing spray capable of bacterial inhibition and H_2S generation for complete diabetic wound healing. Chem. Mater. *33*, 7972–7985.
206. Longchamp, A., Kaur, K., Macabrey, D., et al. (2019). Hydrogen sulfide-releasing peptide hydrogel limits the development of intimal hyperplasia in human vein segments. Acta Biomater. *97*, 374–384.
207. Sun, X., Kong, B., Wang, W., et al. (2015). Mesoporous silica nanoparticles for glutathione-triggered long-range and stable release of hydrogen sulfide. J. Mater. Chem. B *3*, 4451–4457.
208. Xia, W., Yan, T., Wen, L., et al. (2022). Hypothermia-triggered mesoporous silica particles for controlled release of hydrogen sulfide to reduce the I/R injury of the myocardium. ACS Biomater. Sci. Eng. *8*, 2970–2978.
209. Liu, B., Liang, S., Wang, Z., et al. (2021). A tumor - microenvironment - responsive nanocomposite for hydrogen sulfide gas and trimodal - enhanced enzyme dynamic therapy. Adv. Mater. *33*, 2101223.
210. Chen, F. E., Mandel, R. M., Woods, J. J., et al. (2021). Biocompatible metal–organic frameworks for the storage and therapeutic delivery of hydrogen sulfide. Chem. Sci. *12*, 7848–7857.
211. Allan, P. K., Wheatley, P. S., Aldous, D., et al. (2012). Metal–organic frameworks for the storage and delivery of biologically active hydrogen sulfide. Dalton Trans. *41*, 4060.
212. Chen, W., Chen, M., Zang, Q., et al. (2015). NIR light controlled release of caged hydrogen sulfide based on upconversion nanoparticles. Chem. Commun. *51*, 9193–9196.
213. Li, H., Yao, Y., Shi, H., et al. (2019). A near-infrared light-responsive nanocomposite for photothermal release of H_2S and suppression of cell viability. J. Mater. Chem. B *7*, 5992–5997.
214. Tande, A. J. and Patel, R. (2014). Prosthetic joint infection. Clin. Microbiol. Rev. *27*, 302–345.
215. Arciola, C. R., Campoccia, D. and Montanaro, L. (2018). Implant infections: adhesion, biofilm formation and immune evasion. Nat. Rev. Microbiol. *16*, 397–409.
216. Wang, T.-Y., Zhu, X.-Y. and Wu, F.-G. (2023). Antibacterial gas therapy: strategies, advances, and prospects. Bioact. Mater. *23*, 129–155.
217. Holt, J., Hertzberg, B., Weinhold, P., et al. (2011). Decreasing bacterial colonization of external fixation pins through nitric oxide release coatings. J. Orthop. Trauma *25*, 432–437.
218. Wang, J., Wang, L., Pan, J., et al. (2021). Magneto - based synergetic therapy for implant - associated infections via biofilm disruption and innate immunity regulation. Adv. Sci. *8*, 2004010.
219. Li, Y., Liu, X., Li, B., et al. (2020). Near-infrared light triggered phototherapy and immunotherapy for elimination of methicillin-resistant staphylococcus aureus biofilm infection on bone implant. ACS Nano *14*, 8157–8170.
220. Li, M., Aveyard, J., Fleming, G., et al. (2020). Nitric oxide releasing titanium surfaces for antimicrobial bone-integrating orthopedic implants. ACS Appl. Mater. Interfaces *12*, 22433–22443.
221. Zhang, G., Wu, Z., Yang, Y., et al. (2022). A multifunctional antibacterial coating on bone implants for osteosarcoma therapy and enhanced osteointegration. Chem. Eng. J. *428*, 131155.
222. Davidge, K. S., Sanguinetti, G., Yee, C. H., et al. (2009). Carbon monoxide-releasing antibacterial molecules target respiration and global transcriptional regulators. J. Biol. Chem. *284*, 4516–4524.
223. Nobre, L. S., Seixas, J. D., Romão, C. C., et al. (2007). Antimicrobial action of carbon monoxide-releasing compounds. antimicrob. Agents Chemother. *51*, 4303–4307.
224. Wareham, L. K., Poole, R. K. and Tinajero-Trejo, M. (2015). CO-releasing metal carbonyl compounds as antimicrobial agents in the post-antibiotic era. J. Biol. Chem. *290*, 18999–19007.
225. Klinger-Strobel, M., Gläser, S., Makarewicz, O., et al. (2016). Bactericidal effect of a photoresponsive carbon monoxide-releasing nonwoven against staphylococcus aureus biofilms. Antimicrob. Agents Chemother. *60*, 4037–4046.
226. Wegiel, B., Larsen, R., Gallo, D., et al. (2014). Macrophages sense and kill bacteria through carbon monoxide–dependent inflammasome activation. J. Clin. Invest. *124*, 4926–4940.
227. Yuan, Z., Wu, J., Fu, Z., et al. (2022). Polydopamine - mediated interfacial functionalization of implants for accelerating infected bone repair through light - activatable antibiosis and carbon monoxide gas regulated macrophage polarization. Adv. Funct. Mater. *32*, 2200374.
228. Mendes, S. S., Miranda, V. and Saraiva, L. M. (2021). Hydrogen sulfide and carbon monoxide tolerance in bacteria. Antioxidants *10*, 729.
229. Su, Z., Kong, L., Dai, Y., et al. (2022). Bioresponsive nano-antibacterials for H_2S-sensitized hyperthermia and immunomodulation against refractory implant–related infections. Sci. Adv. *8*, 1701.
230. Su, N., Villicana, C. and Yang, F. (2022). Immunomodulatory strategies for bone regeneration: A review from the perspective of disease types. Biomaterials *286*, 121604.
231. Kzhyshkowska, J., Gudima, A., Riabov, V., et al. (2015). Macrophage responses to implants: prospects for personalized medicine. J. Leukoc. Biol. *98*, 953–962.
232. Fullerton, J. N. and Gilroy, D. W. (2016). Resolution of inflammation: a new therapeutic frontier. Nat. Rev. Drug Discov. *15*, 551–567.
233. Newman, H., Shih, Y. V. and Varghese, S. (2021). Resolution of inflammation in bone regeneration: from understandings to therapeutic applications. Biomaterials *277*, 121114.
234. Ding, J., Venkatesan, R., Zhai, Z., et al. (2020). Micro- and nanoparticles-based immunoregulation of macrophages for tissue repair and regeneration. Colloids Surf. B Biointerfaces *192*, 111075.
235. He, J., Chen, G., Liu, M., et al. (2020). Scaffold strategies for modulating immune microenvironment during bone regeneration. Mater. Sci. Eng. C *108*, 110411.
236. Korhonen, R., Lahti, A., Kankaanranta, H., et al. (2005). Nitric oxide production and signaling in inflammation. Curr. Drug Target -Inflamm. Allergy *4*, 471–479.
237. Lo Faro, M. L., Fox, B., Whatmore, J. L., et al. (2014). Hydrogen sulfide and nitric oxide interactions in inflammation. Nitric Oxide *41*, 38–47.
238. Palmieri, E. M., Gonzalez-Cotto, M., Baseler, W. A., et al. (2020). Nitric oxide orchestrates metabolic rewiring in M1 macrophages by targeting aconitase 2 and pyruvate dehydrogenase. Nat. Commun. *11*, 698.
239. Won, J., Kim, W. J., Shim, J. S., et al. (2022). Guided bone regeneration with a nitric - oxide releasing polymer inducing angiogenesis and osteogenesis in critical - sized bone Defects. Macromol. Biosci. *22*, 2200162.
240. Qi, M., Ren, X., Li, W., et al. (2022). NIR responsive nitric oxide nanogenerator for enhanced biofilm eradication and inflammation immunotherapy against periodontal diseases. Nano Today *43*, 101447.
241. Liu, T., Han, Q., Pan, Y., et al. (2021). Carbon monoxide-releasing molecule-3 regulates the polarization of lipopolysaccharide-induced macrophages. Inflammation *44*, 1737–1749.
242. Liu, C., Du, Z., Ma, M., et al. (2020). Carbon monoxide controllable targeted gas therapy for synergistic anti-inflammation. iScience *23*, 101483.
243. Zhang, J., Tong, D., Song, H., et al. (2022). Osteoimmunity - regulating biomimetically hierarchical scaffold for augmented bone regeneration. Adv. Mater. *34*, 2202044.
244. Whiteman, M., Li, L., Rose, P., et al. (2010). The effect of hydrogen sulfide donors on lipopolysaccharide-induced formation of inflammatory mediators in macrophages. Antioxid. Redox Signal. *12*, 1147–1154.
245. Huang, C. W., Feng, W., Peh, M. T., et al. (2016). A novel slow-releasing hydrogen sulfide donor, FW1256, exerts anti-inflammatory effects in mouse macrophages and in vivo. Pharmacol. Res. *113*, 533–546.
246. Loi, F., Córdova, L. A., Pajarinen, J., et al. (2016). Inflammation, fracture and bone repair. Bone *86*, 119–130.
247. Mancini, L., Moradi-Bidhendi, N., Becherini, L., et al. (2000). The biphasic effects of nitric oxide in primary rat osteoblasts are cGMP dependent. Biochem. Biophys. Res. Commun. *274*, 477–481.
248. Wimalawansa, S. J. (2010). Nitric oxide and bone. Ann. N. Y. Acad. Sci. *1192*, 391–403.
249. Nichols, S. P., Storm, W. L., Koh, A., et al. (2012). Local delivery of nitric oxide: targeted delivery of therapeutics to bone and connective tissues. Adv. Drug Deliv. Rev. *64*, 1177–1188.
250. Kalyanaraman, H., Schall, N. and Pilz, R. B. (2018). Nitric oxide and cyclic GMP functions in bone. Nitric Oxide *76*, 62–70.
251. Hankenson, K. D., Dishowitz, M., Gray, C., et al. (2011). Angiogenesis in bone regeneration. Injury *42*, 556–561.
252. Fukumura, D., Kashiwagi, S. and Jain, R. K. (2006). The role of nitric oxide in tumour progression. Nat. Rev. Cancer *6*, 521–534.
253. Yang, Q., Yin, H., Xu, T., et al. (2020). Engineering 2D mesoporous silica@MXene - integrated 3D - printing scaffolds for combinatory osteosarcoma therapy and NO - augmented bone regeneration. Small *16*, 1906814.
254. Li, J., Song, L., Hou, M., et al. (2018). Carbon monoxide releasing molecule-3 promotes the osteogenic differentiation of rat bone marrow mesenchymal stem cells by releasing carbon monoxide. Int. J. Mol. Med. *41*, 2297–2305.
255. Behera, J., Tyagi, S. C. and Tyagi, N. (2019). Role of hydrogen sulfide in the musculoskeletal system. Bone *124*, 33–39.
256. Liu, Y., Yang, R., Liu, X., et al. (2014). Hydrogen sulfide maintains mesenchymal stem cell function and bone homeostasis via regulation of Ca^{2+} channel sulfhydration. Cell Stem Cell *15*, 66–78.
257. Zheng, Y., Liao, F., Lin, X., et al. (2017). Cystathionine γ-lyase–hydrogen sulfide induces runt-related transcription factor 2 sulfhydration, thereby increasing osteoblast activity to promote bone fracture healing. Antioxid. Redox Signal. *27*, 742–753.
258. Song, A. and Hua, Y. (2020). Cystathionine γ-lyase-H_2S facilitates mandibular defect healing via inducing osteogenic differentiation of bone marrow mesenchymal stem cells. Arch. Oral Biol. *117*, 104821.

259. Liu, Y., Liu, J., Li, X., et al. (2017). Exogenous H_2S prevents high glucose-induced damage to osteoblasts through regulation of KATP channels. Biochimie ***137***, 151–157.
260. Zhai, Y., Behera, J., Tyagi, S. C., et al. (2019). Hydrogen sulfide attenuates homocysteine - induced osteoblast dysfunction by inhibiting mitochondrial toxicity. J. Cell. Physiol. ***234***, 18602–18614.
261. Ma, J., Fu, Q., Wang, Z., et al. (2019). Sodium hydrosulfide mitigates dexamethasone - induced osteoblast dysfunction by interfering with mitochondrial function. Biotechnol. Appl. Biochem. ***66***, 690–697.
262. Xu, Z.-S., Wang, X.-Y., Xiao, D.-M., et al. (2011). Hydrogen sulfide protects MC3T3-E1 osteoblastic cells against H_2O_2-induced oxidative damage —implications for the treatment of osteoporosis. Free Radic. Biol. Med. ***50***, 1314–1323.
263. Papapetropoulos, A., Pyriochou, A., Altaany, Z., et al. (2009). Hydrogen sulfide is an endogenous stimulator of angiogenesis. Proc. Natl. Acad. Sci. ***106***, 21972–21977.
264. Zhou, X., Liu, J., Zheng, Y., et al. (2022). SM22α-lineage niche cells regulate intramembranous bone regeneration via PDGFRβ-triggered hydrogen sulfide production. Cell Rep. ***39***, 110750.
265. Gambari, L., Amore, E., Raggio, R., et al. (2019). Hydrogen sulfide-releasing silk fibroin scaffold for bone tissue engineering. Mater. Sci. Eng. C ***102***, 471–482.
266. Raggio, R., Bonani, W., Callone, E., et al. (2018). Silk fibroin porous scaffolds loaded with a slow-releasing hydrogen sulfide agent (GYY4137) for applications of tissue engineering. ACS Biomater. Sci. Eng. ***4***, 2956–2966.
267. Al-Bishari, A. M., Yie, K. H. R., Al-Baadani, M. A., et al. (2021). JK-2 loaded electrospun membrane for promoting bone regeneration. Mater. Sci. Eng. C ***130***, 112471.
268. Eastell, R., O'Neill, T. W., Hofbauer, L. C., et al. (2016). Postmenopausal osteoporosis. Nat. Rev. Dis. Primer ***2***, 1–16.
269. Weitzmann, M. N. and Pacifici, R. (2006). Estrogen deficiency and bone loss: an inflammatory tale. J. Clin. Invest. ***116***, 1186–1194.
270. Wimalawansa, S. J. (2008). Nitric oxide: novel therapy for osteoporosis. Expert Opin. Pharmacother. ***9***, 3025–3044.
271. Hukkanen, M., Platts, L. A. M., Lawes, T., et al. (2003). Effect of nitric oxide donor nitroglycerin on bone mineral density in a rat model of estrogen deficiency-induced osteopenia. Bone ***32***, 142–149.
272. Kalyanaraman, H., Ramdani, G., Joshua, J., et al. (2017). A novel, direct NO donor regulates osteoblast and osteoclast functions and increases bone mass in ovariectomized mice: bone anabolic effects of a novel NO donor. J. Bone Miner. Res. ***32***, 46–59.
273. Ye, J., Jiang, J., Zhou, Z., et al. (2021). Near-infrared light and upconversion nanoparticle defined nitric oxide-based osteoporosis targeting therapy. ACS Nano ***15***, 13692–13702.
274. Lee, J., Kim, D., Park, S., et al. (2023). Nitric oxide - releasing bioinspired scaffold for exquisite regeneration of osteoporotic bone via regulation of homeostasis. Adv. Sci. ***10***, 2205336.
275. Van Phan, T., Sul, O.-J., Ke, K., et al. (2013). Carbon monoxide protects against ovariectomy-induced bone loss by inhibiting osteoclastogenesis. Biochem. Pharmacol. ***85***, 1145–1152.
276. Tseng, F.-J., Chia, W.-T., Wang, C.-H., et al. (2015). Carbon monoxide inhibits receptor activator of NF-κB (RANKL)-induced osteoclastogenesis. Cell. Physiol. Biochem. ***36***, 1250–1258.
277. Bak, S.-U., Kim, S., Hwang, H.-J., et al. (2017). Heme oxygenase-1 (HO-1)/carbon monoxide (CO) axis suppresses RANKL-induced osteoclastic differentiation by inhibiting redox-sensitive NF-κB activation. BMB Rep. ***50***, 103–108.
278. Grassi, F., Tyagi, A. M., Calvert, J. W., et al. (2016). Hydrogen sulfide is a novel regulator of bone formation implicated in the bone loss induced by estrogen deficiency: hydrogen sulfide deficiency mediates ovariectomy induced bone loss. J. Bone Miner. Res. ***31***, 949–963.
279. Gambari, L., Lisignoli, G., Cattini, L., et al. (2014). Sodium hydrosulfide inhibits the differentiation of osteoclast progenitor cells via NRF2-dependent mechanism. Pharmacol. Res. ***87***, 99–112.
280. McInnes, I. B. (2011). The Pathogenesis of Rheumatoid Arthritis. N. Engl. J. Med. ***365***, 2205–2219.
281. Sulzbacher, I. (2013). Osteoarthritis: histology and pathogenesis. Wien. Med. Wochenschr. ***163***, 212–219.
282. Perretti, M., Cooper, D., Dalli, J., et al. (2017). Immune resolution mechanisms in inflammatory arthritis. Nat. Rev. Rheumatol. ***13***, 87–99.
283. Spiller, F., Oliveira Formiga, R., Fernandes Da Silva Coimbra, J., et al. (2019). Targeting nitric oxide as a key modulator of sepsis, arthritis and pain. Nitric Oxide ***89***, 32–40.
284. Yeo, J., Lee, Y. M., Lee, J., et al. (2019). Nitric oxide-scavenging nanogel for treating rheumatoid arthritis. Nano Lett. ***19***, 6716–6724.
285. Kim, T., Suh, J. and Kim, W. J. (2021). Polymeric aggregate - embodied hybrid nitric - oxide - scavenging and sequential drug - releasing hydrogel for combinatorial treatment of rheumatoid arthritis. Adv. Mater. ***33***, 2008793.
286. Chen, X., Liu, Y., Wen, Y., et al. (2019). A photothermal-triggered nitric oxide nanogenerator combined with siRNA for precise therapy of osteoarthritis by suppressing macrophage inflammation. Nanoscale ***11***, 6693–6709.
287. Megías, J., Guillén, M. I., Bru, A., et al. (2008). The Carbon monoxide-releasing molecule tricarbonyldichlororuthenium (II) dimer protects human osteoarthritic chondrocytes and cartilage from the catabolic actions of interleukin-1β. J. Pharmacol. Exp. Ther. ***325***, 56–61.
288. Guillen, M. I., Megias, J., Clerigues, V., et al. (2008). The CO-releasing molecule CORM-2 is a novel regulator of the inflammatory process in osteoarthritic chondrocytes. Rheumatology ***47***, 1323–1328.
289. Ferrandiz, M. L., Maicas, N., Garcia-Arnandis, I., et al. (2007). Treatment with a CO-releasing molecule (CORM-3) reduces joint inflammation and erosion in murine collagen-induced arthritis. Ann. Rheum. Dis. ***67***, 1211–1217.
290. Tao, S., Cheng, J., Su, G., et al. (2020). Breathing micelles for combinatorial treatment of rheumatoid arthritis. Angew. Chem. Int. Ed. ***59***, 21864–21869.
291. Yang, G., Fan, M., Zhu, J., et al. (2020). A multifunctional anti-inflammatory drug that can specifically target activated macrophages, massively deplete intracellular H_2O_2, and produce large amounts CO for a highly efficient treatment of osteoarthritis. Biomaterials ***255***, 120155.
292. Sieghart, D., Liszt, M., Wanivenhaus, A., et al. (2015). Hydrogen sulphide decreases IL - 1β - induced activation of fibroblast - like synoviocytes from patients with osteoarthritis. J. Cell. Mol. Med. ***19***, 187–197.
293. Ha, C., Tian, S., Sun, K., et al. (2015). Hydrogen sulfide attenuates IL-1β-induced inflammatory signaling and dysfunction of osteoarthritic chondrocytes. Int. J. Mol. Med. ***35***, 1657–1666.
294. Wang, B., Shao, Z., Gu, M., et al. (2021). Hydrogen sulfide protects against IL - 1β - induced inflammation and mitochondrial dysfunction - related apoptosis in chondrocytes and ameliorates osteoarthritis. J. Cell. Physiol. ***236***, 4369–4386.
295. Li, L., Fox, B., Keeble, J., et al. (2013). The complex effects of the slow-releasing hydrogen sulfide donor GYY4137 in a model of acute joint inflammation and in human cartilage cells. J. Cell. Mol. Med. ***17***, 365–376.
296. Burguera, E. F., Vela-Anero, Á., Magalhães, J., et al. (2014). Effect of hydrogen sulfide sources on inflammation and catabolic markers on interleukin 1β-stimulated human articular chondrocytes. Osteoarthritis Cartilage ***22***, 1026–1035.
297. Vela-Anero, Á., Hermida-Gómez, T., Gato-Calvo, L., et al. (2017). Long-term effects of hydrogen sulfide on the anabolic-catabolic balance of articular cartilage in vitro. Nitric Oxide ***70***, 42–50.
298. Yu, Y., Wang, Z., Yang, Q., et al. (2021). A novel dendritic mesoporous silica based sustained hydrogen sulfide donor for the alleviation of adjuvant-induced inflammation in rats. Drug Deliv. ***28***, 1031–1042.
299. Geng, W., Liu, X., Tao, B., et al. (2023). Nitric oxide scavenging and hydrogen sulfide production synergistically treat rheumatoid arthritis. Adv. Healthc. Mater. ***12***, 2202380.

ACKNOWLEDGMENTS

This work was financially supported by grants from the National Natural Science Foundation of China (Grant No. 82001965 and 82272157), Shenzhen Science and Technology Research Funding (JCYJ20190806165616542).

AUTHOR CONTRIBUTIONS

A. G. and H. W. supervised and revised the manuscript. Y. X. and Y. L. wrote and edited the manuscript. All authors contributed to the article and approved the submitted version.

DECLARATION OF INTERESTS

The authors declare no competing interests.

LEAD CONTACT WEBSITE

http://htod.siat.ac.cn/index.php/Team/detail.shtml?id=4&cid=11
http://htod.siat.ac.cn/index.php/Team/detail.shtml?id=36&cid=11